



Project funded by the European Commission under the 6th (EC) RTD Framework Programme (2002- 2006) within the framework of the specific research and technological development programme "Integrating and strengthening the European Research Area"



Project UpWind

Contract No.:
019945 (SES6)

"Integrated Wind Turbine Design"

SMART ROTOR BLADES AND ROTOR CONTROL FOR WIND TURBINES

State of the Art

Knowledge Base Report for UpWind WP 1B3

AUTHOR:	Thanasis Barlas
AFFILIATION:	Delft University Wind Energy Research Institute (DUWIND)
ADDRESS:	Kluyverweg 1, 2629 HS Delft, The Netherlands
TEL.:	+31 (0)15 27 82877
EMAIL:	a.barlas@tudelft.nl
FURTHER AUTHORS:	T. Hulskamp (DUWIND), J.W. van Wingerden (DUWIND), A. Mroz (IPPT PAN), P. van Langen (ECN), M. Landa (IT ACSR), S. Apiñaniz (Robotiker)
REVIEWER:	Project members
APPROVER:	

Document Information

DOCUMENT TYPE	Deliverable
DOCUMENT NAME:	Smart Rotor Blades and Rotor Control for Wind Turbines – State of the Art
REVISION:	
REV.DATE:	
CLASSIFICATION:	R1: Restricted to project members
STATUS:	Final

Abstract: This report presents an overview of available knowledge, literature and research regarding the application of smart structures and smart control on wind turbine rotors. A summary of existing knowledge in the field is presented. It covers existing literature in rotorcraft applications, smart materials, smart actuators, computational simulations, experiments on active smart control, and recent research regarding wind turbine applications. Also a summary of concepts for smart wind turbine blades, regarding control surfaces, actuators, sensors, controllers and design issues is analyzed and provided as an overview of potential solutions for smart rotor control for wind turbines.

Contents

1. Introduction.....	5
2. Existing Literature – Research.....	6
2.1 Helicopter Literature - Research	6
2.2 Wind Turbine Literature – Research	17
2.2.1 NREL.....	17
2.2.2 DUWIND (TUDelft)	23
2.2.3 ADAPWING (Risø)	28
2.2.4 C. van Dam (Univ. California).....	37
3. Potential for UpWind.....	42
3.1 Control surfaces.....	42
3.1.1 Full-span pitch control	42
3.1.2 Part-span pitch control.....	47
3.1.3 Trailing edge flaps	48
3.1.4 Micro tabs.....	50
3.1.5 Active twist	52
3.1.6 Variable camber	53
3.1.7 Inflatable structures	55
3.1.8 Boundary layer suction	56
3.1.9 Synthetic jets	57
3.1.10 Passive control concepts.....	59
3.1.11 Non-aerodynamic control concepts	60
3.2 Actuators.....	61
3.2.1 Actuator requirements	61
3.2.2 Conventional actuators.....	61
3.2.3 Smart material actuators	63
3.3 Sensors.....	79
3.3.1 Electrical type strain sensors	79
3.3.2 Optical type strain sensors	80
3.3.3 Accelerometers.....	81
3.3.4 Acoustic emission monitoring.	81
3.4 Control	83
3.4.1 Modern control for load reduction	83
3.4.2 Load reduction with smart rotor	85
3.4.3 Repetitive learning control.....	85
3.4.4 Positive position feedback control	86
3.5 Modeling-Tools	89
3.5.1 Requirements for modelling of smart wind turbine rotors	89
3.5.2 Theoretical tools	90
3.5.3 Software tools.....	91
3.6 Design considerations.....	93
Bibliography.....	95

STATUS, CONFIDENTIALITY AND ACCESSIBILITY									
Status			Confidentiality				Accessibility		
S0	Approved/Released		R0	General public			Private web site		
S1	Reviewed		R1	Restricted to project members	*		Public web site	*	
S2	Pending for review	*	R2	Restricted to European. Commission			Paper copy		
S3	Draft for comments		R3	Restricted to WP members + PL					
S4	Under preparation		R4	Restricted to Task members +WPL+PL					

PL: Project leader**WPL:** Work package leader**TL:** Task leader

Chapter 1

1 Introduction

The size of wind turbine blades has been steadily increasing over the past years. Rotors of 120m diameter are now a reality. The growth in blade length tends to make the blades a larger proportion of the total system cost. With the intention to lower the cost per wind turbine (or keep it steady while increasing the size), new trends and technological improvements have been a primary target of research and development.

Such trends include increasing power performance, reducing weight, reducing design margins, designing for higher life cycles, improving materials, using new design tools, improving blade geometry and reducing loads. Reducing the cost of wind turbine blades has an effect on the costs of energy, but only a small percentage of the total. However, if an innovative blade design can result in decrease in loading, the general cost will decrease, as rotor loads affect the loading of other components, as the drive train and the tower [1] [2].

Design loads on wind turbines are generally divided into ultimate (extreme) loads and fatigue loads. Fatigue loads are a key factor for the design of wind turbines. Reducing fatigue loads can result in a significant reduce in cost, thus can reduce maintenance requirements and improve reliability.

The general aim of many research and development programs in this area is focusing on developing new technology capable of considerably reducing fatigue loads on wind turbines. Many concepts exist and have been considered in the past. The recent trend in this field (recent for wind turbine applications, but investigated for aircraft and helicopter applications) includes the integration of “smart” structures and “smart” control in wind turbine blades. This means the implementation of efficient, innovative actuators which control certain aerodynamic surfaces, which, through the combination of sensors and controllers provide active dynamic “smart” control. As Chopra states: “A smart structure involves distributed actuators and sensors and one or more microprocessors that analyze the responses from the sensors and use integrated control theory to command the actuators to apply localized strains/displacements to alter system response”[7]. The target of this control for wind turbine applications is mainly the reduction of fluctuating (fatigue) loads, especially in the flap-wise blade direction.

This report presents an overview of studied literature for the application of smart dynamic rotor control on wind turbines. This literature covers studies for helicopter active control concepts, smart actuator design concepts, experimental tests and computational models. The general concept is multidisciplinary, so many different technology and theory fields have to be combined and considered. Finally, a summary of available options are presented and various design issues are discussed.

Chapter 2

2 Existing Literature – Research

In this chapter, existing knowledge from research in the field of smart structures for rotor control is presented. The first part (2.1) describes the available state-of-the art in research and technology applied in rotorcraft systems. This part provides also an introduction to smart materials, actuators and possible applications. Only a summary of recent progress is presented, since research on smart rotor control for helicopter applications is vast. The second part (2.2) describes the up-to-date research in application of smart rotor concepts for wind turbines. The field is still new, but available and most important ongoing projects are presented.

2.1 Helicopter Literature - Research

The application of control surfaces on blades for aerodynamic control is a technique traditionally used since the beginning of aircraft technology. The concept of active control on a blade by using smart structures (actuators, sensors, controllers) has been thoroughly studied in the field of helicopter technology. The interest for smart rotor control in helicopter rises mainly because of the importance of vibration and noise reduction at the rotor. In this literature field a lot of topics have been studied, including control surface concepts, smart materials, smart actuators, design options, control strategies, modeling and experimental testing.

In 1996 [3] and 2004 [4] Straub published summary reports of available technological knowledge in smart structures for rotor control (reports prepared for Mc Donnell Douglas Helicopter Systems and the Boeing Company). In these, he summarizes existing studies in smart rotor control (mainly work of Chopra), he specifies the requirements needed for helicopter rotor control (actuation requirements, bandwidth), describes some concepts of aerodynamic control and actuators and studies basic efficiency of smart materials (Fig. 1-4). Specifically, for control concepts, he summarizes pitch control, twist control, camber control and moveable control surfaces (trailing edge flaps or servo tabs actuated by a smart material tube). Furthermore, a selection of smart materials is analyzed (piezoelectric, electrostrictive, magnetostrictive, shape memory alloys and electrorheological fluids). Finally, some smart actuator design concepts are suggested (bender elements, stack actuator, actuator tube, ultrasonic motors). Based on the results of this study, it was concluded that rotor control using smart materials is feasible if advances in smart materials are combined with rotor design for low control loads and motions. Specifically, Straub concludes that servo flap control with discrete actuators driving hinged rotor control surfaces emerges as the most suitable rotor control mechanization for smart material actuation. He suggests that rotor design must be tailored for the control concept, latest advances in smart materials must be employed and several types of smart materials must be combined in an actuator for best performance.

Based on the summary work, Straub published the second report [4] for Boeing specifying a smart rotor design for active control (Fig. 5). A blade with integrated smart actuators was designed. A piezoelectric-driven trailing edge flap was used for vibration, noise and aerodynamic performance improvements, and a Shape Memory Alloy (SMA)-driven trailing edge trim tab for in-flight blade tracking. The sizing parameters were calculated using CFD. The first smart actuator consists of two piezo stack columns mechanically amplified through a push-pull rod, which connects them to the trailing edge flap. The second actuator consists of two SMA tubes connected through a linkage to the trailing edge tab. Actuator performance and robustness was evaluated from a series of tests. An analytical model was developed which shows reduction by over 80% in vibratory hub loads with flap angles less than 2 degrees and a 5 db noise reduction. Straub concludes that all the requirements for the control systems were met and design has been optimized through the tests. But, not full rotating tests were conducted and no closed-loop control was applied.

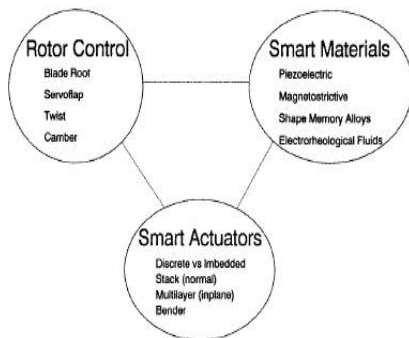


Fig. 1: Smart Structure concept [3]

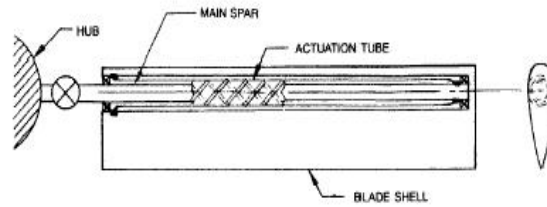


Fig 2: Actuator tube [3]

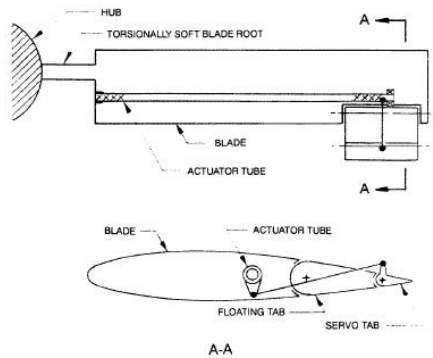


Fig 3: Servo flap [3]

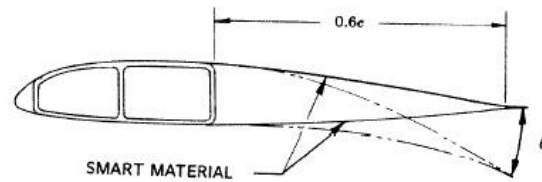


Fig 4: Camber control [3]

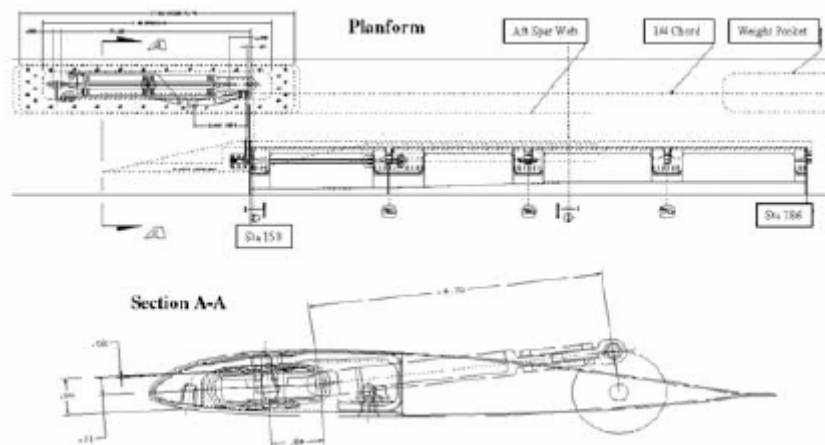


Fig. 5: Straub's smart blade – actuator design [4]

The most important state-of-the art summary report of smart structures and integrated systems (with application to rotorcraft) was published by Chopra [7]. For more than 10 years he has been active in the research field of smart structure applications to rotorcraft. An overview of available smart actuators and sensors is presented (Fig. 6-15), but more detailed information is provided for piezoelectric actuators and sensors which are considered more feasible for rotorcraft applications.

The static and dynamic strain of piezoelectric actuators (mostly PZT-5H) is presented, but also the drift, hysteresis and manufacturing issues. The frequency response of piezoelectric sensors is analyzed. Furthermore, a comparison between different models of smart beams (beams equipped with smart actuators), and between different models of smart plates (plates equipped with smart actuators) is made.

Next, a thorough survey on Shape Memory Alloys (SMA) is presented. Modeling, strain-stress performance, behavior under various loading, and specific actuator options are analyzed. Chopra states that more research on accurate models for SMAs, and more detailed Finite Element Method simulations should be made. But, mostly innovations are needed to increase frequency response of SMA actuators. About Magnetostrictive and Electrostrictive materials and their use as actuators, it is mentioned that simplified constitutive relations and detailed electromechanical/magnetomechanical characteristics are not yet available so research must continue in order to be used as actuators in specific applications.

Furthermore, the application of smart actuators on rotorcraft is discussed. Mainly, required mechanical amplification (for larger stroke) and issues on power and leverage amplification are discussed. Generally, for rotorcraft applications, moderate actuation force and large deflections are required. The use of these forms of mechanical amplification (level/frame methods) trades force with displacement and provides required performance. Piezo stack actuators, benders, and most important design concepts of amplification mechanisms are specified.

Finally, a summary of research in rotorcraft application of smart structures is presented. It focuses on experiments and design models. The main smart structure concepts involve leading and trailing edge flaps actuated by smart material actuators, controllable camber/twist blades with embedded piezoelectric elements/fibers and active blade tips actuated with tailored smart actuators. For flap actuation concepts range from piezobimorphs, piezostacks, and piezoelectric/magnetostrictive-induced composite coupled systems.

Specifically, Koratkar and Chopra built 1.83 m diameter scaled rotor models with trailing edge flaps actuated by piezobimorphs (Fig. 16 a). Froude-scaled models were built and tested in a vacuum chamber and on a hover tower and finally Mach-scaled rotor models in closed-loop testing in the wind tunnel. Using a neural network controller, with a flap deflection of ± 5 degrees, individual blade control resulted in over 80% reduction in vibratory hub loads. Moreover, Lee and Chopra built a model of a blade section of 30 cm length with trailing edge flaps actuated with piezo-stacks, using a double lever (L-L) amplification mechanism (Fig. 16 c). The expected increased performance of flaps at different operating conditions was shown (e.g. ± 10 degrees at 36 m/s). Bernhard and Chopra built a 1.83 m diameter Mach-scaled smart active-tip rotor actuated with piezo induced bending-torsion coupled composite beam (Fig. 16 e). The achieved tip pitch deflections were 1.7 to 2.9 degrees. Chen and Chopra built a 1.83 m diameter Froude-scaled rotor model with controllable twist blades actuated by embedded multilayered piezoceramic elements (Fig. 16 d). The results in rotor vibration were less than the target values, but showed the potential partial load vibration suppression. Also, Roger and Hagoon, Derham and Hagood and Cesnic and Shin developed Mach-scaled models with controllable twist utilizing embedded active fiber composites. Although the results, regarding performance, were not as high as expected, showed enormous potential for full scale rotor applications. Regarding SMA actuators, Chopra investigated the application by developing a blade section model with tab actuated by SMA wires (Fig. 16 b). The performance in terms of deflection was good, although the frequency response of SMA actuator was poor. Chopra has over a decade of experience in modeling and developing various smart control systems for vibration and noise reduction in helicopters. Presenting all of his work is beyond the targets of the present report. Most important references can be found in Chopra's review report [7].

Actuators	PZT-5H	PVDF	PMN	Terferrol DZ	Nitinol
Actuation mechanism	Piezoceramic	Piezofilm	Electrostrictive	Magnetostrictive	Shape memory alloy
Free strain Δ , μ strain	1,000	700	1,000	2,000	60,000
Modulus E 10^6 psi	10	0.3	17	7	4 for (martensite) 13 for (austenite)
ϵ_{\max} for aluminum beam $t_b/t_c = 10$	350	10	500	580	8,500
Band width	High	High	High	Moderate	Low
Strain-voltage linearity	First-order linear	First-order linear	Nonlinear	Nonlinear	Nonlinear

Fig. 6: Comparison of actuators [7]

Sensor	Resistance gauge 10-V excitation	Semiconductor gauge 10-V excitation	Fiber optics 0.04-in. interferometer gauge length	Piezofilm 0.001-in. thickness	Piezoceramics 0.001-in. thickness
Sensitivity	30 V/ ϵ	1000 V/ ϵ	10^6 deg/ ϵ	10^4 V/ ϵ	2×10^4 V/ ϵ
Localization (inches)	0.008	0.03	0.04	<0.04	<0.04
Bandwidth	0 Hz acoustic	0 Hz acoustic	0 Hz acoustic	0.1 Hz GHZ	0.1 Hz GHZ

Fig. 7: Comparison of sensors [7]

Coefficient	PZT-5H	PZT-8	PVDF
d_{31}	-274×10^{-12} m/V	-97	18-24
d_{32}	-274×10^{-12} m/V	-97	2.5-3
d_{33}	593×10^{-12} m/V	225	-33
d_{15}	741×10^{-12} m/V	330	—
Relative permittivity ϵ_{33}	3400	1000	—
Free-strain range	-250 to +850	$\mu\epsilon$	—
Poling field dc	12 kV/cm	5.5	—
Depoling field ac	7 kV/cm	15	—
Curie temperature	193°C	300	—
Dielectric breakdown	20 kV/cm	—	—
Density	7500 kg/m ³	7600	—
Open circuit stiffness E_{11}	62 GPa	87	—
Open circuit stiffness E_{33}	48 GPa	74	—
Compressive strength (static)	>517 MPa	>517	—
Compressive depoling limit	30 MPa	150	—
Tensile strength (static)	75.8	75.8	—
Tensile strength (dynamic)	27.6 MPa	34.5	—

Fig. 8: Piezoelectric characteristics [7]

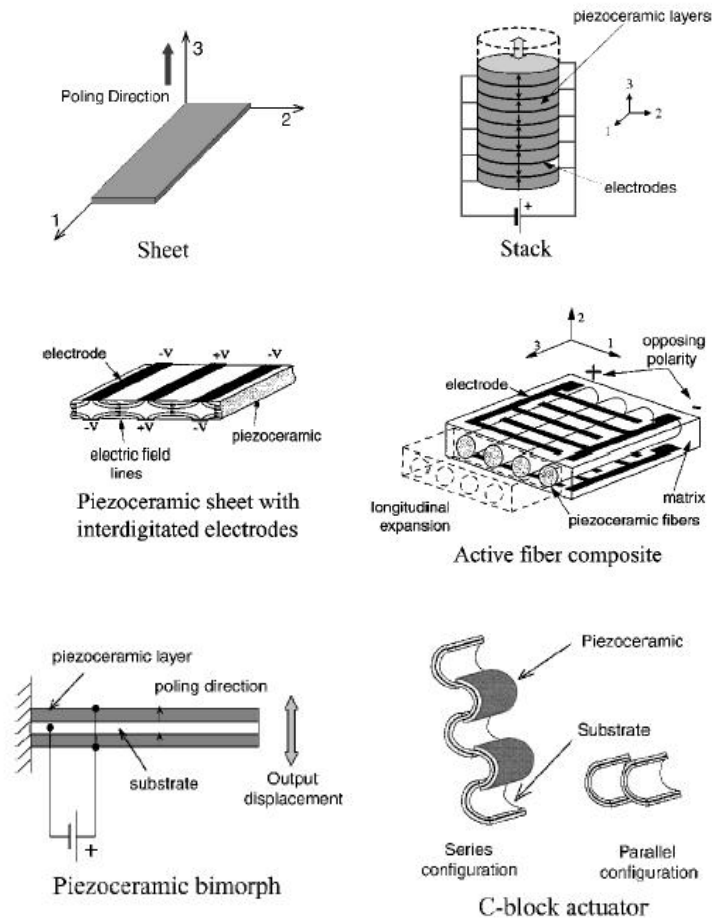


Fig. 9: Different types of actuators [7]

Coefficient/ property	Unit	Value	Coefficient/ property	Unit	Value
σ_{cf}^s	Pa	$1.38e+6$	A_s	$^{\circ}\text{C}$	52
σ_{cr}	Pa	$1.72e+6$	A_f	$^{\circ}\text{C}$	65
C_A	$\text{Pa}/^{\circ}\text{C}$	$8e+6$	$M_{s(\text{Tanaka})}$	$^{\circ}\text{C}$	43.5
C_M	$\text{Pa}/^{\circ}\text{C}$	$12e+6$	$M_{f(\text{Tanaka})}$	$^{\circ}\text{C}$	40.7
E_A	Pa	$45e+9$	$M_{s(\text{Brinson})}$	$^{\circ}\text{C}$	55
E_M	Pa	$20.3e+9$	$M_{f(\text{Brinson})}$	$^{\circ}\text{C}$	42

Fig. 10: Thermomechanical properties of SMA wires [7]

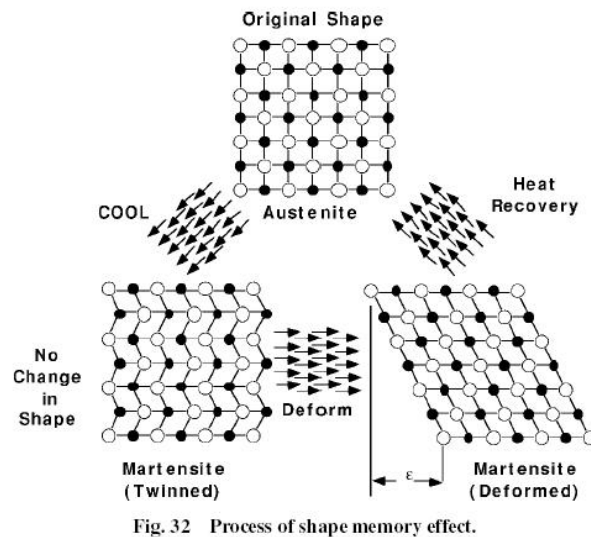


Fig. 32 Process of shape memory effect.

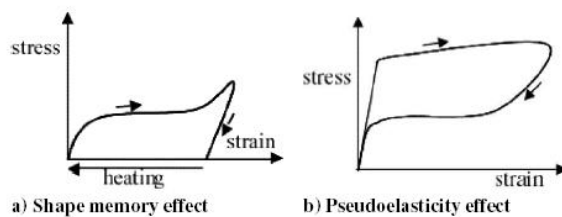


Fig. 11 Stress-strain behavior of SMA [7]

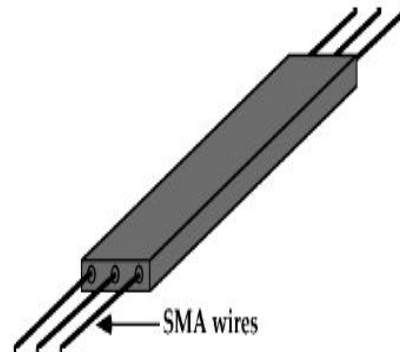


Fig. 12: Graphite-Epoxy beam with SMA wires [7]

Part/material no.	Operating voltage, V	Maximum strain, μ strain	Block force (BF), lb	Normalized block force, ksi	Strain-force index	Energy density, ft-lb-slug
MM 8M (70018)	360	254	128	1.05	0.133	1.27
MM 5H (70023-1)	200	449	101	0.83	0.180	1.80
MM 4S (70023-2)	360	497	143	1.17	0.291	2.78
PI P-804.10	100	1035	1133	7.31	3.783	36.72
PI PAH-018.102	1000	1358	1505	9.71	6.593	62.95
XI RE0410L	100	468	95	5.16	1.207	11.52
XI PZ0410L	100	910	70	3.58	1.629	15.55
EDO 100P-1 (98)	800	838	154	2.00	0.838	8.00
EDO 100P-1 (69)	800	472	50	0.66	0.156	1.49
SU 15C (H5D)	150	940	266	7.48	3.516	33.57
SU 15C (5D)	150	1110	274	7.70	4.274	40.80

Fig 13: Comparative test evaluation of commercially available piezo-stack actuators [7]

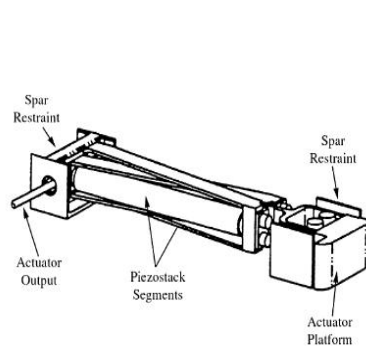


Fig. 14: X-Frame actuator [7]

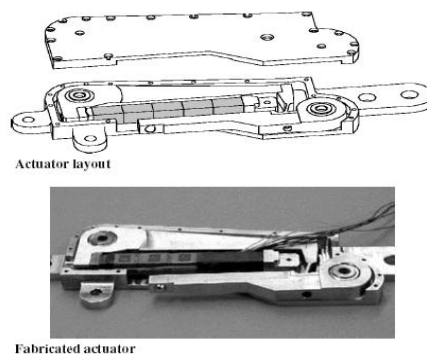
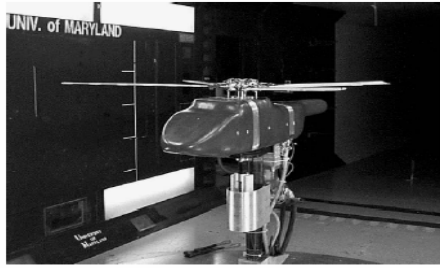


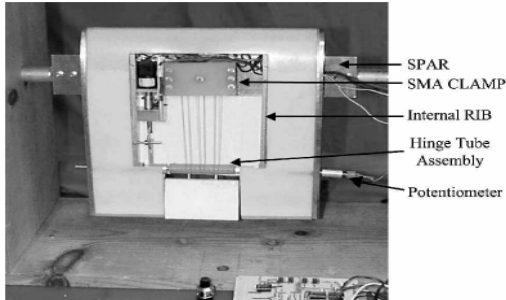
Fig.15: L-L amplification mechanism [7]



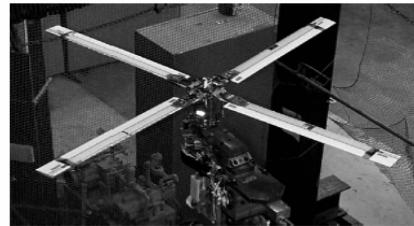
a) Piezobimorph-actuated flap: 6-ft-diam rotor model test in Glenn L. Martin wind tunnel; successfully tested in both open- and closed-loop studies



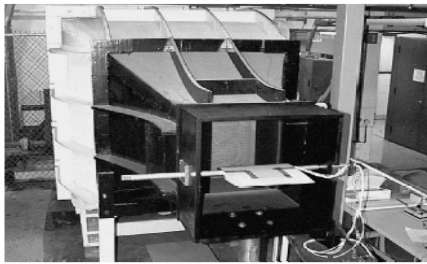
d) Active twist blade with embedded piezoactuators 6-ft-diam rotor test in Glenn L. Martin wind tunnel; produced ± 0.5 -deg blade twist up to 5/rev excitation



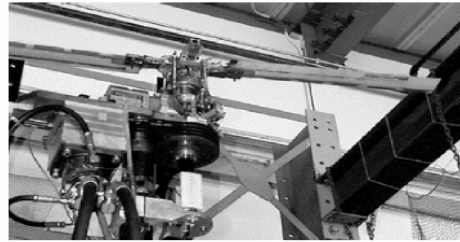
b) Blade-tab-actuated with shape memory alloys actuator; wing section tested in open-jet wind tunnel; produced tab deflections of over 20 deg



e) Smart tip rotor model (diam 6 ft) on hover stand, actuated with composite bending-torsion coupling and piezos; produced ± 2 deg tip deflections up to 5/rev



c) Piezostacks-actuated flap: full-scale wing section model tested in open-jet wind tunnel; produced ± 6 -deg flap deflection



f) Froude-scale rotor model (6 ft diam) on hover tower with piezobimorph-actuated flaps

Fig. 16: Smart rotor development at Alfred Gessow Rotorcraft Center, by I. Chopra [7]

The most recent research in active rotor control using smart devices is that in ADASYS project. It is a joint task between Eurocopter, EADS CRC, Daimler Chrysler Research Labs and DLR [9, 10]. The work was presented during European Rotorcraft Forum sessions taking place the 4 previous years. For the first time, a full scale rotor was developed, based on the hingeless system of the BK117/EC145. A piezoelectric actuator concept was chosen and developed for active trailing edge flap control. A monolithic co-fired multilayer stack actuator (so called "DWARF") was utilized. Three trailing edge flaps (15% chord length – flap angle ± 10 degrees) were used on each blade. The preloaded piezo actuators were connected to the flaps using a tension rod. Wind tunnel experiments of both 2d and rotating cases, bench testing of key components, centrifugal tests and whirl tower tests confirmed the efficiency of the actuation system in achieving necessary flap deflections and identified the aerodynamic and dynamic parameters. Algorithms with the control target of minimizing noise and vibration for individual blade control (IBC), were used for the development of the flap controller. The controller consists of 4 PID channels and a set of Kalman filters, and is combined with the traditional cyclic/collective primary controller of the helicopter. A PC with dSPACE was used for the real-time controller. The active smart control rotor and the control systems were equipped on a BK117. Real flight tests were performed during level flight, climb, descent and maneuver flight. All results are impressive and show reduction in vibratory forces (Fig. 22).

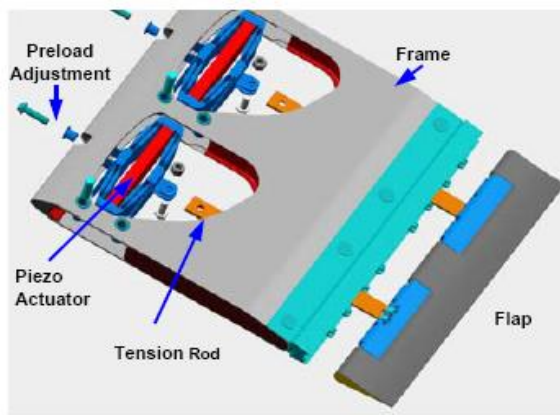


Fig. 17: Flap and actuators unit assembly [9]



Fig. 18: Blade with flaps on whirl tower

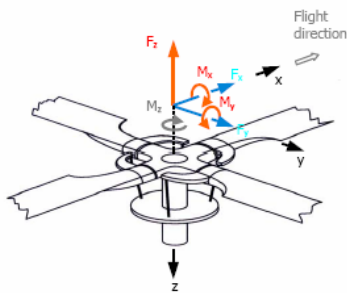


Fig. 19: Hub loads for feedback control [10]

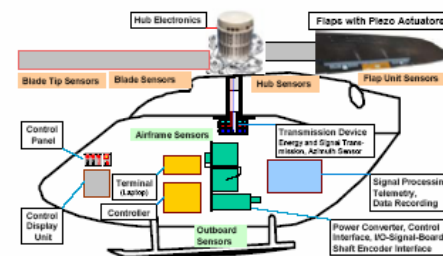
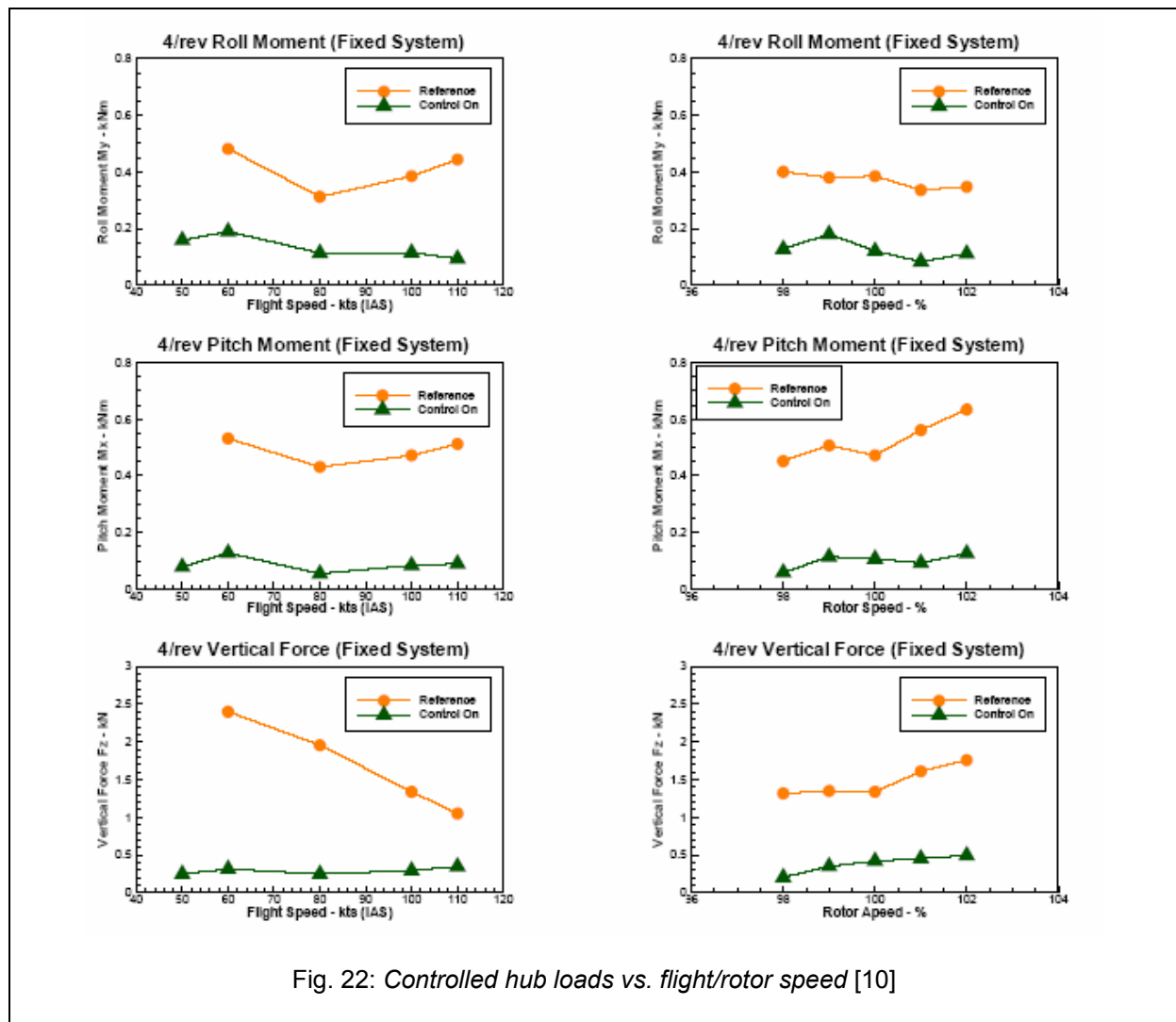


Fig. 20: Systems on helicopter [10]



Fig. 21: First flight of a the BK117 S7045 with active trailing edge flaps [10]



Of course, a thorough investigation about active flow techniques and adaptive wings has been conducted over the year for aircraft applications too. Some overview references are presented below. The helicopter research efforts were analyzed in detail since the similarity with wind turbine applications is great. A detailed overview of all active control research for fixed wings applications is outside the target of this report.

An extensive study of literature on theory, simulation and experiments in active flow control is given in [38]. Overview of possible flow control strategies is given, referenced to relevant literature and categorized by the type of actuation (passive or active) and by means by which the actuation changes in response to flow change (open loop, closed loop, optimal control). Some issues concerning the CFD are also addressed. Another overview of active flow control technology is given in [39]. This contribution is oriented towards airplane wing structure. A concept of adaptive wing using translational actuators is discussed in chapter 3.1, whereas variable camber flaps are discussed in chapter 3.3. Concepts of adaptive wing and adaptive rotor blades are overviewed in [40].

2.2 Wind Turbine Literature – Research

This part of the overview summary on available literature and research of interest for smart rotor applications focuses on progress related to wind turbine applications. Although the amount of available progress in this specific field is quite new and can not be compared to the available progress in rotorcraft, inspired by these similar applications and by the need for more advanced active control, research programs investigate the possibilities for such concepts in wind turbines. Some of the most important projects (most of them recent and ongoing) are summarized.

2.2.1 NREL

An early first approach regarding investigation of using aerodynamic control devices for wind turbine control was made by NREL during 1995-1998. The work is described in [11, 12, 13]. Although this work focused on using aerodynamic devices for braking purposes, and no research is included for smart actuation or active load control, this contribution was a preliminary step and is considered important in quantifying certain preliminary parameters for the design of such devices. In [11], five trailing edge devices were investigated to determine their use as wind turbine aerodynamic brakes. There were compared mainly according to the achieved lift to drag ratio reduction and drag increase. The spoiler-flap concept was considered the best choice. In [12] extensive 2D wind tunnel tests of these devices were conducted analyzing various aerodynamic parameters for a range of angles of attack, control configurations and sizes. The control devices were evaluated also numerically using a computer program (WIND). The overall performance of a wind turbine with such aerodynamic control devices was predicted running simulations for various configurations (parametric fixed device configurations). The spoiler-flap configuration exhibited a large negative suction coefficient over a broad angle-of-attack range and good turbine braking capabilities. In [13], an experiment using a 20kW horizontal-axis wind turbine that incorporated variable-span, trailing edge aerodynamic control devices is presented. The target of these rotational, atmospheric tests was to quantify the influence of span-wise 3D effects, by comparing aerodynamic parameters with the 2D experimental data from the previous research work. Although during the tests, only fixed configurations of three trailing edge devices were used, this research work is of great importance, since it comprises a realistic investigation of the aerodynamic parameters associated with control devices used in variable span-wise length and the 3D flow effects associated with their performance. Specifically, a “softening” of the stall behavior (ΔC_L around stall) was observed, compared with the infinite span (2D) results. Also, it is stated that the 2D experiments underpredicted the effective reduction in lift for short span devices near the tip. The reason is suggested to be connected with the effect of strong shed vorticity due to the device uploading, which reduces the lift in the inboard section, thus enhancing the performance of the device (Fig. 25). Such effects are considered of great importance when designing variable span-length aerodynamic control devices for rotational applications, based on 2D measurements and modeling. Finally some approximate expressions for relating 2D and 3D drag effects are discussed.

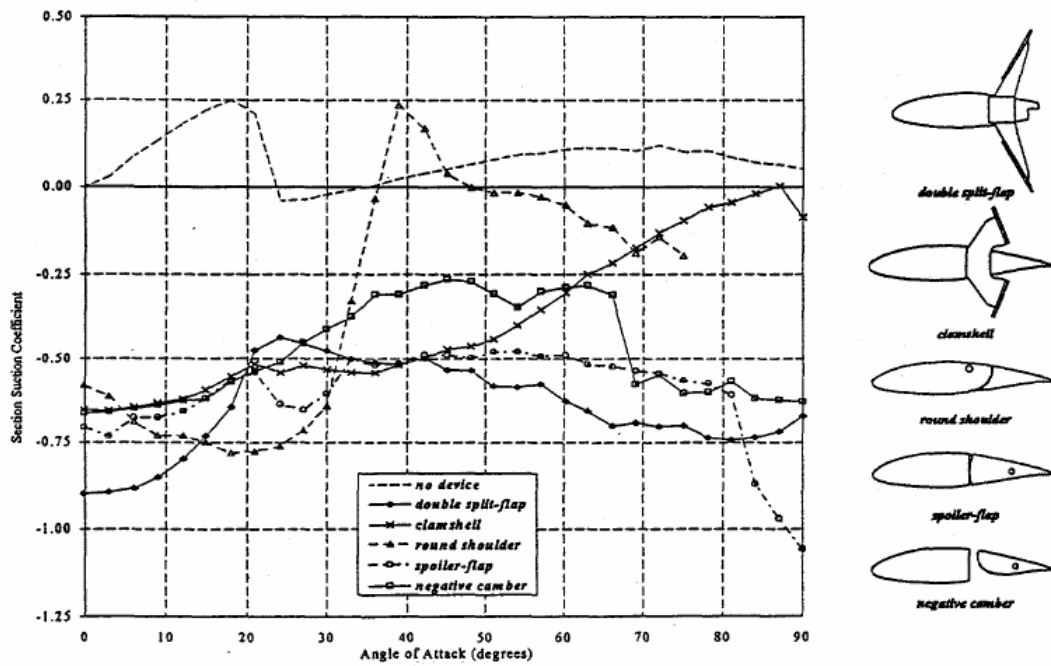


Fig. 23: Effectiveness of trailing edge aerodynamic control surfaces (brakes) [11]

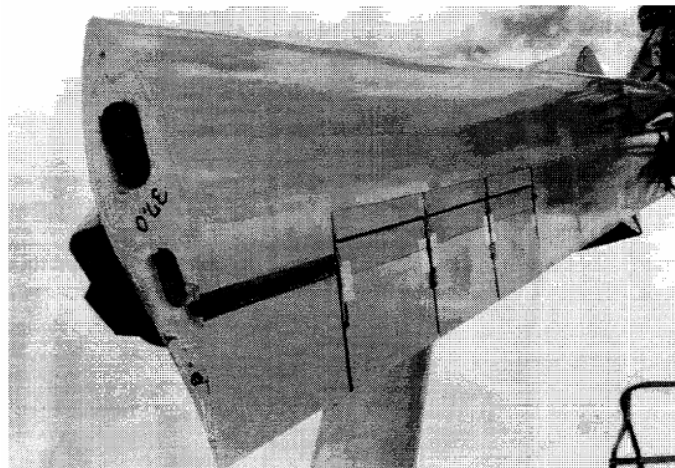


Fig. 24: Variable span flaps on the rotating test blade [13]

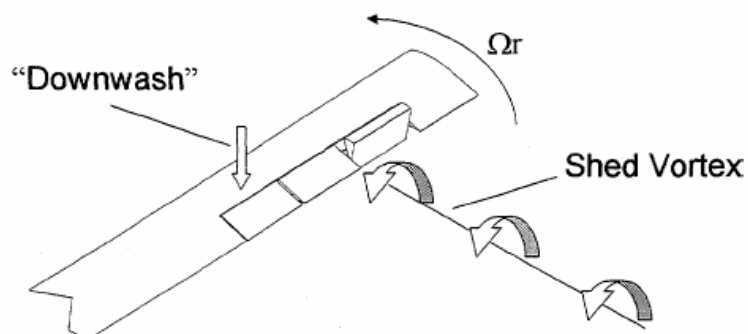


Fig. 25: The span -wise effects on the effectiveness of the flaps [13]

A recent research direction at NREL is the investigation of active control of rotor aerodynamics and rotor geometry for wind turbines. Preliminary results of this effort are presented in [36]. This study focuses on exploring two categories of aerodynamic modification. The first is geometry control, based on variable-length blades. The second is use of active aerodynamic control devices including: flaps, slats, ailerons, MEM tabs, vortex generators and camber control. The control algorithms of such devices will employ linear state-space methods that include also individual blade pitch control. For the variable-diameter rotor concept power performance and loads calculations were calculated using MSC-ADAMS. The desired blade tip extension position was calculated using a linear function of wind speed and applied using a state space model based algorithm. The results show increased power over the wind speed range, but also increased peak and fatigue loads as expected. The biggest challenge is such a concept is the design and operation of the mechanism for the extension of the tip (a rack and pinion with a servo motor were selected). For the aerodynamic devices, microtabs based on the work of van Dam [27, 28, 29, 30, 31, 32, 33], were firstly chosen for investigation, and preliminary results are presented. The aerodynamic effects of these devices were incorporated only in form of adjustment in static lift and drag based on the experimental and computational results of van Dam. The micro tab effects were lumped into three regions of the blade: inboard, midspan and outboard. A control strategy based on a LQR state space controller was developed, which includes individual blade pitch control and controls the turbine operation differently into distinct operation regions. A step change in logarithmic wind shear exponent was simulated and control response for traditional PI for blade pitch, Individual Pitch and Microtab control were compared in reduction of blade tip deflection. Also peak and fatigue loads were calculated based on IEC load cases. The variations in tip deflection were quickly reduced with the MEM tabs. The loads are also reduced by using the aerodynamic control devices. The approach of NREL is interesting in quantifying load reductions and performance changes, although no dedicated aerodynamic model was provided for realistic simulation of the unsteady behavior of such devices (the microtabs were deployed immediately, with no time lags and the controller is ideal).

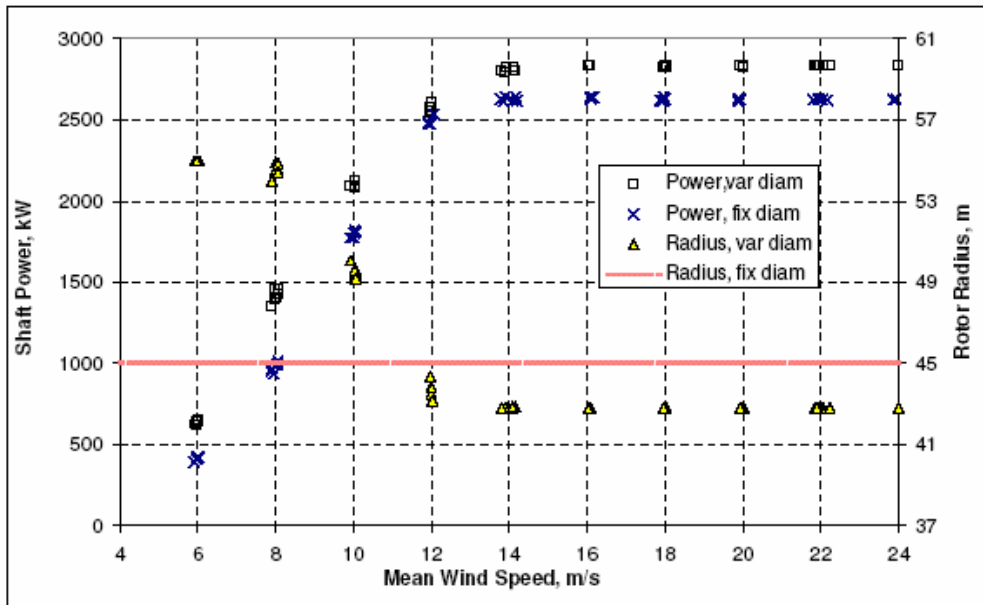


Fig. 26: Power performance achievements with variable diameter rotor [36]

Load Component	Baseline		Variable Diam		% change
	Maximum	Load Case	Maximum	Load Case	
Root Edge bending, kNm	2,350	ECD_R	2,580	ECD 10m/s	9.8
Root Flap bending, kNm	5,010	ECD_R	5,590	PP 22m/s	11.6
Main shaft bending, kNm	3,760	ECD_R	4,350	ECD 10m/s	15.7
Main shaft torque, kNm	1,780	PP 24m/s	1,830	PP 24m/s	2.8
Tower top roll, kNm	2,080	PP 24m/s	2,120	PP 24m/s	1.9
Tower top tilt, kNm	-6,070	ECD_R	-6,600	ECD 10m/s	8.7
Tower top yaw, kNm	2,840	PP 24m/s	3,490	ECD 8m/s	22.9
Tower base, kNm	49,670	EWM 1 year	52,260	EWM 1 year	5.2
Blade Tip Deflection, m	5.06	ECD_R	7.98	ECD 8m/s	57.7

Fig. 27: Peak loads changes with variable diameter rotor [36]

Load Component	SN slope	Baseline	Var Diam	% change
Root Edge bending, kNm	15	2594.0	3084.5	18.9
Root Flap bending, kNm	15	2756.9	2945.6	6.8
Main shaft bending, kNm	8	1,950.0	2,107.5	8.1
Main shaft torque, kNm	12	717.7	747.7	4.2
Tower top roll, kNm	8	513.9	531.2	3.4
Tower top tilt, kNm	8	1,623.6	1758.1	8.3
Tower top yaw, kNm	8	1,621.7	1681.0	3.7
Tower base, kNm	4	6,283.5	7,090.5	12.8

Fig. 28: Fatigue loads changes with variable diameter rotor [36]

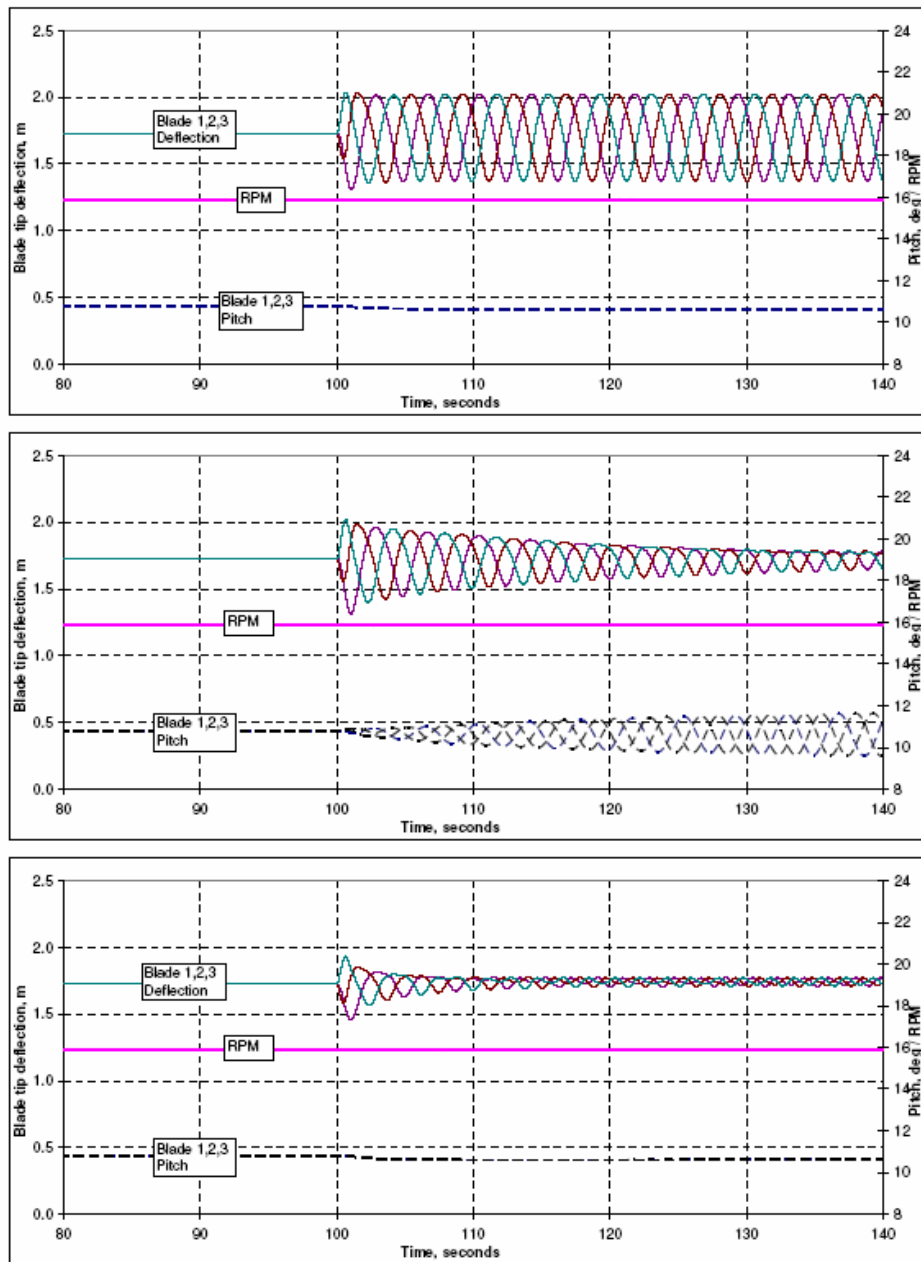


Fig. 29: Reduction in tip deflection for a step change in wind shear with traditional PI blade pitch, Individual Pitch and Microtab control (top to bottom) [36]

Load Component	Baseline		Aero Controls		% change
	Maximum	Load Case	Maximum	Load Case	
Root Edge bending, kNm	2,350	ECD_R	2,690	ECD_R	14.5
Root Flap bending, kNm	5,010	ECD_R	4,730	ECD_R	-5.6
Main shaft bending, kNm	3,760	ECD_R	3,420	ECD_R	-9.0
Main shaft torque, kNm	1,780	PP 24m/s	1,660	PP 22m/s	-6.7
Tower top roll, kNm	2,080	PP 24m/s	1,970	PP 24m/s	-5.3
Tower top tilt, kNm	-6,070	ECD_R	-5,760	ECD_R	-5.1
Tower top yaw, kNm	2,840	PP 24m/s	2,790	PP 24m/s	-1.8
Tower base, kNm	49,670	EWM 1 year	49,670	EWM 1 year	0.0
Blade Tip Deflection, m	5.06	ECD_R	4.67	ECD_R	-7.7

Fig. 30: Peak load reduction with Microtab control [36]

Load Component	SN slope	Baseline	Aero Controls	% change
Root Edge bending, kNm	15	2594.0	2543.5	-1.9
Root Flap bending, kNm	15	2756.9	2166.7	-21.4
Main shaft bending, kNm	8	1,950.0	1446.5	-25.8
Main shaft torque, kNm	12	717.7	729.9	1.7
Tower top roll, kNm	8	513.9	510.3	-0.7
Tower top tilt, kNm	8	1,623.6	1363.3	-16.0
Tower top yaw, kNm	8	1,621.7	1387.2	-14.5
Tower base, kNm	4	6,283.5	5342.0	-15.0

Fig. 31: Fatigue load reduction with Microtab control [36]

2.2.2 DUWIND (TUDelft)

An important research work, concerning feasibility studies on smart dynamic rotor control for wind turbine applications, has been conducted by Marrant, van Holten and Kuik for the STW project Smart Dynamic Rotor Control for Large Offshore Wind Turbines. It has been summarized in a series of reports prepared for NOVEM (de Nederlandse Organisatie voor Energie en Milieu). The first report [15] deals with the inventory of rotor design options and possible load reductions. The fluctuating loads on a wind turbine are described and possibilities of influencing fatigue loads or structural loads are discussed. Active rotor control concepts are presented which include pitch control concepts (collective, cyclic, higher harmonic), individual blade control (part-span pitch, aileron control, active twist) and active damping of blade and tower vibrations. Also semi active and passive control options are discussed (passive tips, self-twisting blades, compliant blades). Concluding, individual pitch control was considered as the most powerful strategy (because of the ability to reduce aerodynamic loads both due to temporal and spatial variances in inflow) but active structural damping was also considered interesting (for reducing the loads due to axial tower mode and blade flapwise bending mode).

The second report [14] summarizes present techniques with regard to sensors, actuators, aerodynamic constructions and control strategies and their application on large offshore pitch regulated variable-speed wind turbines. Regarding sensors, strain gauges, accelerometers and force sensors were analyzed. Piezoelectric force sensors at the blade root were considered a feasible solution for the measurement of aerodynamic loads. Optical fibers were considered expensive and not well established for measuring strains on blades. Passive accelerometers were considered a good solution due to their low bandwidth and low frequency limit. Regarding control strategies, four control strategies that had been developed to actively suppress vibrations in rotorcraft are analyzed: a feed forward adaptive control algorithm (Broadband filtered X-LMS and tonal control), a Fourier synthesis algorithm, a real-time adaptive neural network controller and an iterative learning controller. Some important considerations regarding the connection between controller design and wind turbine design are also pointed out. Regarding actuators, many categories are analyzed: conventional (pneumatic, hydraulic, electro-motors), smart materials (electrorheological, magnetorheological, shape memory alloys (SMA), electrostrictive, piezoelectric, magnetostrictive).

A summary of analysis about smart materials and their use as actuators is presented:

SMA

Pros:

- SMA's lead to small size, internal material-based mechanisms for single unit actuators.
- They exhibit excellent cycling performance in repeated loading.
- The actuation signal can be diverse: heat via electrical signals, hot water, hot air, laser or infrared rays.
- SMA's have a fracture toughness and energy absorption which is better than almost any other metal.

Cons:

- They show slow response time as compared to other smart material components (e.g. piezo-ceramics).
- Energy requirements for actuating the shape memory effect are relatively high [2].
- Nonlinear hysteresis (12-38%) and thermomechanical response characteristics are an essential feature: this results in difficult modelling and design of actuators for consistent repeatable operation.
- Creep is very common and can occur all the way up to 11% under nominal stress conditions.
- The shape memory effect is very much limited to a certain thermal range, requiring very precise actuation.
- The electrical connection is difficult (no solder or braze works): only crimping, swaging and other forced contact methods will work.
- Active strain often fails the adjacent structure and substrates.
- Machining is difficult if not impossible.
- Building composite shafts or beams with embedded shape memory alloys is a challenge and needs focused effort.
- Composite charging is an adverse side effect.
- Fibre pull-out is a problem.

ElectrostrictivePros:

- Small hysteresis levels above the Curie temperature: small thermal expansion.
- Lightweight construction permits control without severely affecting passive dynamics.
- Nonlinear constitutive relations permit tuning of field-strain ratios.
- Unpoled nature of materials can lead to extended performance over piezoelectric elements.
- Broadband frequency response.

Cons:

- Nonlinear strain-field relations and field-dependant parameters.
- Temperature dependency of elements manifested in temperature dependent parameters.

Piezoelectric:Pros:

- Relative temperature insensitivity and linear response at low excitation levels
- Lightweight construction and flexibility as sensors and actuators in a large variety of applications
- Broadband frequency response
- Their health status can be measured by applying an electric field and measuring their impedance.

Cons:

- Significant hysteresis at large electric field levels.
- Brittleness and small tensile strength of PZT's.
- Weak electromechanical coupling coefficients for PVDF's.
- Piezoelectric effect generated through poling can decay, thus leading to aging effects and performance degradation. This can be solved by regular repoling (depending on the PZT, maybe several times a day).

Also, certain amplifying mechanical devices (L-L, X-frame, C-block, Recurved) are analysed (originating from rotorcraft research). Furthermore, aerodynamic rotor control concepts are summarised (full-span and part-span pitch control, blade twist control, MEM tabs, camber control, aileron control-flaps). Aerodynamic control with trailing edge flaps or MEM tabs are considered the most feasible concept (high frequency capabilities, good structural and safety features).

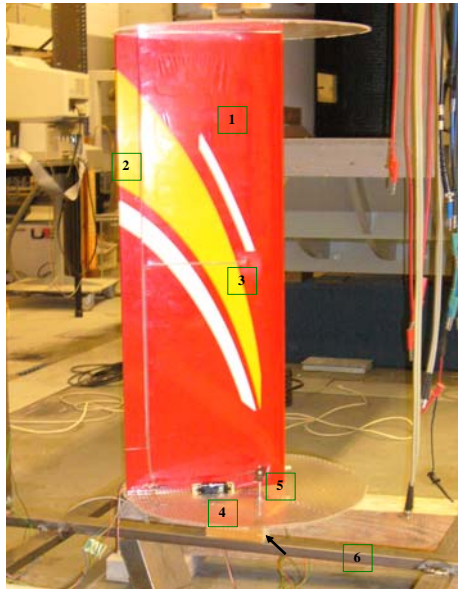
The third report [16] summarizes theoretical and software tools, which are necessary for the design of a smart rotor. Also hardware for testing of a smart rotor is mentioned. It is assumed that existing quasi-steady BEM models are not enough for smart rotor applications, vortex methods may be more reliable and unsteady aerodynamics are very important for the simulation of the fluctuating inflow and loads. It is also stated that new reliable dynamic models for smart materials and control algorithms must be incorporated. Regarding software tools, WOBBE is mentioned for stability calculations, and PHATAS/FOCUS, DAWIDUM and ADAMS for load calculations. For controller requirements, a PC with Matlab/dSPACE is necessary. Concerning hardware and testing mainly wind tunnel and laboratory requirements are discussed.

In a final report of the project, the sense and feasibility of a large-scale program on smart rotor research is discussed. With the target to reduce fatigue and peak loads the main possibilities suggested are: reduction of aerodynamic load fluctuations, active aerodynamic damping of structural modes and optimal control through cyclic blade root stiffness variation and passive rotor control. The first one is considered as more feasible due to existing knowledge.

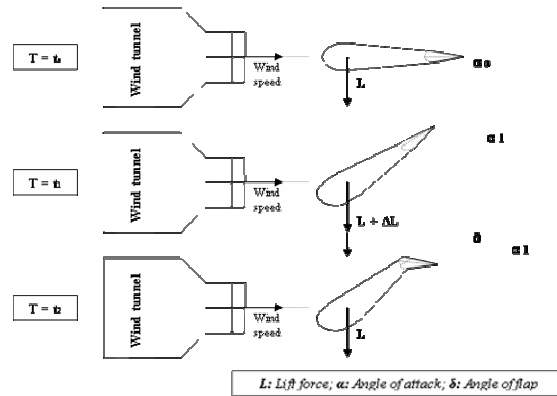
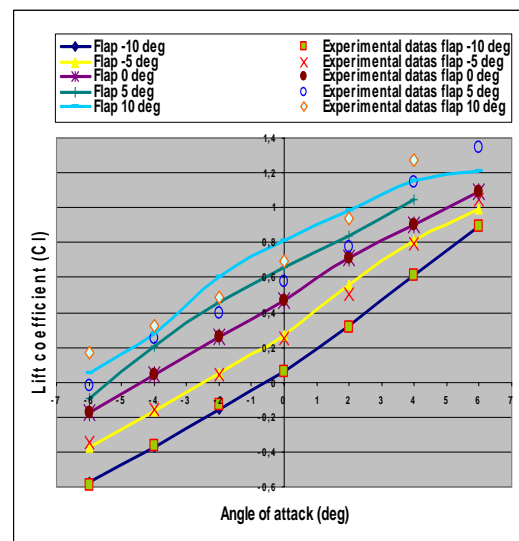
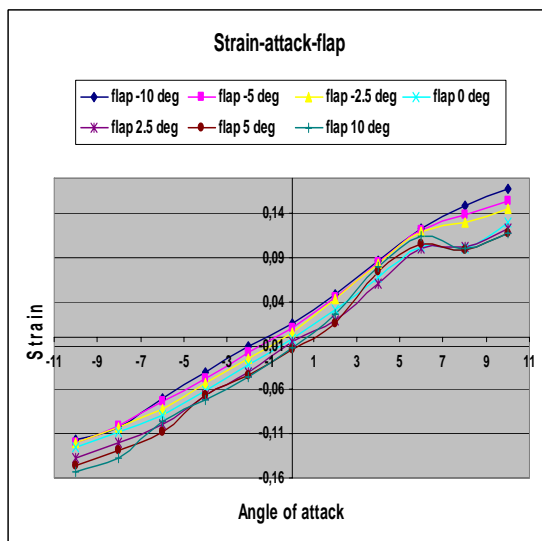
An interesting first approach to the application of active control on wind turbine blades was that of Aguirre at the TUDelft [34]. A blade section with a trailing edge flap was used for the wind tunnel experiment. Strain gauges were implemented for measuring the lift change on the blade, potentiometers for measuring the pitch angle and the flap angle and servomotors as actuators for changing the pitch angle and the flap angle. The experimental procedure was based on the idea of changing the pitch angle of the blade (so the angle of attack – in order to simulate disturbances in inflow experienced by wind turbine blades) and then, using a real time controller, activating the flap in order to reduce the changes in lift. Steady measurements were firstly performed for different angles of attack and flap. For designing the controller, no mathematical model was used, but system identification in order to determine the dynamics of the system. The system identification process uses the measured input and output signals of the system in order to determine the transfer function that describes the dynamics. Then, as the target of this experiment, the dynamic model of the process is implemented in a simple feedback controller (e.g. PID) and dSPACE / Matlab is used for real-time control. Unfortunately no model could be build because of the disturbances in the signals. The

disturbances came mainly from the vibrations on the blade, the lack of robust sensors (strain gauges not perfect for such applications), the lack of filters and the wind tunnel inflow. Generally, a mistake in this approach was the lack of proper dynamic design of the system before the experiment. The system for active control purposes should be designed in detail before wind tunnel experiments in order to be appropriate for control purposes. Also, better equipment should be used (accelerometers as sensors, not step actuators like servomotors and blade stiffness and eigenfrequencies appropriate for measuring). This experiment was a good simple approach to use active control on a blade and showed the challenges and requirements for such efforts.

Also, at DUWIND, during the research work concerning the project Smart Dynamic Rotor Control for Large Offshore Wind Turbines and the combination with UpWind's WP 1B3, ongoing research is in progress. Research focuses on aerodynamics, structural dynamics and control concerning smart rotor concepts. An aeroelastic model has been developed. Aerodynamics is based on BEM theory. It includes unsteady aerodynamics model of airfoil with TE flap based on the work of Leishman [83] and simple dynamics for the blade (flapping degree of freedom), tower (fore-aft degree of freedom) and shaft (torsional degree of freedom). Also, unsteady wind input (wind shear, tower shadow, turbulence) and a dynamic inflow model are included. Controllers for pitch and flap actions are designed and implemented. The package is developed in Matlab Simulink environment and is called WIMSIM. The NM80 wind turbine is simulated for different flap configurations and controllers. Furthermore, preliminary structural models of smart materials are being developed. These include Shape Memory Alloy (SMA) stress, strain, temperature relation models and Piezoceramic (PZT) models for different piezoelectric bender configurations based on Classic Laminate Plate Theory. Various prototypes of piezo-based trailing edge flaps are under development and an experimental setup is being prepared. The experiment will test a blade section model with actively controlled trailing edge flaps and show results for load alleviation. The trailing edge flaps will be made of the piezoelectric bender prototypes mentioned and active control will be incorporated with a real-time digital controller in the Low Speed Wind Tunnel of TUDelft. The target is to actively control the aerodynamic surfaces-actuators in order to reduce different kind of prescribed and random unsteady aerodynamic forcing. All the research work carried out now by DUWIND is in progress and no official publications have been made yet.

Fig. 32: *Blade with sensors / actuators* [34]

1. Experimental blade
2. Flap of the blade
3. Strain gauges
4. Flap servomotor
5. Flap potentiometer
6. Pitch servomotor

Fig. 33: *Control strategy* [34]Fig. 34: *Static measurements* [34]

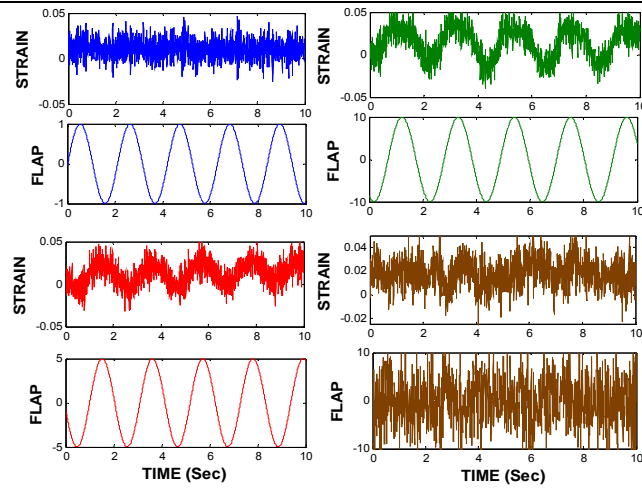


Fig. 35: Signals and disturbances for flap sine deflection – strain [34]

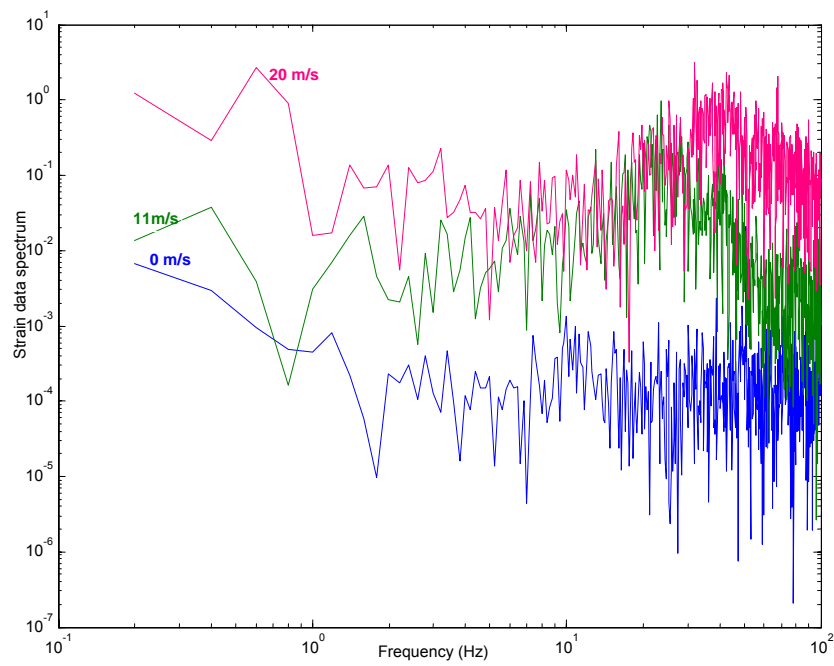


Fig. 36: Power spectrum of strains at 0, 11, 20 m/s [34]

2.2.3 ADAPWING (Risø)

A very important contribution to the research about smart rotor control for wind turbines is made by the wind energy research group of Risø, the National Laboratory in Denmark. Through the project Adapwing (Adaptive wing geometry for reduction of wind turbine loads), the possibilities of eliminating the fast fluctuating loads on wind turbines as a consequence of the turbulence in the wind and the tower shadow through the use of adaptive wing geometry regulation are being investigated. By cooperation between researchers and students from DTU many interesting reports have been presented. All cover computational studies on variable geometry airfoils using aero-servo-elastic models. Firstly, in the MSc thesis of Basualdo, a two-dimensional model is developed [17, 20]. The aerodynamics is described using Thin Airfoil Theory for attached, irrotational, incompressible flow and solved numerically using a Panel Method for steady and unsteady situations. The structural model consists of two degrees of freedom (edgewise, flapwise), expressed by spring and damper models. For control, a simple PD control algorithm is used, with a target control strategy to minimize the tip deflection variation of the blade. The results show the potential of such a control. The standard deviation of the airfoil displacements has been reduced to 25 % of the value corresponding to no control, during the 2 sec. simulations. In all the other simulations (e.g. 100 sec, gust) the decrease in the displacement amplitudes is evident. But, it must be pointed that the model consists of a simple control simulation, not taking into account any delays caused by aerodynamics, actuator performance or noise (Fig. 37-43).

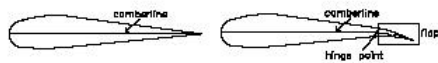


Fig. 37: Airfoil model [17]

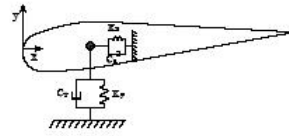


Fig. 38: Structural model [17]

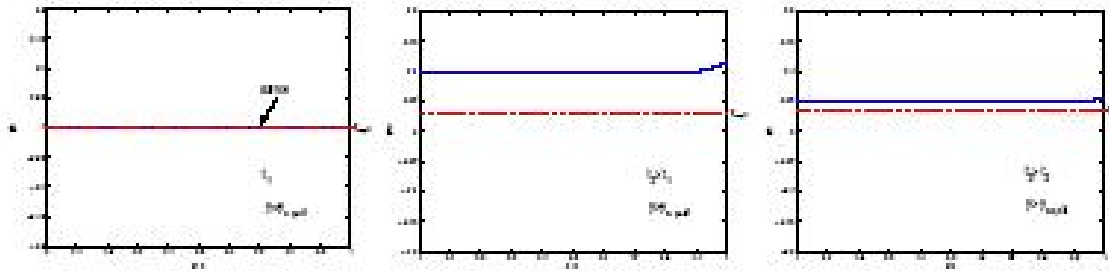


Fig. 39: Sequence of flap actuation response during increase in inflow [17]

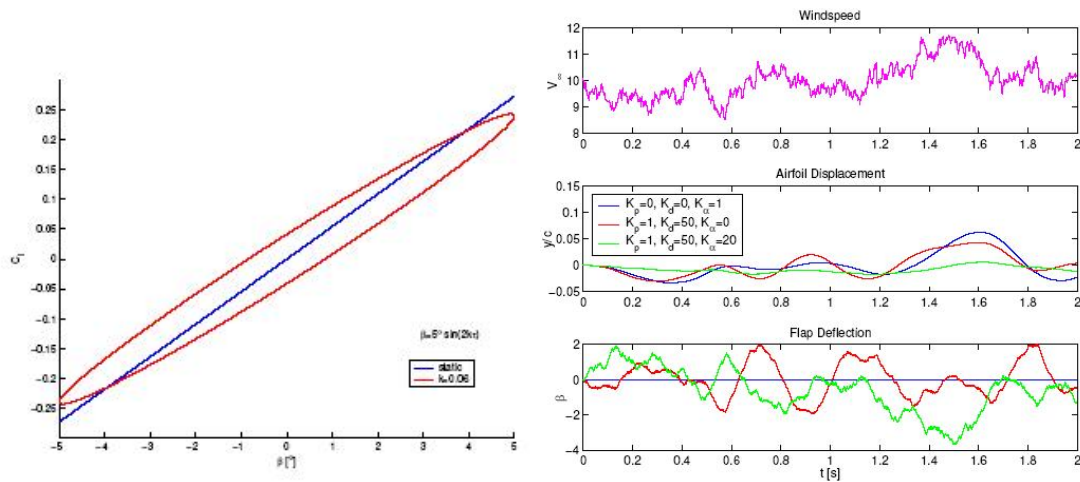


Fig. 40: Dynamic lift loop [17]

Fig. 41: Displacement and flap deflections as a function of time, for various control strategies [17]

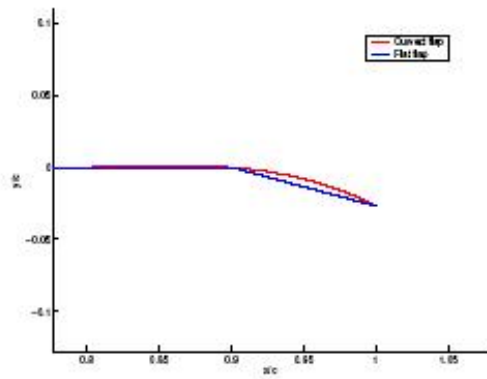


Fig. 42: Curved and flat flap configurations [17]

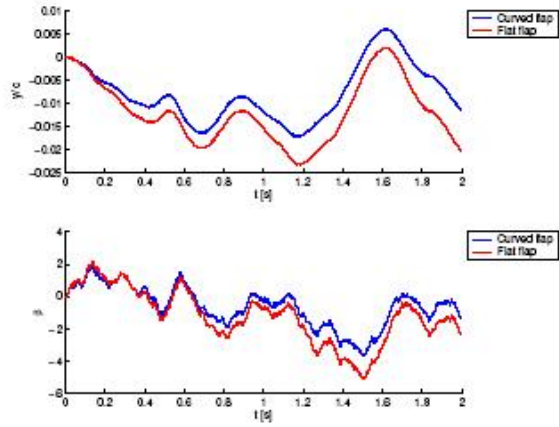


Fig. 43: Displacement and flap deflections for curved and flat flap [17]

In the work of Trolborg, as for his MSc thesis, a 2D computational study is being performed [18, 21]. The aerodynamic characteristics of the Risø-B1-18 airfoil equipped with different compliant trailing edge flaps are calculated. The solver used was Ellipsys2D (in-house RANS code) with a $k-\omega$ SST turbulence model for fully turbulent flow, at $Re=1.6$ million. The calculations on the baseline airfoil were compared with experimental data and showed perfect agreement. A comparison with the potential theory solver developed by Gaunna [26] (based on Theodorsen's theory) is also made. The influence of various key parameters such as flap shape, flap size, and oscillating frequencies was investigated so that an optimum design is suggested: A moderately curved flap with flap chord to airfoil curve ratio between 0,05 and 0,10. Finally a study was conducted on an oscillating airfoil fitted with an oscillating flap, with the objective to prescribe the motion of the flap so that the lift remained constant (Fig. 44-46).

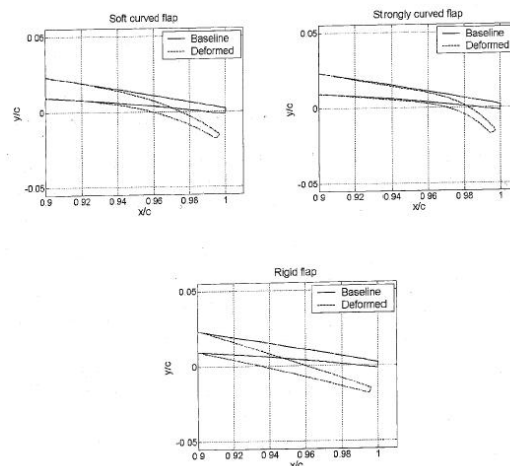


Fig. 44: Flap configurations and static results [18]

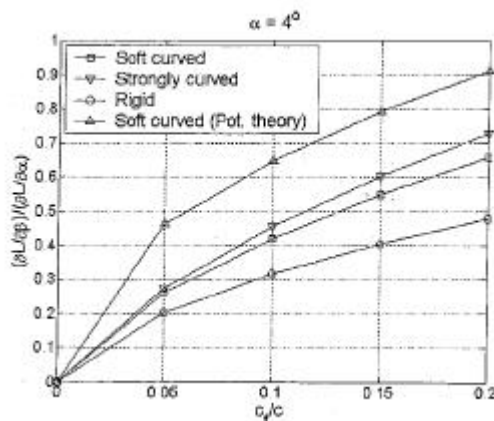


Fig. 45: Flap effectiveness [18]

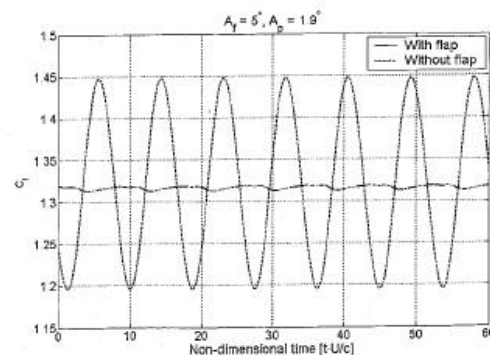


Fig. 46: Lift signal comparison of oscillating airfoil with and without flap [18]

In the work of Andersen, as for his MSc thesis, 2D and 3D aeroservoelastic models have been developed [19, 22, 23, 24]. 2D: The aerodynamic model is work of Gaunaa and consists of a 2D unsteady potential flow model for a variable geometry airfoil (small angles of attack/flap deflections, attached flow, no viscous effects). The structural model consists of three degrees of freedom (edgewise, flapwise, rotational), expressed by spring and damper models. The wind input model is a turbulence field given by the model of P. Veers. A PID and a LQR controller were modeled with different strategies (minimizing deflection either in x , y or θ direction). Regarding results, for a 60 second simulation, the variances in normal load have been reduced 75% and for the traverse load a reduction of 45% was obtained. 3D: The aerodynamic model includes a BEM model with various 3D corrections and a flap model which include effects of the wake history. Unsteady aerodynamics is described by the model of Gaunaa using the indicial response formulation. The structural blade model comprises a cantilever beam, with modal expansion of blade and camberline deformations. The wind input model is a 3D turbulence field given by the model of P. Veers (wind shear and tower effects are also included). A PID controller is implemented to control the flaps with different control strategies minimizing deflection either in x , y or θ direction). Effects of system time lag, flap power consumption and signal noise are also included. Optimal positioning and size of discrete and separated flaps is investigated. The model is created for a V66 blade from Vestas. The equivalent flapwise blade root moment is reduced 61% using 7 meter TE flaps with infinite power available for the flap actuators. TE flaps with 1% cross sectional blade mass gives a reduction of 60% when flap actuators consume 100W/m maximum. The potential drops to 41% when signal noise is added to the control.

All important results from the computational work in Adapwing have been included in a series of publications [20, 21, 22, 23, 24].

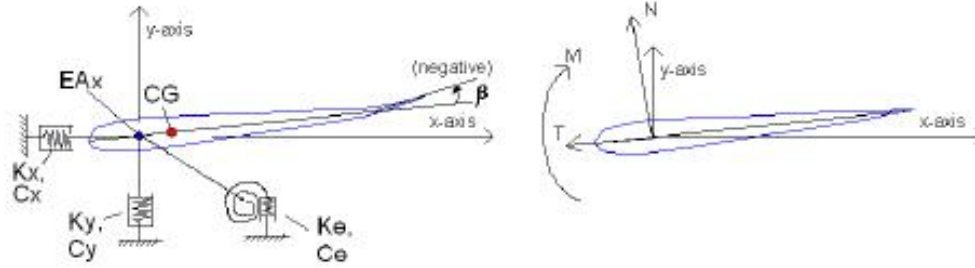


Fig. 47: Structural model

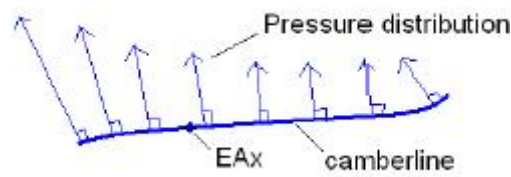


Fig. 48: Output of aerodynamic model [19]

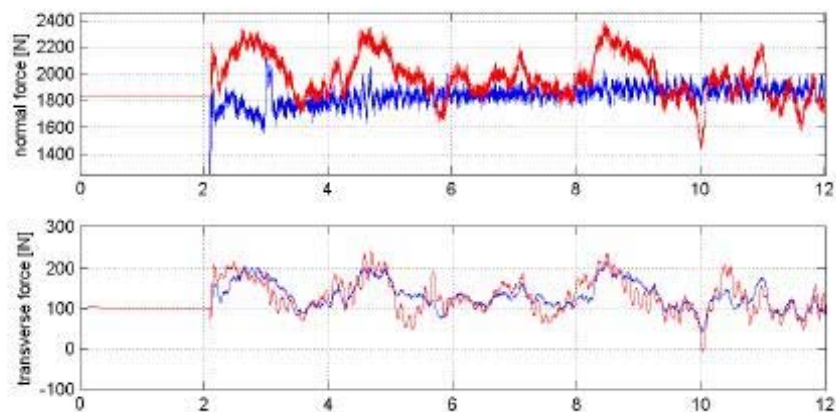
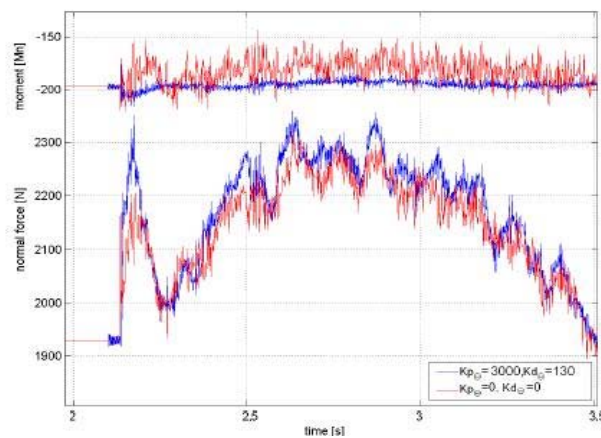


Fig. 49: Reduction in normal and traverse force using target x,y [19]

Fig. 50: Reduction in bending moment and normal force using target θ [19]

Through the project Adapwing, as have been mentioned previously, computational studies were performed in order to find general design directions for deformable controllable airfoil geometry. The choice, as can be seen through the computational studies, was deformable trailing edge flaps. An experimental setup for wind tunnel tests was prepared. The actuator/control surface chosen was a piezoceramic uniform bender actuator (Thunder TH-6R) (Fig. 51). So, no discrete servo or hinge flap was used but just a piezo-bender device which serves as both a flap and actuator. The flap had 10% chord length and could operate with deflection between -5 and +5 degrees. Firstly, the actuator performance was measured [25]. Through static and dynamic tests, the deflections of the bender were studied at various voltage inputs. An important result was that the actuator response showed a clear hysteresis loop. Optimal voltage operation regions were found (Fig. 52, 53). A blade section was constructed base on the Risø-B1-18 Airfoil. A number of Thunder actuators were glued to the trailing edge. Static and dynamic measurements were performed studying the pitch change and flap change and their behaviour together at different frequencies of operation (Fig. 54, 55). Not active controller was implemented. Unfortunately, there are no official publications available regarding this experiment yet.



Fig. 51: The Thunder TH-6R piezo actuator [25]

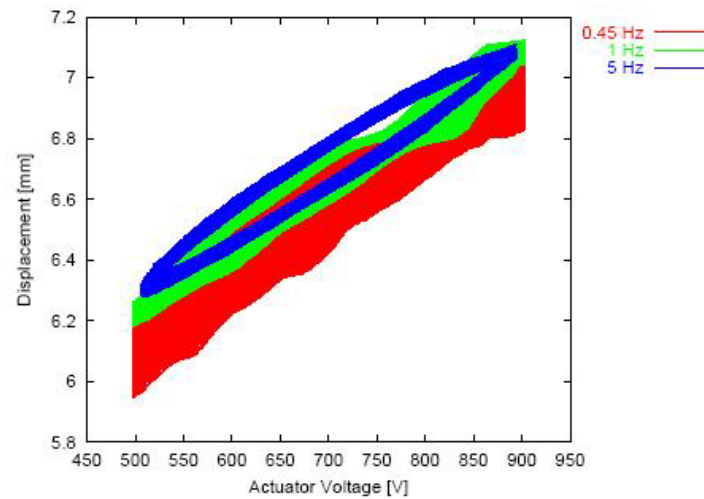


Fig. 52: Displacement of the actuator for different voltage / frequencies [25]

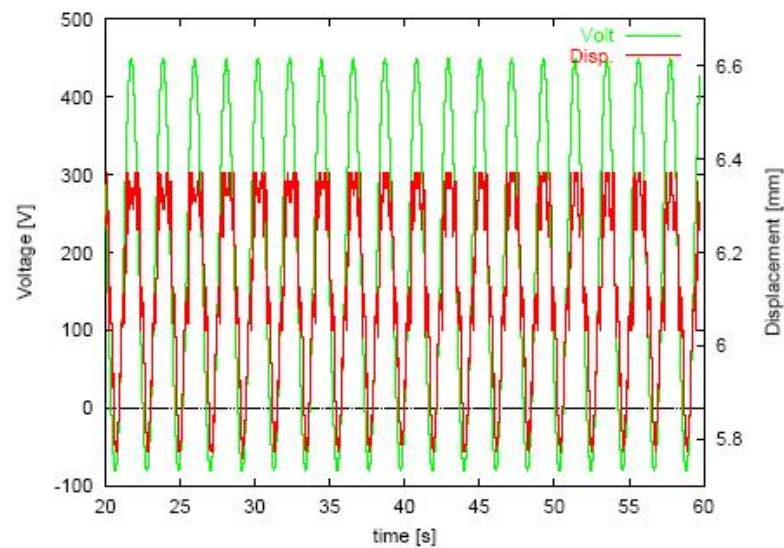


Fig. 53: Displacement / voltage of actuator in time [25]



Fig. 54: The wind tunnel test setup

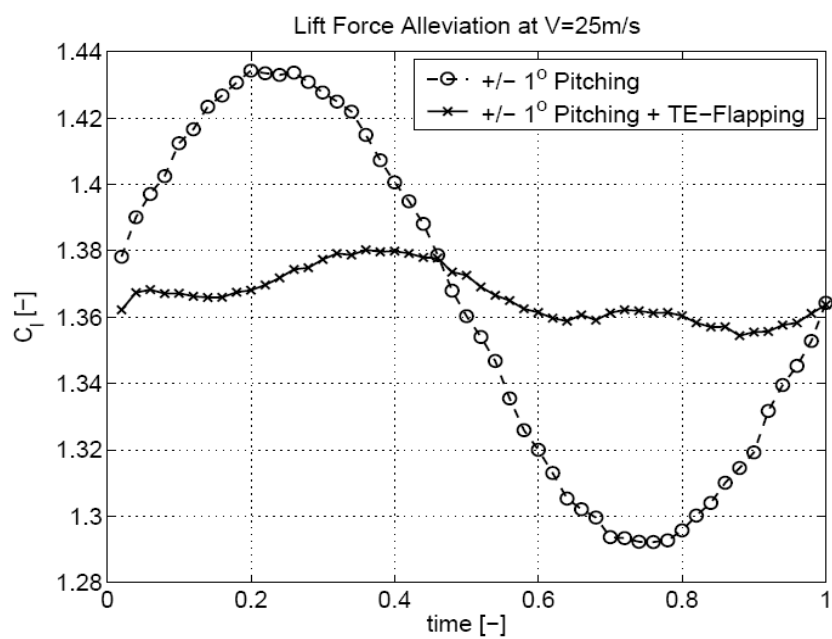


Fig. 55: Preliminary Experimental results

2.2.4 C. van Dam (Univ. California)

Following a different approach, van Dam [27, 28, 29, 30, 31, 32, 33] at the University of California, has focused on active load control for wind turbine blades using Micro Electrical Translational Tabs (MEM). In his work he summarises computational and experimental work, which proves the feasibility of such a concept for active load control. The Microtabs are mounted near the trailing edge of the rotor blades, deploy normal to the surface, and have maximum deployment height on the order of the boundary-layer height. The effect of these devices on the change in lift (due to camber change) is calculated. The effect of varying tab location, height and width is simulated using CFD. Results show an increase of 50% for C_l in the linear range of the lift curve. Also, data showed that a 1% of chord tab placed at 5% of chord from the trailing edge provided the best compromise for lift, drag and volume constraints in the trailing edge. Furthermore, 3D CFD simulations were conducted in order to investigate the effect of gaps or serrations in the tabs (because solid tabs suffer from vortex shedding). They show distinct relationships between tab-gap sizing and the resulting level of load control. The feasibility of the concept is generally shown and basic design formulations have been concluded through this computational work. C. van Dam proceeds with unsteady CFD simulations to investigate the behaviour of deploying microtabs [33]. Unsteady 2d compressible Navier-Stokes solver OVERFLOW 2 was used. Microtab heights on the order of 1% of chord, deployed on the order of one characteristic time unit were utilized. Also a deployed spoiler device on the upper side was investigated. The unsteady effects of tab deployment time, deployment height and freestream angle of attack on aerodynamic responses were investigated [Fig. 61-63]. Two external validation studies were performed for fixed microtabs and deployed spoiler. This study showed that there are no surprising deployment effects that make microtabs less attractive as active load control devices.

Van Dam in connection to numerical simulations has conducted series of experiments in order to show the design, fabrication and aerodynamic control performance of Micro Electrical Mechanical Tabs (MEMs). Although the term MEM refers also to the actuation procedure (electrical motor actuation – mechanical sliding movement), it is mainly used to describe the Gurney-flap like translational tabs. 2D experiments in the UC Davis Wind Tunnel were performed in order to calculate the aerodynamic performance of fixed and actively controlled MEM tabs. The experiments were conducted at $Re=1 \times 10^6$ for the two blade sections (fixed tabs and remotely controlled integrated tabs) for different locations and heights (for the fixed tab) and compared to CFD calculations. Results show good aerodynamic performance as it can be seen at the figures and the experimental setup promises a robust and reliable design for actively controlled aerodynamic purposes (detailed research in actuator options for translational tabs is not presented). Results show an increase of 50% for C_l in the linear range of the lift curve. Also, data showed that a 1% of chord tab placed at 5% of chord from the trailing edge provided the best compromise for lift, drag and volume constraints in the trailing edge. Some other conclusions are: Tab height is more important design factor than tab location, pressure side is more sensitive to tab configuration than suction side, effectiveness on the upper surface is reduced at high angles of attack.

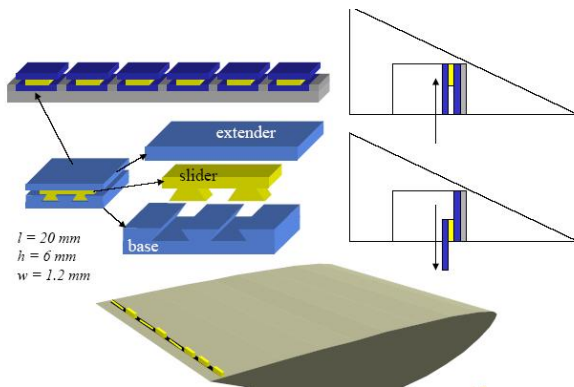


Fig. 56: MEM tab assembly and motion [28]

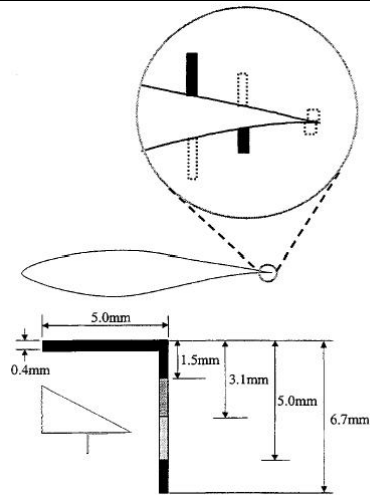


Fig. 57: Solid tab locations/ dimensions [28]



Fixed Solid Tab Model



Integrated Microtab Model

Fig. 58: Experimental blade section models with MEM tabs [31]

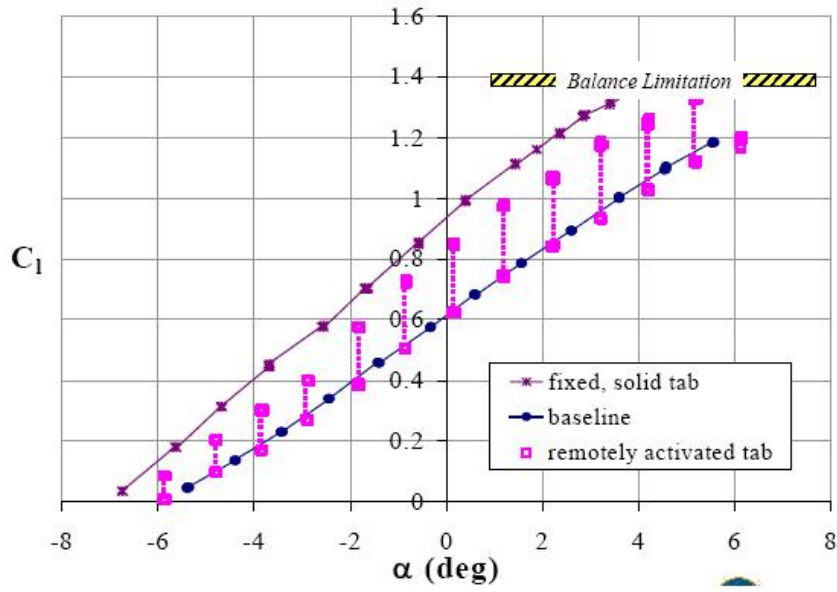
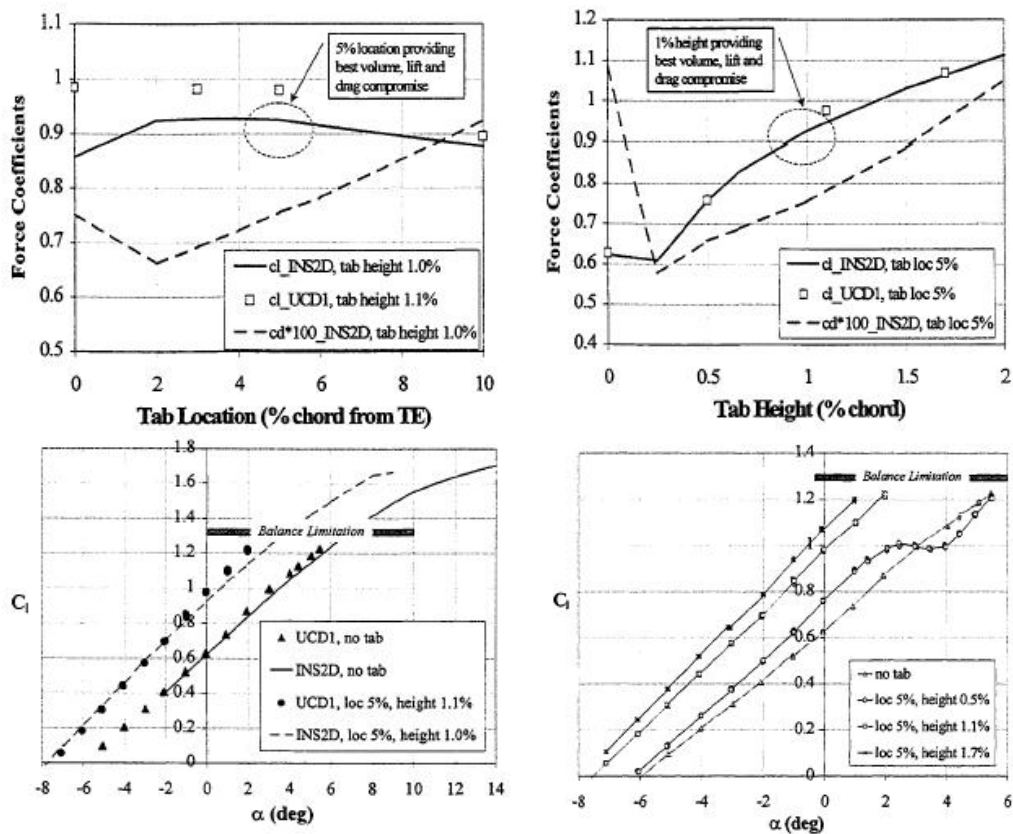


Fig. 59: Tab results (GU(25)-5(11)8, $Re=1.0 \times 10^6$, 1%c tabs, 5%c from TE) [31]



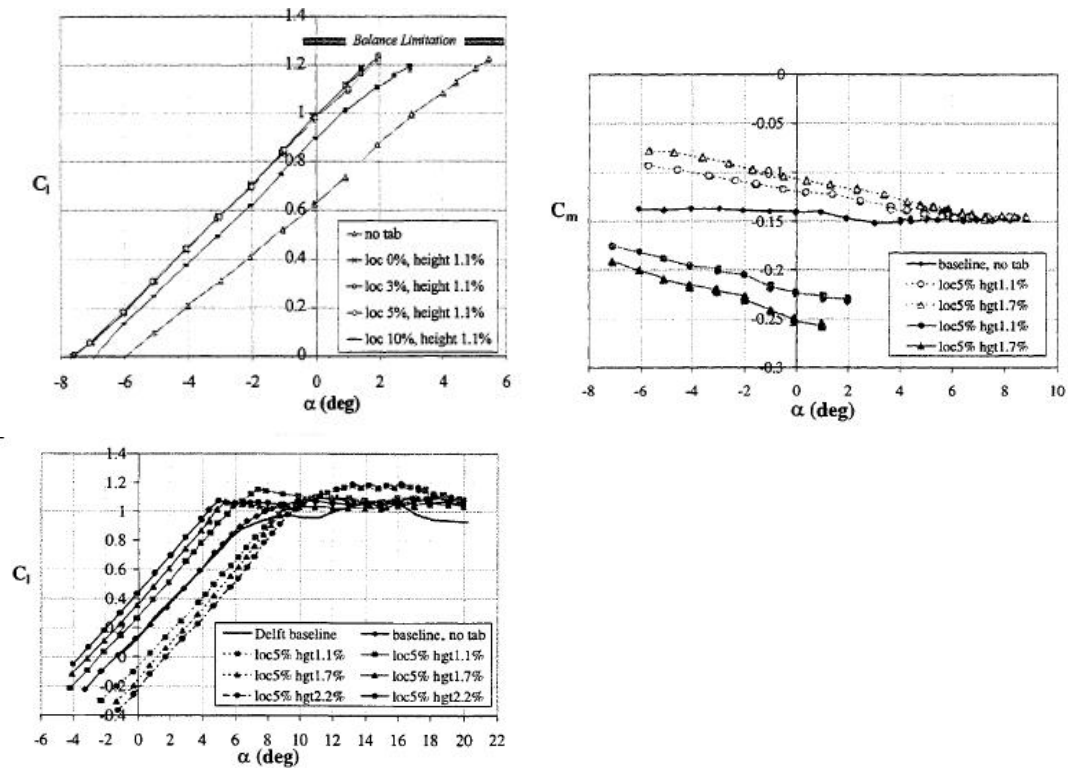


Fig. 60: Experimental results (and comparison to CFD) showing the effect of tabs dimensions and location on aerodynamic forces [28]

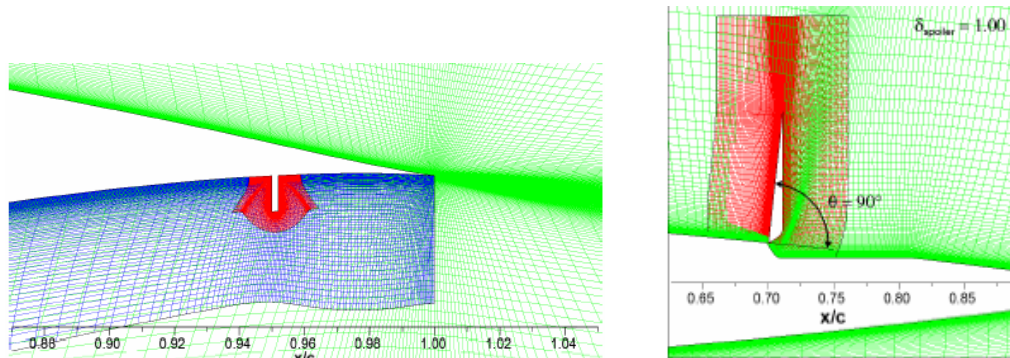


Fig. 61: Microtab and spoiler grids for unsteady CFD simulations [33]

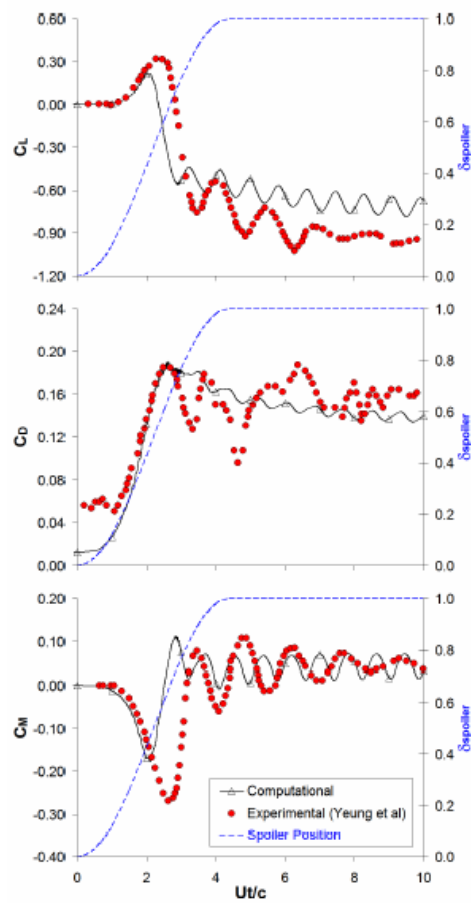


Fig. 62: Transient aerodynamic response for deployed tab (CFD-experiment) [33]

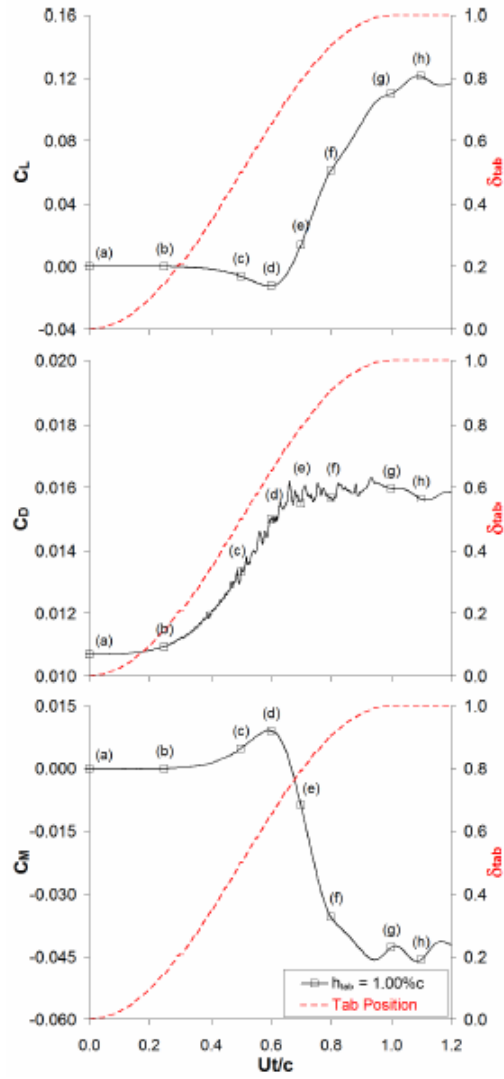


Fig. 63: Transient aerodynamic response for deployed spoiler

Chapter 3

3 Potential for UpWind

UpWind Work Package 1B3 focuses on the alleviation of blade loads by applying smart active (distributed) control. In order to prove the feasibility of this target and analyze its function, all available options and concepts regarding all the components of a smart rotor blade application must be compared, analyzed and quantified. This review about the potential use of available options comprises the first preliminary stage of the research regarding their feasibility and performance.

In this chapter, the potential application of smart structures on wind turbines for rotor control is analyzed. All available concepts for aerodynamic control surfaces are presented, different kinds of actuators, sensors and controllers are analyzed and modeling/available tools and design issues are discussed. This part comprises a first attempt for smart rotor concept comparison and it is mainly based on existing knowledge from review studies for wind turbines, smart materials and smart actuators [5, 6, 7, 8, 14, 15, 16, 101, 102, 103] and research from different fields summarized in the relevant references.

3.1 Control surfaces

This part focuses on different concepts of aerodynamic control surfaces proposed to be used for active control purposes. The concepts focus on the use of deformable shape of the airfoil or the manipulation of the boundary layer. The geometry of the devices, the function and quantification (if available) of their performance are analyzed. Also, references to design considerations as reliability, maintenance, structural feasibility and actuation options are made. Finally, passive control solutions are reviewed and some non-aerodynamic control device solutions are presented.

3.1.1 Full-span pitch control

Pitch control is the traditional concept used for most of the modern state-of-the-art wind turbines for power regulation and load reduction. Although (both full-span and part-span pitch) is not considered as a 'smart' control concept, it will be discussed first. Actuation systems (mainly electrical motors or hydraulic) are located at the hub and pitch the blades in order to change the angle of attack. Blades are traditionally pitched with only one control output and consequently all the blades have the same pitch angle (collective pitch control). Individual pitch control has been proposed for reduction of periodic loads (turbulence, tower shadow, wind shear), by pitching each blade individually. This concept can be extended to multiples of rotational frequency (2p, 3p), so to aim at the reduction of periodic loads which appear in such frequencies [37]. Traditional (collective) pitch control can easily be proven that is not capable of reducing fast fluctuating loads, which is the target of the smart rotor blade concept. Because of the requirement that the existing pitch actuators should pitch the blade in case of an emergency, these actuators are able to pitch the complete blade at a maximum rate of 6° per second. This is large enough to influence the 1P loads on a large wind turbine but will lead to excessive wear of the actuator when used for fatigue load reduction. From a structural point of view, the biggest issues with this design involve the torsional inertia and stiffness of the blade: to obtain pitch at higher frequencies, an enormous amount of mass will have to be moved. Moreover, the forces to move these masses will stress the wind turbine construction itself. Therefore, the construction will have to be stiffened and/or strengthened in the torsional direction. Concerning actuation options for full-span pitch control, electrical motors and hydraulic systems are used. A smart material actuator concept can be used to use full-span pitch control for smart rotor control purposes. This concept requires a torsion tube to be used parallel to the load carrying spar, which provides all-movable blade control. Torsion smart material tubes (torsion tube using piezo-electric fibers or pitch case actuator using SMA fibers) [3] theoretically/conceptually can produce fast enough changes in pitch. The disadvantage of such a concept is that large amount of smart material must be used, which increases

UPWIND

both the weight of the blade and the total cost. Moreover, extra mechanical parts must be placed on the blade, which decreases the reliability of the concept, and increases required maintenance and possibility for lightning strikes too.

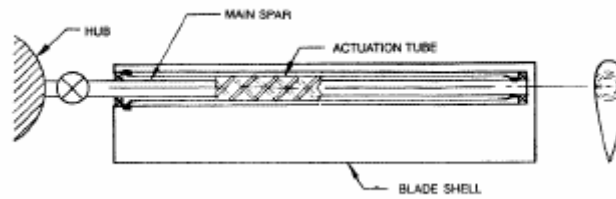


Fig. 64: Torsion tube for full-pitch actuation (using piezo-strips) [3]

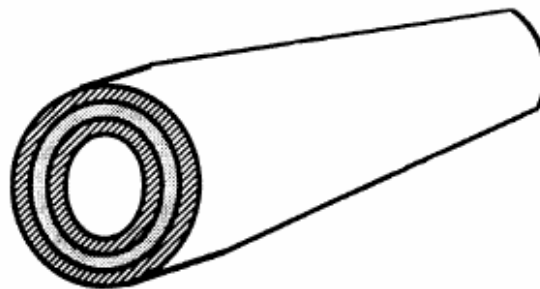
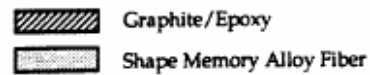


Fig. 65: Pitch case for full-pitch actuation (using SMA fibres) [3]

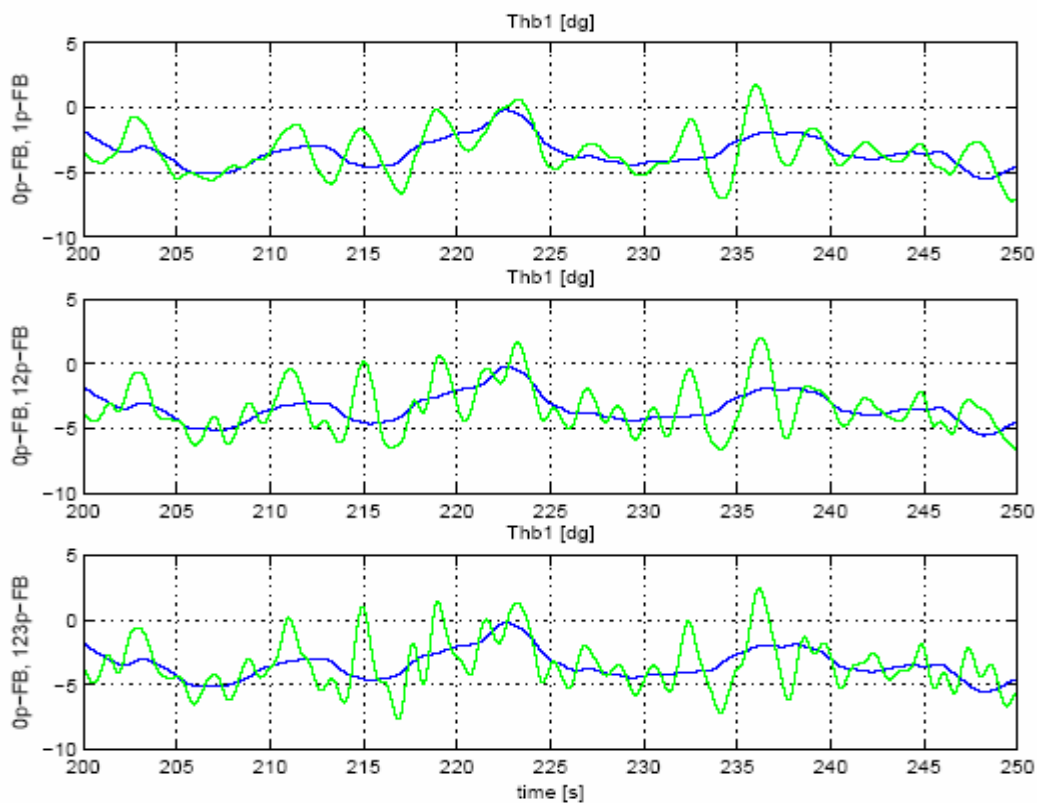


Fig. 66: Pitch angle requirements for 1, 2, 3 p pitch control (green: collective pitch control, blue: individual pitch control)

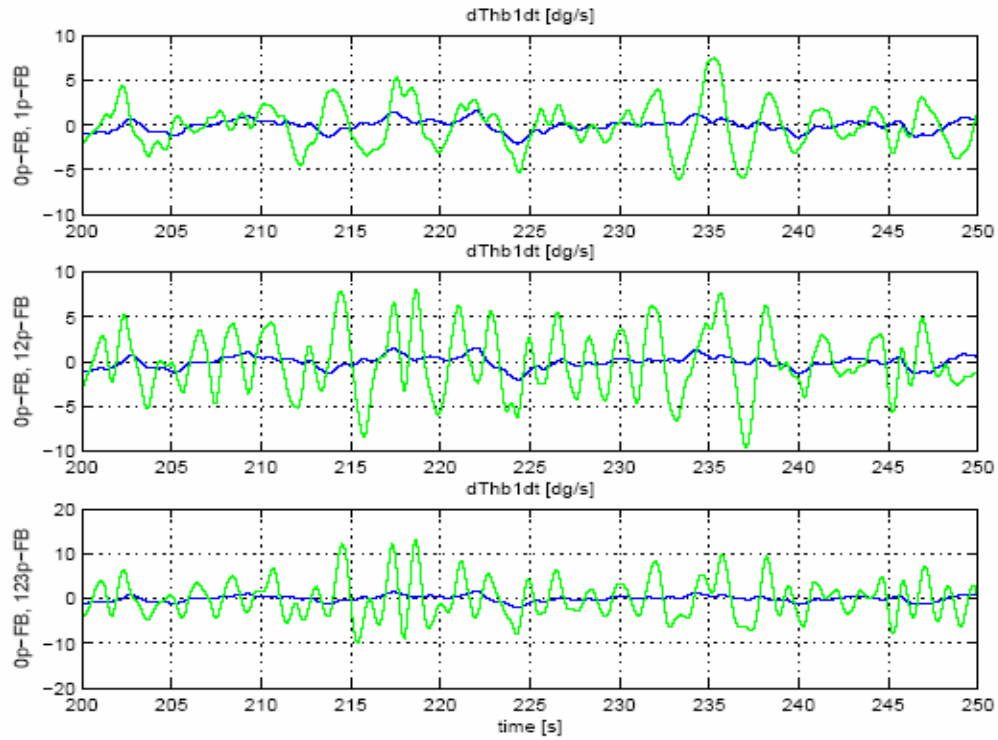


Fig. 67: Pitch speed requirements for 1, 2, 3 p pitch control (green: collective pitch control, blue: individual pitch control)

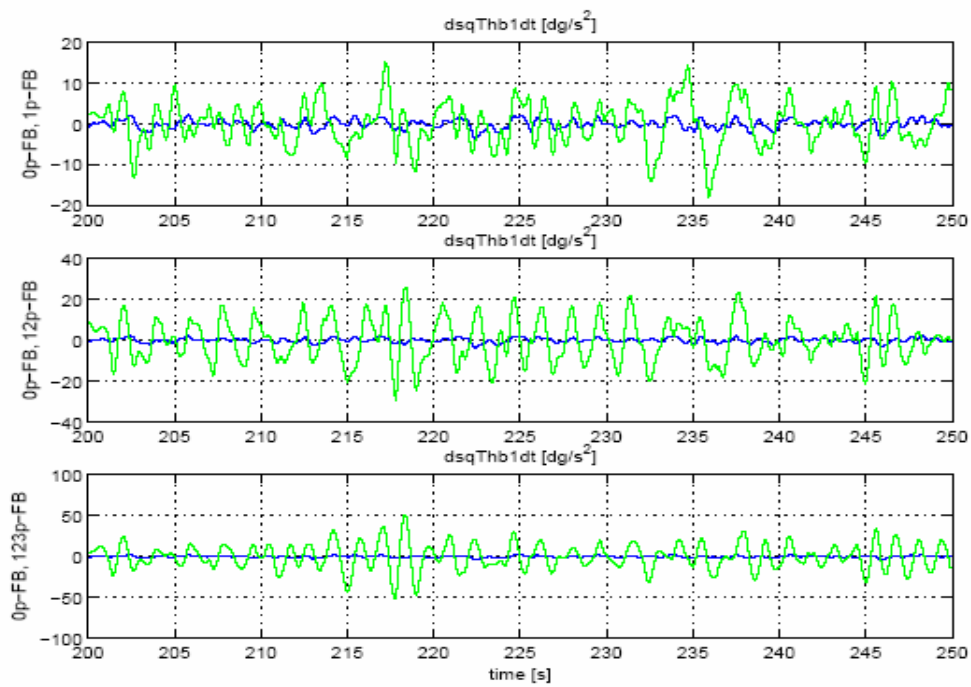


Fig. 68: Pitch acceleration requirements for 1, 2, 3 p pitch control (green: collective pitch control, blue: individual pitch control)

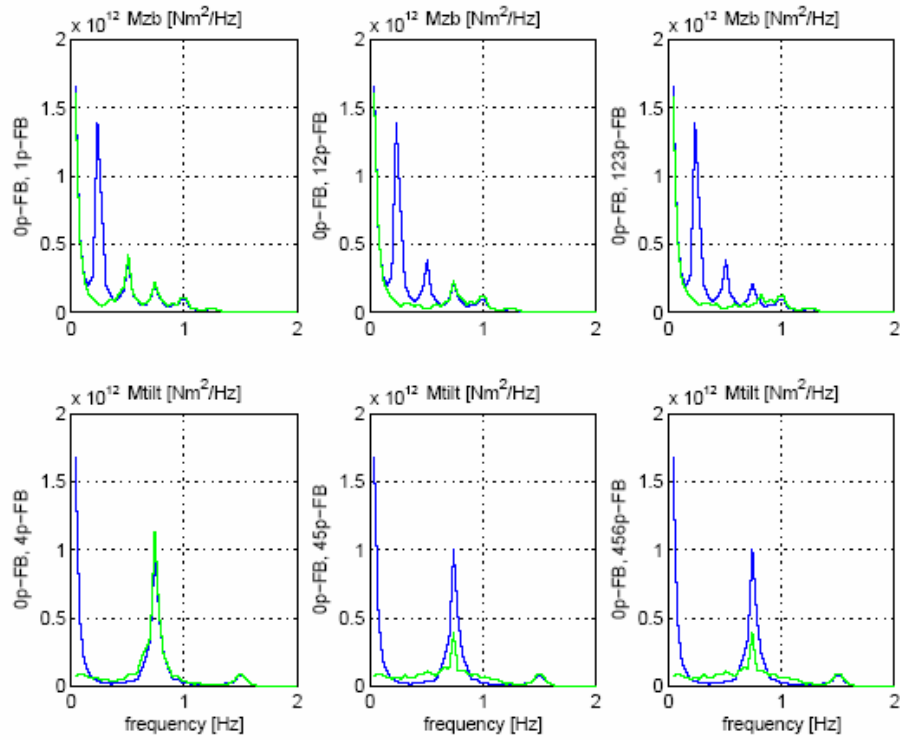


Fig. 69: Autopower spectra of flapwise blade root moment and tiltwise moment in rotor centre (green: collective pitch control, blue: individual pitch control)

(ECN simulations – [37])

3.1.2 Part-span pitch control

In case of a part-span pitch control system, only the tip section of the blade is pitched. Theoretically, this concept seems attractive as large pitch torques are avoided and rapid control can be achieved. In practice, there are important disadvantages: extra mechanical parts on the blade, more difficult maintenance, multiple parts in blades, longer control signal ways. Part-span pitch control has been used in the past as an aerodynamic brake control. Active control of fast fluctuating loads can theoretically be obtained using smart material concepts [3]. Bending torsion coupled piezo actuators in form of a tube can be used to pitch the blade tip. Of course all disadvantages of part-span pitch control make a smart active control version of it not very attractive.

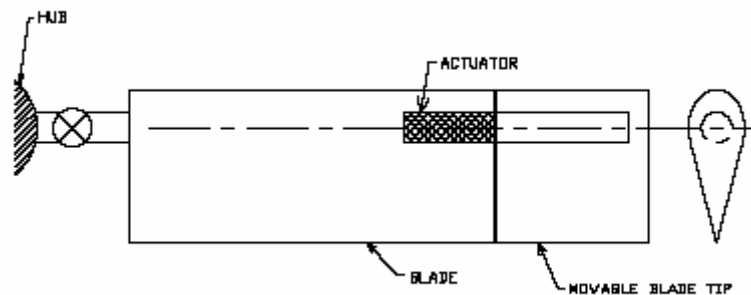
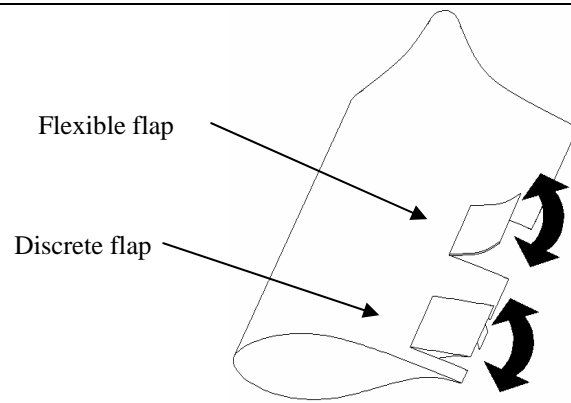
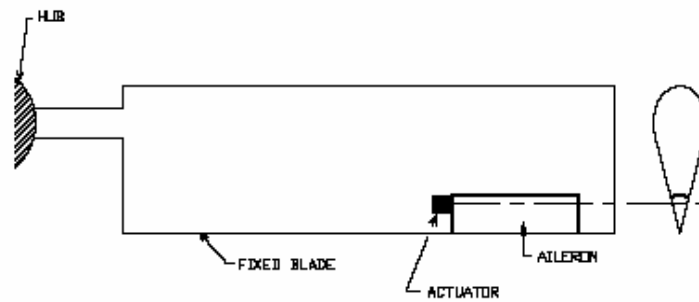
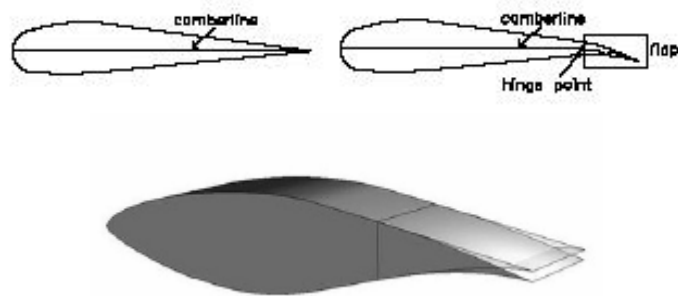


Fig. 70: Part-span pitch control using a smart material tube [3]

3.1.3 Trailing edge flaps

Inspired by existing technology in aircraft and rotorcraft applications, the general concept of a small movable control surface to directly control lift on a blade seems promising. By increasing (deployment on the pressure side) or decreasing (deployment on the suction side) the camber of the airfoil, trailing edge flaps generate substantial change in the lift coefficient of the airfoil (change in maximum lift, lift curve slope and zero-lift angle of attack). Such devices can achieve significant change in lift over a blade with using small surface deflections, have intrinsically better structural and safety features than single shaft mechanism that should operate a tip control surface and have substantial smaller power requirements than for full or part span pitch change control. Trailing edge flaps can be employed in two manners: either as discrete flaps or as continuous deformable trailing edge. Discrete flaps (ailerons - traditionally used in aircrafts) are mounted on the blade (hinged) and require a moment over the hinge to achieve the required position. These kinds of flaps (ailerons) are generally promising, but are not very attractive due to certain reasons: They don't comprise an integrated design solution, all the necessary mounting components are subject to wear and corrosion and the aerodynamic performance is reduced due to the kink (sharp change) in the camber. Also, in this concept the option of a servo-flap can be considered for moving the flap because of the high control forces involved. This concept is unattractive too, as it utilizes more complex mechanical surfaces. Continuous deformable trailing edge (the word flap does not probably apply to this situation – variable trailing edge geometry is more applicable) shows a smooth change in shape, which increases its effectiveness (flap effectiveness parameter and lift to drag ratio - [18]), is an interesting integrated solution for an aerodynamic control device and is composed of very simple and uniform parts. To be actuated, a bending moment must be exerted on the trailing edge. On the other hand, this kind of control has to work against the structural rigidity of the trailing edge (depending on the material) and its skin will probably be subject to severe fatigue. This concept is actually a combination of the idea of an aileron-flap and camber control based on skin deformation.

Considering actuation options for trailing edge flap control surfaces, various options have been proposed. Discrete flaps can be actuated in numerous ways using smart actuators, as it has been proposed for helicopters vibration control. The most common examples are: piezoelectric bender actuators, piezoelectric stack devices, torsion tubes and SMA wires. Smart material actuators, due to their high energy-to-weight ratio, have been used in helicopter research applications to actuate trailing edge flaps. Usually such devices are combined with various forms of mechanical amplification systems (e.g. push rods) in order to achieve large enough deflections. Overview of such solutions is presented in part 3.2. Helicopter rotor trailing-edge devices are subjected to higher aerodynamic loads (compared to their size), they have to operate at higher frequencies and they are subjected to significant centrifugal loads. Large forces have to be tackled in order to achieve required flap movements. Also, maintenance of helicopter parts is a given fact, so complex mechanical devices can be used on the blades. So, although wind turbine blades offer larger space for hosting big actuation devices, blades are most cost driven and requirement needs must be set to minimum, especially for offshore environment. On the other hand, the use of continuous, deformable trailing edge (flexible flaps), does not require the need for a separate actuator and mechanical parts, since the actuator is integrated in (or is part of) the trailing edge. Smart material layers (piezo patches or SMA wires) can be embedded in the material or smart actuators can be mounted on the inside of the airfoil (piezo benders) to pull on the skin. In both configurations, (partially) weak but tough skin sections are needed for easy deformation. In this case the fatigue and corrosion characteristics of the highly stressed (partially) weak skin sections will be determinant for the possibility to use this configuration within active rotor blades placed offshore.

Fig. 71: *Trailing edge flaps*Fig. 72: *Discrete flap* [3]Fig. 73: *Continuous deformable trailing edge* [17, 36]

3.1.4 Micro tabs

The use of microtabs for active control purposes is a rather new aerodynamic concept, derived from an earlier concept of Gurney flaps. Micro tabs are small (deployment height in the order of the boundary layer thickness) translational devices placed near the trailing edge of an airfoil. The deployment (perpendicular to the surface) of such tabs changes the Kutta point, so the effective camber of the airfoil, providing changes in lift. Lift enhancement is achieved by deploying the tab on the lower (pressure) side of the aerofoil, while lift mitigation is achieved by deploying the tab on the upper (suction) side of the aerofoil. For the deployment on the suction side, rotational movement of these tabs (spoiler-like) has been also proposed. These tabs are mainly mentioned as MEM tabs (Micro Electrical Mechanical tabs), as they are based on the concept of microjoinery (dovetail slider joints), actuated/controlled by small integrated electronic circuits. For large scale wind turbine applications, such devices will not probably be in the micro scale and will be actuated in a different way. Micro tabs have been proposed and investigated by van Dam [27, 28, 29, 30, 31, 32, 33]. Their effect on lift has been shown as powerful as conventional control surfaces such as flaps. The minute size of these devices allows for faster response times and, by the use of smart feedback control, can result in the overall reduction of system complexity, weight and cost. As actuation options, either an integrated electronic circuit or various forms of smart material actuators (piezo stacks, piezo benders, SMA wires) can be used. For the rotational (upper side) tab, a mechanical device (e.g. push rod) in combination with a piezo or SMA actuator can be used.

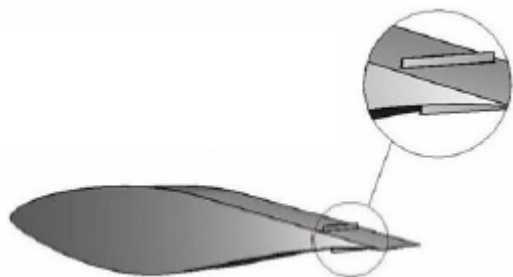


Fig. 74: Micro tab size, position [36]

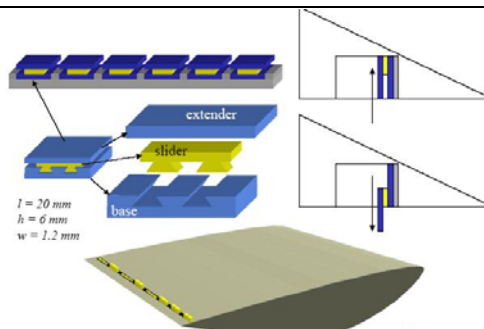


Fig. 75: Dovetail-based translational design [28]

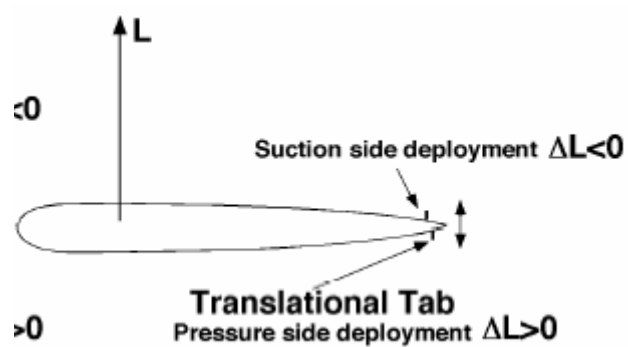


Fig. 76: Micro tab concept [28]

3.1.5 Active twist

The active twist concept focuses on twisting the whole blade (or an outboard part) over its complete span. The twist change results in change in angle of attack (so in lift). The change in pitch is largest at the tip, which is effective for aerodynamic control. Moreover, the change in angle of attack is proportional with the rotational speed, so the change more or less suits the velocity field at each station. The concept is based on the actively controlled tension-torsion coupling. For this, an actuator is integrated within the blade that is made of anisotropic fiber composite material. Research in this concept for helicopter applications, has shown good results in providing aerodynamic control, but still many disadvantages are evident, especially for the large scale application for wind turbine blades. First of all the response times for such a control concept will not be fast enough for active control purposes. Also, the strains and control forces needed to twist the whole blade are estimated to be very high [8]. For actuation purposes, smart materials are attached under the skin in fiber form (piezo or SMA) or in the blade spar. In this way, small twist deflections can be achieved theoretically. This concept will require a torsional weak design of the blade, which may also be critical with respect to flutter. The largest problem with respect to the use of an active twist rotor would be the large scale integration of smart materials (piezo or SMA fiber composites) in the torsion box or complete rotor blade structure. Especially the use of piezo fiber composites would lead to a very heavy and expensive structure. Some results with active twist concepts have been summarized by Chopra [7].

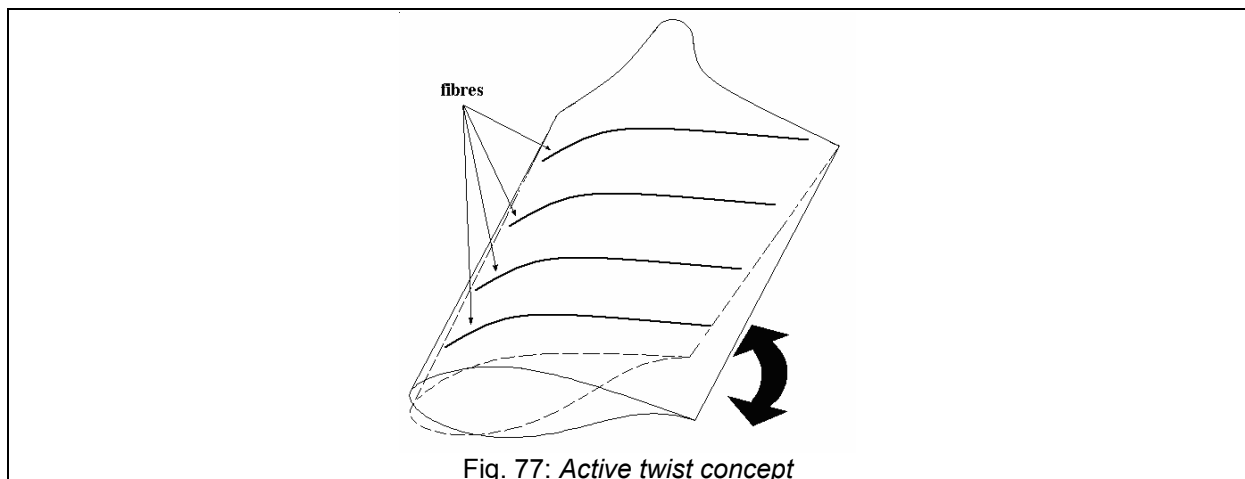


Fig. 77: Active twist concept

3.1.6 Variable camber

Camber control is an effective way of controlling the lift by directly changing the shape of the airfoil. This can be achieved generally by implementing smart materials inside the blade skin. Such actuation process will have to overcome all applied aerodynamic, dynamic and structural forces and deform the inner structure of the airfoil. A lot of concepts have been proposed to this purpose, ranging from accordion-like construction for the center part of the cord to bending the aft section (or just the trailing edge) or dropping the leading edge. The first one can be actuated by an internal framework comprising of SMA wiring or a framework which can be deformed by piezo stacks (or even deformable ribs). For the second type, concepts similar to the continuous deformable trailing-edge can be introduced, as mentioned above (integrated smart material layers or smart embedded actuators). The challenge is that this concept will require very large strains in the skin. Partially weaker skin sections will have to be used for camber control. This is feasibly probably only for small variable geometry surfaces (as mentioned in the trailing edge flap section), in order not to compromise the integrity of the blade structure. Overview of adaptive wings, mainly focusing on aircraft applications, is summarized in papers of Breitbach et al [40] and Stanewsky [39].

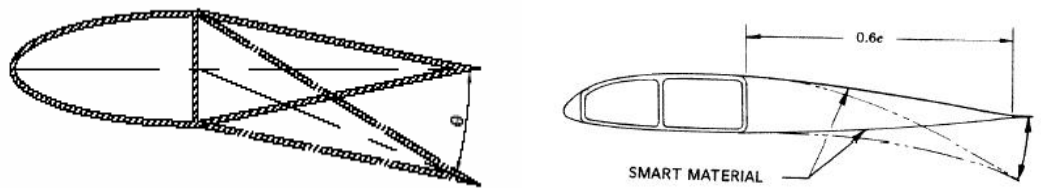


Fig. 78: Camber control concept [3]

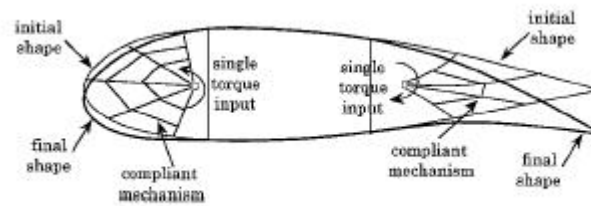


Fig. 79: Leading and trailing edge control by using compliant mechanisms

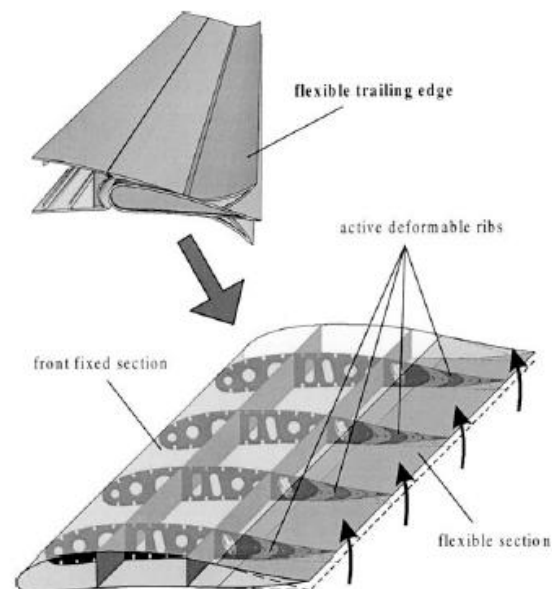


Fig. 80: Trailing edge control by using deformable ribs [40]

3.1.7 Inflatable structures

The concept of using inflatable structures in order to change the airfoil shape is a quite exotic one. The idea is to use flexible blade skin which can be deformed by using inflatable structures. Inflatable structures have been used successfully for aerospace applications [58]. Separate air chambers can be used in order to provide sufficient stiffness in the construction. Inflation and deflation of such chamber can be achieved probably by piston like arrangement or pressure vessel. This concept is still a preliminary idea and could possibly lead to very complex arrangements with extra weight on the blade, extra maintenance requirements and questionable reliability.

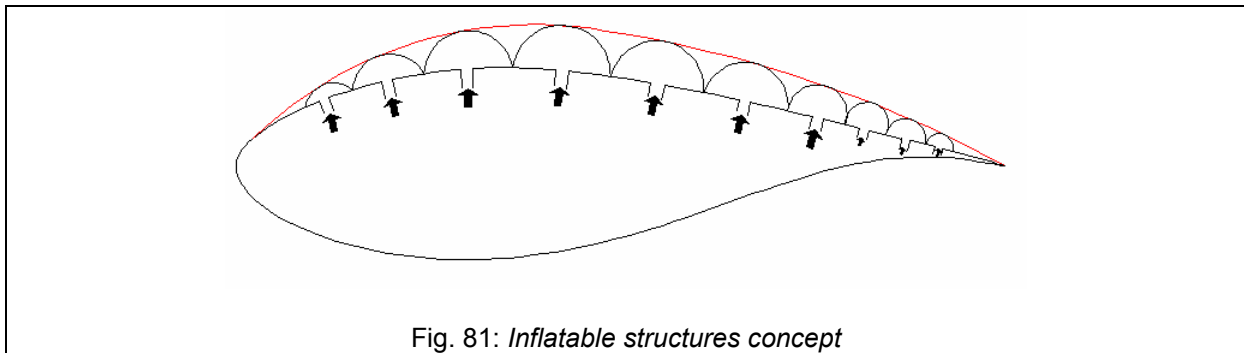


Fig. 81: *Inflatable structures concept*

3.1.8 Boundary layer suction

Boundary layer suction is used on wings to prevent laminar and turbulent separation, by removing flow of low momentum. This technique is also used in some wind tunnels to remove the boundary layer. The method consists in operating a powered system to suck boundary layer flow from closely spaced vertical slots. The technique can be so effective that in laboratory experiments it was observed fully laminar flow for very high Reynolds numbers and supersonic speeds. The corresponding drag levels are very low. The development of a boundary layer suction system is quite complicated, since it involves considerations on optimum slot placement, structural modifications, power system, amount of suction, etc. A successful research project was carried at TUDelft quantifying the concept of active boundary layer suction control. This concept's main interest is the prevention of flow separation and the reduction of drag, but by using actively controlled suction, the virtual shape of the airfoil can be changed, so control in lift can be achieved. Also a project is carried out at TUDelft also for developing perforated composite skin structures for integrated suction on blades. For actuation purposes actively controlled pumps must be used for suction control. This will probably make the concept more complex and increase power and maintenance requirements, but still there is not available research work in using boundary layer suction for active control purposes [104].

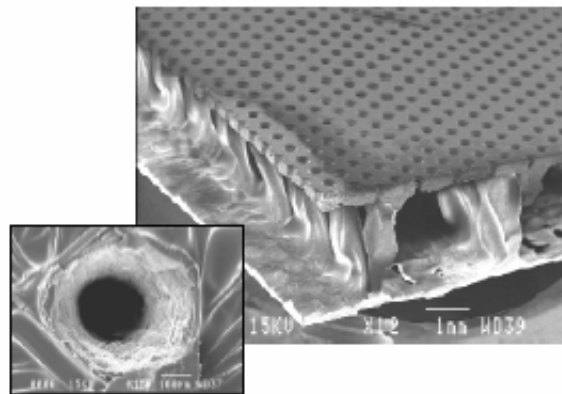


Fig. 82: *Perforated composite skin structure*

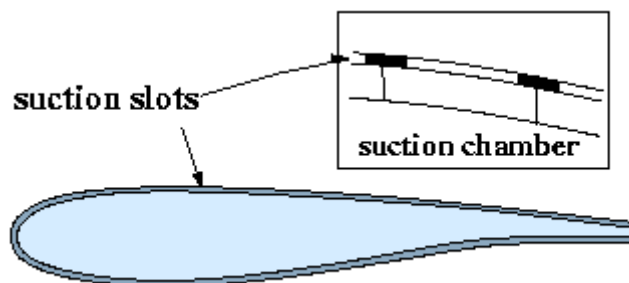


Fig. 83: *Boundary layer suction on airfoil*

3.1.9 Synthetic jets

Another concept of boundary layer manipulation is that of synthetic jets. Synthetic jets are zero-net mass flux jets created by employing an oscillatory surface within a cavity. The jet is formed by alternating momentary ejection and suction of fluid across an orifice and is entirely created from the fluid that is being controlled, so no fluid ducting is necessary. Net momentum addition and a change of direction are obtained, because low momentum flow is removed from the boundary layer during the suction phase and high momentum flow is blown out perpendicular to the surface.

It is shown that these jets can be used to modify the flow field on length scales that are one to two orders of magnitude larger than the characteristic jet length scale (Amitay & Glezer [35]). The commonly used actuators are piezoelectric diaphragms excited in a periodic manner, but other options like smart material actuators are also under consideration.

Synthetic jets can be applied on various ways for flow control. Traditionally synthetic jets are used as a boundary layer manipulation concept. Then, slotted jets are located close to the leading edge of the airfoil and used for separation control at moderate or large angles of attack, thereby altering the airfoil pressure distribution largely. Besides the location and the direction of the jet, two governing dimensionless parameters can be defined for the device. Firstly, the dimensionless frequency:

$$F^+ = \frac{f_e L}{U_\infty},$$

with f_e the actuation frequency, L the characteristic flow length scale (regularly the distance from the jet to the trailing edge) and U_∞ the free stream velocity. And secondly, the momentum coefficient:

$$C_\mu = \frac{\rho_j U_j^2 h}{\frac{1}{2} \rho_\infty U_\infty^2 L},$$

with h the slot width, j the jets properties and ∞ the free stream properties. The momentum coefficient typically lies in the range $10^{-4} < C_\mu < 10^{-2}$, where steady blowing or suction is not effective for lift coefficient changes.

For flow separation control an optimal reduced frequency of order unity is normally found (Greenblatt & Wygnanski [42]), so that the actuation frequency is about the same as the natural vortex shedding frequency. Actuation at this relatively low frequency leads to a coupling with the instabilities in the separating shear layer so that a Coanda-like deflection towards the surface is obtained (Amitay & Glezer [41]).

More recently, the benefit of actuation on a reduced frequency of at least one order of magnitude higher than unity has been shown. A broader effective range and more time-invariant circulation are obtained. Besides, no large scale vorticity concentrations and velocity fluctuations exist and the cross-stream thickness of the wake is smaller (Amitay & Glezer [41]).

Besides boundary layer -or separation- control, synthetic jets can also be used for camber control at lower angles of attack. Although this 'virtual aeroshaping' is a much more immature research area than separation control, high expectations exist.

Virtual shape control near the leading edge has been shown by Vadillo, e.a. ([44]). A small bump with a down-stream high-frequency synthetic jet showed drag reduction at constant lift. In this study, the small upstream flow obstruction was applied to reduce the actuation level.

Because the trailing edge is a more effective location for camber control this position might be used for effective lift changes. It is proposed to use synthetic jets analogous to the microtabs. The drag penalty is highly reduced for a continuous jet in comparison with a small Gurney flap (Traub, e.a [43]). Synthetic jets might be even more effective at a lower momentum coefficient and allow for a simpler construction, since no continuous pumping is needed.

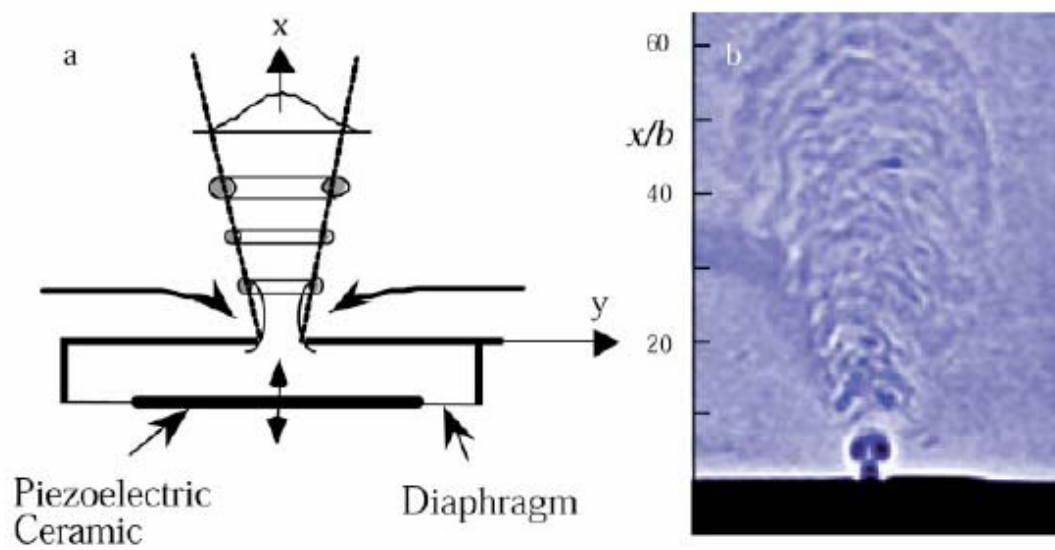
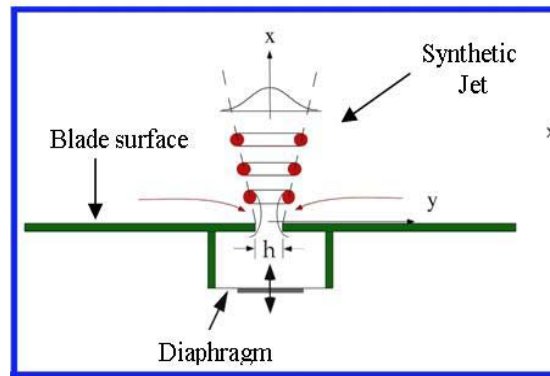


Fig. 84: Synthetic jet layout [35]

3.1.10 Passive control concepts

Passive approaches for aerodynamic control seem attractive due to their simplicity and economy. Mainly such methods make use of aeroelastic tailoring of the composite rotor blades or parts of it. Such structures are used to achieve aerodynamic performance benefits by controlled structural deformation.

An interesting concept is that of passively controlled blade tips. In this experimental concept, centrifugal and aerodynamic forces are used to adjust the pitch angle dynamically in response to rotor speed and wind speed. Some of these ideas have been proposed and investigated in the past (FLEXHAT, TenTorTube). Although passively controlled blade tips have been shown to give a smooth high quality power output, the main problems were the large extra mass, complexity, phase control delays in control for alleviating fluctuating loads and a high level of required maintenance resulting in high costs.

Self-twisting composite blades for passive pitch control have been proposed for speed control and load relief. Aeroelastic tailoring must be used for such concepts to achieve required tension-torsion coupling for self-twisting. Main advantages are the eliminating of moving parts and smooth deformation, but, higher blade mass and not accurate control in the desired operation regions, make such concepts not so favourable. Concepts of compliant blades have also been proposed. The blades can be designed, to automatically and passively feather the blades towards gusts, thus reducing the angle of attack.

Generally, the disadvantages of such passive control concepts lie in the complexity of the design, the fundamental changes in existing blade structural properties and the inability to perfectly control the devices and tune them to respond accurately to specific situations [14].

3.1.11 Non-aerodynamic control concepts

If the reduction of vibrations is the main drive, also damping materials or systems can be employed. This can be attained by implementing materials that are known for their high material damping coefficients, such as foams, but also SMA's and piezo layers. Constrained layer damping can be divided into an active and a passive variant. In case of the active variant an active layer (usually composed of piezo-electric material) exerts an opposing force against the vibrating load carrying structure in phase with the velocity of the structure. A disadvantage of this configuration is the brittleness of the active piezo-electric layer as well as the small tensile strength of piezo-electric materials. This would be very critical for the application within wind turbine rotors. The passive variant makes use of a relatively stiff plate glued against the load carrying structure. The visco-elastic layer is able to increase the damping of the structure in passive way. This passive variant is probably more effective in damping longitudinal vibrations than in damping transverse vibrations of the structure. In wind turbines it is especially in the transverse direction (flap-wise and edge-wise loads) that damping is needed in order to be effective. There are no known cases where these two variants have been applied for the damping of large scale structures [14].

3.2 Actuators

In this part, major smart material based actuation solutions are reviewed. Firstly, requirements concerning actuators for smart active control are summarized. Furthermore, traditional methods of actuation are discussed. Next, major smart materials, smart actuator concepts and existing methods are reviewed. Issues of actuation bandwidth, stroke, force and implementation in our active control objective are presented.

3.2.1 Actuator requirements

Actuators for wind turbine active control will have to be placed on the blades in order to actuate the various aerodynamic control surfaces for fluctuating load reduction. A set of basic actuator requirements for the specific purpose can be proposed:

- Lightweight
- Broadband response
- Large strains
- Minimum delays
- Minimum sensitivity to temperature
- Minimal effect on system dynamics (frequencies, mode shapes)
- Low maintenance requirements
- As low as possible power and voltage requirements
- Stiffness is important because of the disturbing nature of resonances within the actuator assembly.
- To greatly simplify the effective control, a linear behavior of the actuator is recommended.
- Fit within the limited envelope of the cross sections
- Reliable operation in harsh environment (rain, corrosion, humidity, salt, lightning)

The main categories of actuator types are embedded and discrete. These types will be analysed later. Requirements depend strongly on the specific type of actuator and the control surface concept. Concerning weight, the actuators should not increase scientifically the weight of the blades. Although weight requirements for wind turbines are less strict than in helicopter applications, there must be taken into account (especially if it affects the position of the blade centre of gravity (c.g.) with respect to the aerodynamic centre (a.c.) and the elastic axis. Concerning broadband response, depending on the control strategy, the actuator must be dynamically responsive at the frequency range of interest. The wind turbine size pursued in our investigation will affect the control frequency. For example: For a 4 to 5 MW wind turbine, rotating frequencies are in the order of 0.2-0.3 Hz. For individual blade control 3p frequencies (3 times the rotational frequency) must be affected (0.6-0.9 Hz). The actuator bandwidth must be higher than the control frequencies and margins must be added for time lags and delays. As a first estimate, an actuator bandwidth of 1.5-2 Hz seems reasonably enough.

The requirements for actuators are strongly dependent on the control strategy and the specific aerodynamic control concept. General directions of proposed types of actuators have been given in the previous section, specifically for each concept. General analysis of most suitable actuation methods and quantification of important parameters is considered necessary.

3.2.2 Conventional actuators

In this part, conventional solutions for actuation purposes are discussed. Hydraulic, pneumatic and electrical actuators are the most common types of actuators used in various engineering applications and in existing wind turbines for traditional control purposes (blade pitch control, yaw control).

For large loads and large strokes, hydraulic actuators are often used. Although, the necessary frequency ranges for pitch control and the required forces and strokes are no problem for these actuators, detailed requirements for using them for active smart control purposes must be studied. The

main disadvantages regarding hydraulic actuators are considered fluid leakage problems, regular maintenance, space needed for actuators and fluid containment and delays in actuation.

Pneumatic actuators provide weight reduction compared to other kinds of traditional actuators but have certain important drawbacks regarding their use in active smart control applications. These systems suffer usually from leakage problems, require regular maintenance, have reduced frequency range (air is more compressible) and exhibit certain instabilities.

Electro-mechanical actuators are used in most of the modern wind turbines for full-span pitch control. Maintenance requirements are lower compared to other actuation solutions. DC motors are commonly used because of their simplicity and easy-to-control capability. For large control surface actuation purposes (full-span pitch control) electrical motors are not able to achieve fast speeds for active control of fluctuating loads. For small on-the-blade control surface actuation purposes (e.g. flap control), electrical motors can be used, but will impose practical issues like weight, maintenance and power requirements.

3.2.3 Smart material actuators

The concept of smart rotor blade control imposes strict requirements for the installed equipment on the wind turbine blades, especially when considered a scenario for offshore wind turbines. Traditional actuators don't meet minimum requirements for such concepts. Furthermore, proposed concepts of aerodynamic control surfaces (distributed along the blade span) require fast actuation without complex mechanical systems and large energy to weight ratios. Promising solution for this purpose is the use of smart material actuator systems. Generally known types of smart materials are ferroelectric materials (piezoelectric, electrostrictive, magnetostrictive), variable rheology materials (electrorheological, magnetorheological) and shape memory alloys. Piezoelectric materials and shape memory alloys are generally the most famous smart materials used in actuators in various applications. The development of their technology has reached a quite high level and commercial solutions are available and widely used. Piezoelectric materials and shape memory alloys have widely been used in research regarding aircraft and helicopter applications. Some of the other types of smart materials (electrostrictive, electrostrictive) are promising, but still more research has to be carried out to allow this kind of solutions to become easily available for certain applications. Basic characteristics of piezoelectric materials and shape memory alloys, ongoing research and their possible application for actuation, will be analysed in this section.

Piezoelectric materials and actuators overview

Piezo actuators convert electrical energy to mechanical energy. This is why they are referred to as "motors" (often linear motors). For actuation purposes, two widely used piezoelectric materials are piezoceramics (mostly used: lead zirconate titanate –PZT) and piezopolymers (mostly used: polyvinylidene fluoride - PVDF). Also, single crystal PZN-x%PT and Langazsite are promising piezo materials (because of their low density high piezo strain coefficients) but have not been used for actuation purposes yet. PZTs are commonly used for actuation purposes as shape control applications, as they exhibit significant deformations, while PVDFs are used as sensors, since they have a significant weaker electromechanical coupling coefficient than PZTs. Piezoelectric materials exhibit nearly linear field-strain relations for small electric fields, which is of great interest when employing them in control systems. At higher electric fields these materials exhibit significant hysteresis and strain-based non-linearities. Moreover, they have low saturation strains (0.08%), moderate forces and fast response (100 Hz bandwidth) with low power requirements. Lightweight construction and flexibility as sensors and actuators in a large variety of applications makes these smart materials feasible for aerodynamic control in wind turbines, but specific combinations of actuator forms and control surface concepts must be studied for more detailed design of such ideas. Displacements and forces attainable with PZTs depend greatly on the method of actuator/structure integration. Common piezoelectric basic structures are sheets, uniform, bimorph, stacks, tubes and piezoelectric fibre composites. Single sheets can be energized to produce motion in the thickness, length, and width directions. They may be stretched or compressed to generate electrical output. Uniform actuators are bending actuators and consist of a piezo sheet and a substrate. Thin 2-layer elements (bimorphs) are the most versatile configuration of all. They may be used like single sheets (made up of 2 layers), they can be used to bend, or they can be used to extend. "Benders" achieve large deflections relative to other piezo transducers. "Extenders", being much stiffer, produce smaller deflections but higher forces. Multilayered piezo stacks can deliver and support high force loads with minimal compliance, but they deliver small motions. Piezoelectric fiber composite actuators consist of fibers of PZT, instead of layers, embedded in a polymer. These fibers make the actuator more flexible. An actuator tube is a composite tube with imbedded, attached or included piezoelectric materials. Other types of configurations using PZT are considered very feasible for actuation purposes, since they deliver large displacements (usually taking advantage a sort of recompression between their components). Most well known off-the-shelf solutions are the RAINBOW, the THUNDER and the LiPCA actuators. The RAINBOW actuator (Reduced And Internally Biased Oxide Wafer) is a dome-like circular actuator produced by chemically reducing one surface of a high lead containing piezoelectric or electrostrictive wafer with solid graphite in an oxidizing atmosphere at an elevated temperature. The THUNDER actuator (Thin Layer Uniform Ferroelectric Driver and Sensor) is a multi-layer uniform bender piezo actuator made of sandwich-like bonded layers of PZT, aluminium stainless steel using a polyamide adhesive. The bonding produces a pre-stress. The substrate (stainless steel) acts to keep the ceramic in compression and itself in tension. This internal stress gives the actuator the advantage of very large deflections and forces under load. THUNDER applications have been used in various applications, especially in shape control for adaptive structures. LiPCA device system is composed of

a piezoelectric ceramic wafer layer and fiber reinforced light composite layers, typically a PZT ceramic layer is sandwiched by a top fiber layer with low coefficient of thermal expansion (CTE) and base layers with high CTE. When compared to the bare piezoelectric ceramic (PZT), LIPCA has advantages such as high performance, durability and reliability. Such actuators are considered very promising and have been used for vibration control research, but are not yet commercially available. Also, other configurations have been used for helicopter applications, such as the DWARF actuator (a monolithic co-fired multilayer stack actuator) [9, 10].

All the previous innovative piezo-based actuation configurations are able to deliver large displacements which are generally needed for aerodynamic control concepts. But, the selection of actuator types for such application, depend strongly on the control surface design and function. General directions have been given in the previous analysis of the aerodynamic control surfaces. For the control of small discrete surfaces (flaps, microtabs) piezo electric actuators (benders or stacks) can be used for moving the surfaces. For specific design configurations the requirements for displacements and forces must be met. Most smart materials exhibit low strains and moderate forces for large scale applications. In order to make them applicable as discrete actuator devices, amplifiers should be used to increase the strain where force and strain capabilities of the material are interchanged. Several configurations have been proposed (especially in the helicopter literature). Usually, this kind of mechanical amplification systems use parts as rods, arms, frames etc to deliver amplified displacement or power to specific control devices from the actuators. Always a trade-off between force and displacement is taking place. Some interesting devices like these are the L-L, the X-frame the C-block and the Recurved mechanical actuators [Fig. 90]. The first two use piezo-stack devices and the last two bimorph bender actuators. Also, various concepts have been proposed and used for rotorcraft applications, utilizing simple rod concepts or other simple mechanisms. For wind turbine applications, the need for very high forces or displacements are not so strict compared to helicopter blades, since aerodynamic forces (per blade area) and centrifugal forces are smaller. The maintenance requirements also restrict the use of complex devices on the blades. But, if certain actuation properties are needed for specific discrete aerodynamic control surfaces, such concepts should be considered.

Research in piezoelectric materials and actuators

Physical principle

The actuation principle of piezo electric materials is that the material will strain under the application of an electric field. The principle also works in reverse: when a strain is applied, an electric field will be generated in the material. The piezo electric effect was actually observed first in this reverse manner. The word 'piezo electrics' has also been derived from this: 'piezein' ($\pi\epsilon\acute{\iota}\zeta\epsilon\iota\nu$) means 'squeeze' or 'press' in Greek.

The physical principle is as follows [105, 86]: For a material to show the piezo electric effect, the material must have an unsymmetrical lattice. This way, the material is electrically neutral, but will exhibit an electric dipole because the centre of all positive charged particle does not coincide with that of the negative ones. This for instance occurs in the piezo electric ceramic PZT as can be seen below: The central atom is out-of-centre which causes the electric dipole.

When viewing the material on a larger scale, it can be observed that adjacent lattices form area's in which the direction of the out-of-centre position of the centre atom is the same. These area's are called Weiss domains. However, when even stepping back one level further, it can be seen that all Weiss domains are orientated in arbitrary directions. This means that the material from a macroscopic point of view has no net dipole. This can be altered by applying a very high voltage. This operation is called 'poling'. It will cause domains that are in the direction of the applied voltage to grow at the expense of other, adjacent domains. When the voltage is removed, a net dipole remains. There are also piezo electric polymers which exhibit a dipole in there molecular build-up. The most well known is PVDF.

Functionality

After poling, when a positive electric field is applied in the poling direction, the material will elongate in that direction and contract perpendicular to that. Usually, piezo electric materials are produced in thin sheets with even thinner electrodes on both sides. This way, a relative small voltage applied over the thickness generates a high, evenly distributed electric field through the thickness. The constitutive behavior of a piezo electric material is usually described in the following way [87, 88, 7]:

$$\begin{Bmatrix} \varepsilon_1 \\ \varepsilon_2 \\ \varepsilon_3 \\ \gamma_{23} \\ \gamma_{31} \\ \gamma_{12} \end{Bmatrix} = \begin{bmatrix} S_{11} & S_{12} & S_{13} & 0 & 0 & 0 \\ S_{12} & S_{22} & S_{23} & 0 & 0 & 0 \\ S_{13} & S_{23} & S_{33} & 0 & 0 & 0 \\ 0 & 0 & 0 & S_{44} & 0 & 0 \\ 0 & 0 & 0 & 0 & S_{55} & 0 \\ 0 & 0 & 0 & 0 & 0 & S_{66} \end{bmatrix} \begin{Bmatrix} \sigma_1 \\ \sigma_2 \\ \sigma_3 \\ \tau_{23} \\ \tau_{31} \\ \tau_{12} \end{Bmatrix} + \begin{bmatrix} 0 & 0 & d_{13} \\ 0 & 0 & d_{31} \\ 0 & 0 & d_{33} \\ 0 & d_{15} & 0 \\ d_{15} & 0 & 0 \\ 0 & 0 & 0 \end{bmatrix} \begin{Bmatrix} E_1 \\ E_2 \\ E_3 \end{Bmatrix} + \begin{Bmatrix} \alpha_1 \\ \alpha_2 \\ \alpha_3 \\ 0 \\ 0 \\ 0 \end{Bmatrix} T$$

A few remarks will have to be made with this:

- The coefficients d_{33} and d_{31} are very, very small. The strain of piezo material is usually in the order of 10^{-4} or $\approx 0.1\%$.
- The coefficient d_{33} is usually bigger than d_{31} . This means that the strain caused by given voltage is higher in the thickness direction than in-plane. However, since we are talking about sheet material, the dimensions in the thickness direction are much smaller. Thus, the displacement through the thickness is almost negligible. In the next section some means of employing the d_{33} effect are described.
- It can be seen that the piezo electric effect is very similar to thermal expansion. This is very helpful in understanding and modeling the effect. However, the piezoelectric effect is much larger ($[d]\{E\} > \{\alpha\}\Delta T$).
- When embedding, attaching or assembling piezo material in any form in a construction, it can be seen that the amount of strain that can be attained, is very much dependent on the stiffness of the structures. This determines how much the structure "pushes back". The strain-force behavior of a piezo electric is characterized by two quantities: the free strain (Δ) and the blocking force. The first tells you how far the material will strain under a given voltage and the second one which force is required to keep the material from deforming. This also shows why PVDF is not very suited for actuation of rigid structures: because its intrinsic stiffness is very low, it is also not capable of exerting force on its environment. For this reason, and because it is light, PVDF is usually used for sensing applications.

Amplification

As mentioned before, there are some ways of amplifying the strain of a piece of piezo electric material. The most elegant way is to use the d_{33} effect. Two options have been developed until today. First of all, one can stack a series of disks or small patches on top of each other, each patch with its own electrode. This is called a 'piezo stack'. See Fig. 85. By applying the same voltage to each patch, a high field in the poling direction is attained. Moreover, because the dimension of the piezo material in its doping direction is increased, so is its displacement. However, the displacements are still very small; a typical stack of several centimeters can only attain about 100 μ m but large forces can be exerted this way.

Another way of implementing the d_{33} effect is to produce fibers and pole those fibers in their longitudinal direction. Then these fibers are embedded in a polymer and on the surface of this so called Active Fiber Composite [89] electrodes are applied. Because these electrodes are not far apart, again a high electrical field in the poling direction is applied. These plies can in turn be embedded into fiber reinforced polymers. See Fig. 85.

A special type of these active fiber composites are called MFC's [90] (Macro Fiber Composites), developed by NASA. MFC's are produced by sawing very fine strips from a patch and embedding those in epoxy between Kapton film (Fig. 92).

Another way to amplify the displacement of a piezo based actuator is to apply sheet material in a bender, either as an unimorph, with a patch on one side, or as a bimorph with a patch on each sides. This way, the small strain of the piezo patch can be used to obtain relatively large deflections of the bender. The behavior of such a bender is quite accurately described by extending the Classical Laminate Theory (CLT) with piezoelectric effects analogous to thermal expansion as explained before. But other models which incorporate out-of-plane shear have also been developed [7]. When applying piezo patches in laminates, one must be aware that a piezo patch strains in all in-plane directions when a field is applied. However, usually we want to bend or strain the construction in one direction. Barret [91] therefore introduced the Directionally Attached Piezoelectric (DAP) or Enhanced Directionally Attached Piezoelectric (EDAP). This basically comes down to using narrow strips or special adhesion strategies to exploit the expansion in only one direction.

There are also ways of increasing the deflection of these benders. This is done by introducing a geometrical non-linearity by axially compressing the bender [92] or using the thermal mismatch

between the components to introduce a buckled shape. This effectively reduces the intrinsic stiffness of the bender, allowing it to bend further. Although not properly researched yet, it can be assumed that the behavior under loading is also worse because its resistance against external loading is also lower.

To types of benders that make use of the thermal mismatch are called Thunders [93, 94] and LiPCA's [95, 96, 97]. The Thunder actuators consist of a piezo ceramic sheet that is laminated between a thin steel plate and an even thinner aluminum foil by means of an adhesive. This laminate is cured at about 300°C and when it cools, the difference in Coefficient of Thermal Expansion (CTE) causes a bend, and even slightly domed shape of the bender. LiPCA's, Lightweight Piezo Ceramic Actuators, are based on the same principle, but they are produced by laminating a piezo patch between glass-epoxy and carbon or epoxy plies. See the figure below (Fig. 93) for a build-up of both actuators. Another type called Rainbow Actuators work through the same principle.

Modeling the behavior of these benders is quite hard due to the non-linearities. Therefore in these cases, the Rayleigh-Ritz technique is implemented. With this technique, a certain shape for the parameterized displacement field is assumed. Secondly, the second order derivatives of these displacements are taken to calculate the strains. These are then, together with the constitutive equations (based on the CLT) substituted into the equation for the potential energy. Finally, the potential energy is differentiated to the unknown coefficients of the assumed displacement field and set equal to zero (minimum of potential energy). Thus we have n equations with n unknowns, where n is the number of terms describing the shape of the bender. This (possibly non-linear) system of equations can be solved and the precise shape is obtained. The non-linearities are introduced by using the second order derivatives of the displacement field for the strain.

Finally there are also mechanical ways of amplifying the displacement of a piezo based actuator. Usually in these a piezo stack is used to drive some sort of lever mechanism. An example of this is the double-L amplifier, displayed in Fig. 90.

Applications

In the above, it has been explained that piezo electrics are suitable for situation where high frequency, low displacement capabilities are wanted. In the case of piezo ceramics also high forces can be exerted. This means that up to now, piezo electrics are mainly used as (ultrasonic) transducers and actuators in mechatronics, e.g. in the manufacturing of electronic circuits or as stabilizers in digital photo cameras.

Additionally, a lot of research has been conducted into the embedding of piezo electrics in constructions for sound mitigation and shape control. Again, small strain and displacement, but high frequency applications are researched here. The shape control research in the field of aeronautics has been mostly aimed at morphing wings for Unmanned Autonomous Vehicles (UAV's) and helicopter blades [92, 98, 3]. An often presented solution is to embed strips under a 45° angle to a spar box or tube to twist the structure. This way the angle of attack of a wing or rotor can be controlled (see Fig. 94). An alternative for composite structures is to use an angled laminate and extending it with longitudinally embedded piezo electrics.

On the other hand, piezo electrics also have a sensor function, converting mechanical in electrical energy. In this role, they are used in scales, sonar equipment or as an alternative for strain gages.

Hysteresis and depoling

Up till now, the material has been described as a material which can be deformed to ones wishes by applying a voltage in the poling direction. However, there are some complications and limitations to this.

First of all, most piezo electrics exhibit some capacitance. This means that when a voltage is applied the material will be electrically charged, creating a opposing field. Thus, piezo electrics can not be used for very low frequency or static applications. Secondly, when loaded dynamically, piezo electric materials show significant hysteresis [87, 7]. This is believed to be caused by the deformation of non-aligned domains. And finally, there are also some conditions that will destroy the piezo electric effect of the material. These are:

- High temperatures. The temperature that will depole the piezo electric material is called the Curie temperature.
- High pressures. When piezo electrics are subjected to very high (compressive) pressures, the domains may flip 90°, reducing or destroying the piezo electric effect.
- High voltages. When a voltage is applied against the poling direction the same effect as with high pressures may be observed. The field at which this occurs is called the depolarization field [99]. A high field, opposing the poling the direction may cause both 90 and 180° switching of domains.

Piezo electric materials

Already two materials have been mentioned but here we will elaborate more on materials and their properties. The most implemented piezo electric materials are ceramics. Of this group of materials PZT is the most used. However, of PZT two variants exist: 5A and 5H [87, 101]. The second has a coupling coefficient which is about twice as high as that of 5A, resulting in twice as much strain for a given voltage and thickness. However, the Curie temperature and depolarization field are considerably lower. That is why 5A (lower coupling coefficient, but higher Curie temperature) is used in Thunder and LiPCA actuators because these have to be cured at higher temperatures. A big drawback of both variants of PZT is their brittleness.

Alternatives are the earlier mentioned PVDF [106], but as also mentioned before, due to this material's low intrinsic stiffness, it has limited actuator capabilities. Moreover, its coupling coefficient is also considerably lower. A final possible alternative is called Languisite [8]. This is a piezo electric crystal that is grown under very high pressure. The crystal has a lower coupling coefficient than PZT, but a very high Curie temperature and depolarization field. Thus, when high voltages are applied, similar performances can be attained. It is also much less brittle and lighter than PZT. However, the crystal is very limitedly available and thus even more expensive than PZT. Below a table with the properties of the different piezo electric materials can be found.

However, Languisite is not one specific material, but rather a family of materials. Furthermore, the d-matrix of Languisite is also different. The properties of the Languisite family are therefore presented in a different table. For comparison, the properties of PZT-5A are also displayed in. Unfortunately, no data on the coercive field was available.

		PZT 5A	PZT 5H	PVDF
Piezo-electric Coefficient [pm/V]	d_{31}	-190	-320	14/2
	d_{33}	390	650	-34
Curie Temperature [°C]	T_{Curie}	350	230	90
Depoling Field [MV/m]	E_{depole}	0.7	0.55	150
Young's Modulus [GPa]	E_3	52	50	0.9
	E_1	66	62	2.5/2.1

Properties of PZT and PVDF

Note: Since PVDF has a different physical make-up than the others, the values are also different in background. For instance, the maximal voltage is not related to "classical" depolarization. Moreover, since the material shows in-plane anisotropy, two in-plane values are mentioned.

		LGS	LGT	LGN	PZT-5A
Independent piezo electric coefficient [pm/V]	d_{11}	6.15	7.06	7.41	-190 (d_{31})
	d_{14}	-6.01	-4.32	-6.16	390 (d_{33})
Curie Temperature [°C]	T_{Curie}	1470			350
Young's Moudulus [GPa]	E_3	192	191	193	52
	E_1	112	109	110	66

Piezoelectric and mechanical properties of Languisite crystals

The structure of the d-matrix is as follows:

$$\begin{bmatrix} 0 & 0 & d_{11} \\ 0 & 0 & d_{12} \\ 0 & 0 & 0 \\ 0 & 0 & d_{14} \\ 0 & d_{25} & 0 \\ 0 & d_{26} & 0 \end{bmatrix}$$

Bohm [100] reports that due to the symmetry of the crystal, only two parameters, which are displayed in the previous table are independent. The relation to the others is as follows:

$$d_{12} = -d_{11}$$

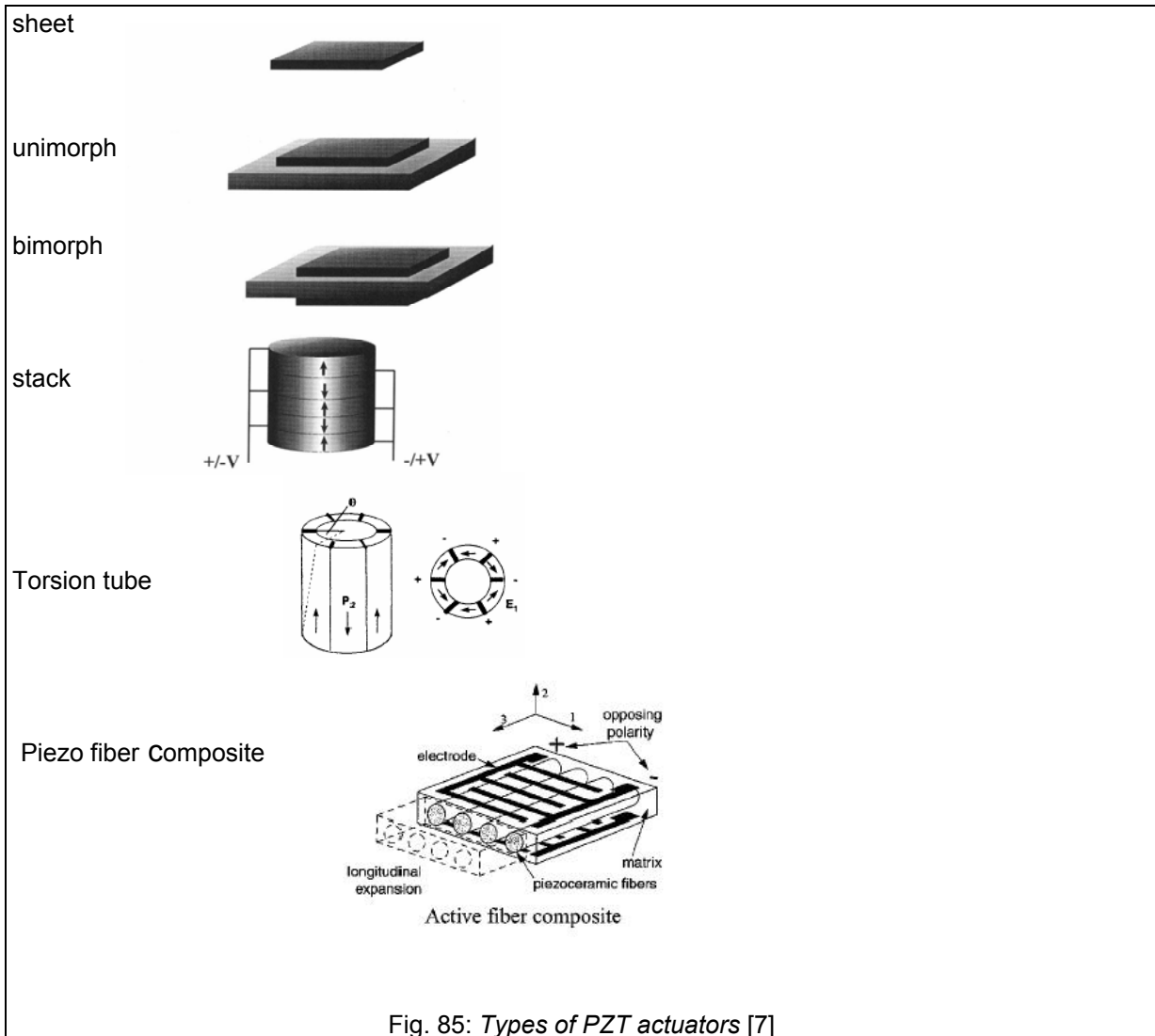
$$d_{25} = -d_{14}$$

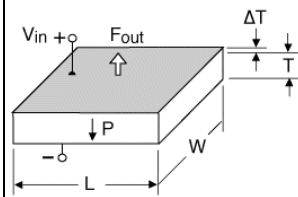
$$d_{26} = 2d_{11}$$

Additionally, the compliance matrix is also displayed:

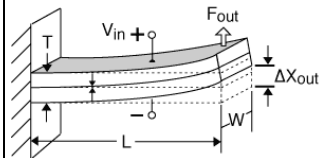
$$\begin{bmatrix} S_{11} & S_{12} & S_{13} & S_{14} & 0 & 0 \\ S_{12} & S_{22} & S_{23} & -S_{14} & 0 & 0 \\ S_{13} & S_{23} & S_{33} & 0 & 0 & 0 \\ S_{14} & -S_{14} & 0 & S_{44} & 0 & 0 \\ 0 & 0 & 0 & 0 & S_{44} & S_{14} \\ 0 & 0 & 0 & 0 & S_{14} & 2(S_{11} - S_{12}) \end{bmatrix}$$

Finally, its composition is described. The Langasite (LGS) crystal is a Lanthane-Gallium-Silicium-Oxide crystal, with the scientific notation: $\text{La}_3\text{Ga}_5\text{SiO}_{14}$. With LGT, also called Langatite, the Silicium is replaced by Tantale ($\text{La}_3\text{Ga}_{5.5}\text{Ta}_{0.5}\text{O}_{14}$) and with LGN by Niobium: $\text{La}_3\text{Ga}_{5.5}\text{Nb}_{0.5}\text{O}_{14}$.

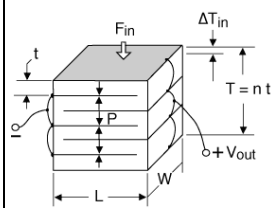




sheet layout and function



bimorph layout and function



stack layout and function

Fig. 86: Extensive and bending function of PZT actuators [101]

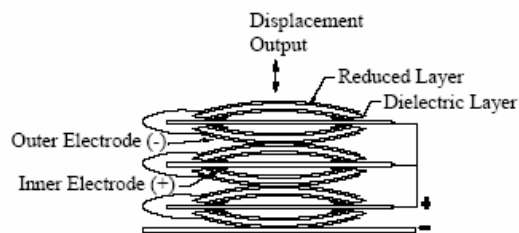


Fig. 87: The RAINBOW actuator in stack

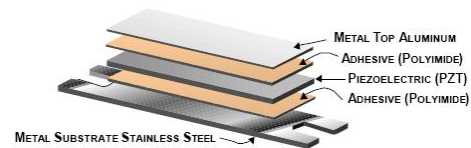


Fig 88: The THUNDER actuator [102]

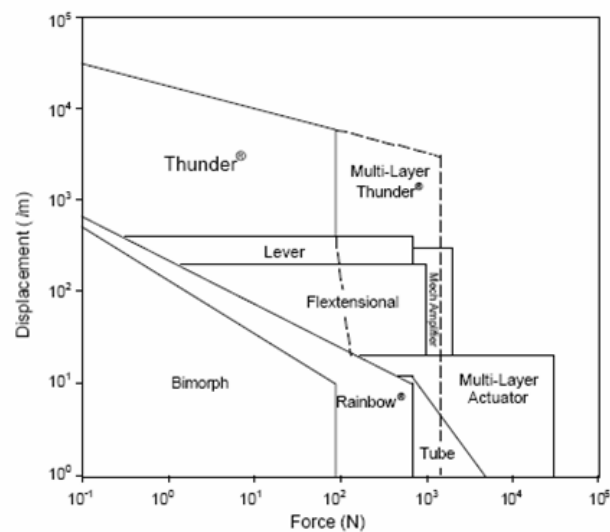


Fig. 89: General comparison of PZT actuators [102]

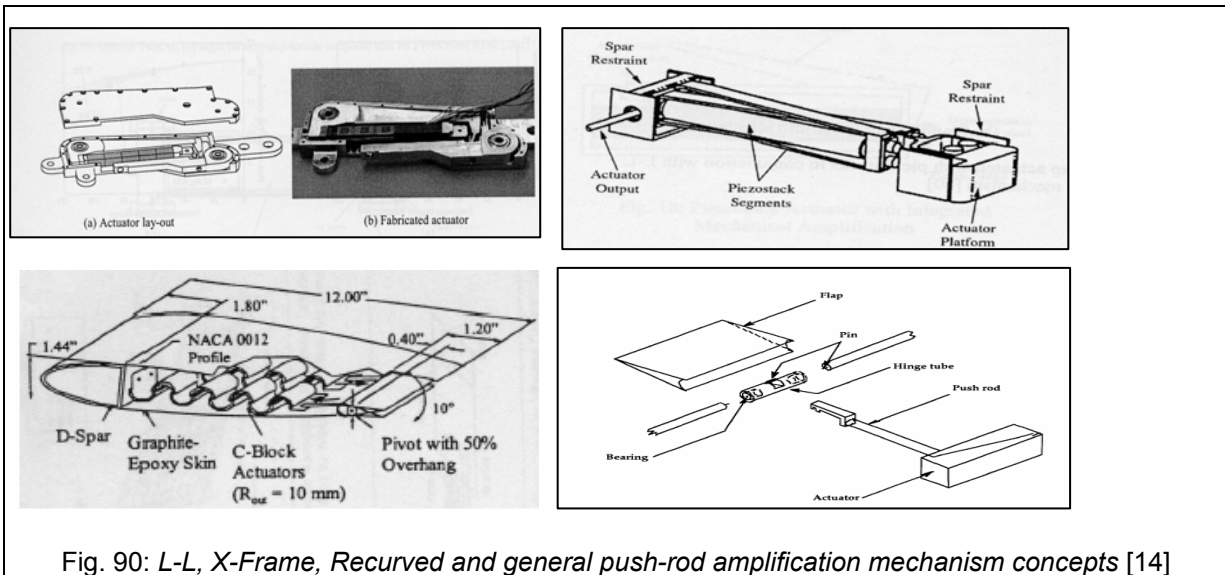


Fig. 90: L-L, X-Frame, Recurved and general push-rod amplification mechanism concepts [14]

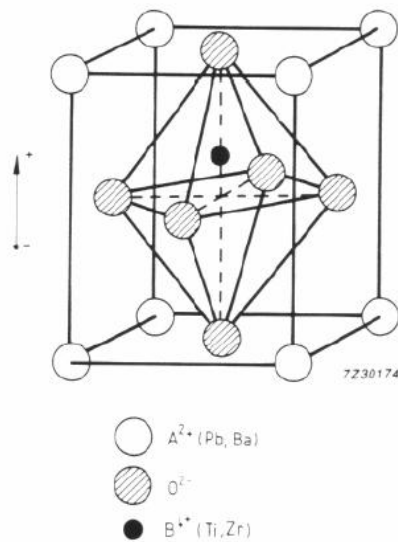


Fig 91: The PZT Crystal

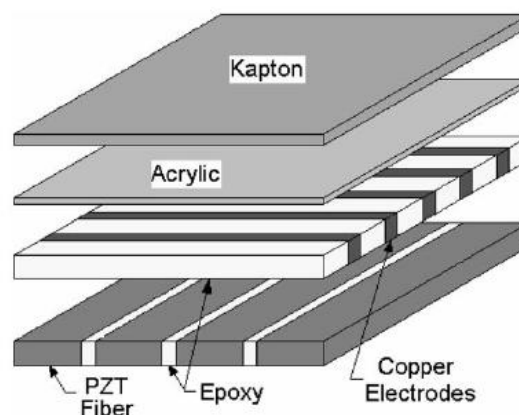


Fig. 92: Macro Fiber Composite build-up

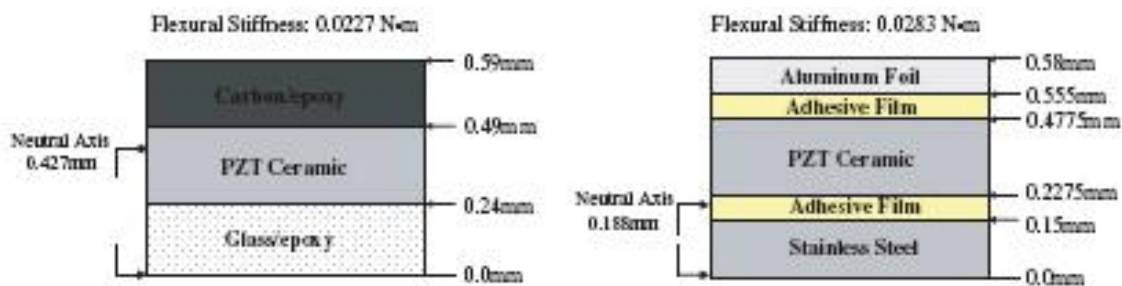
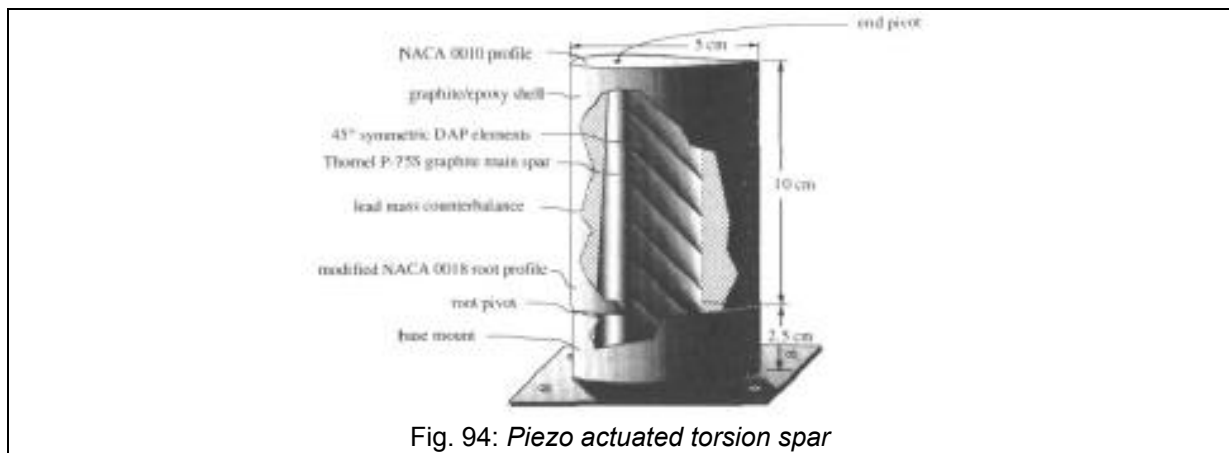


Figure 93: Build-up of Thunder (left) and LiPCA (right) actuators



Shape Memory Alloys and actuators overview

Although the almost linear behavior of piezo actuators makes them attractive for control purposes, shape memory alloy based actuators are promising for a different reason: their large produced strain capability. Shape memory alloys (SMA) are able to sustain and recover relative large strains (up to 10%) without undergoing plastic deformation. Most popular SMAs are Ni-Ti ("Nitinol" – mostly used), Cu-Zn-Al and Cu-Zn-Al-Mn. Fundamental to shape memory alloys is the so-called shape memory effect. Once deformed at low temperature, SMAs can return to their original shape after heating above the transition temperature. This is of course a reversible process. The process followed is: Austenite -> cooling -> martensite -> heat recovery -> austenite. The process of heat cooling and heat recovery gives the SMAs low response times and bandwidth. Heat sink devices can be used for improving the cooling procedure (e.g. Peltier elements). Also, all non-linear effects (hysteresis, creep) comprise a disadvantage for control use. Better dynamic models are needed to describe their behavior. SMAs are drawn into barstock, rod, wire, tubing, sheets and foils, and can be imbedded, attached or included in a composite tube. Discrete coil springs when large forces and small displacements are required, are. With such custom forms SMAs are a promising solution for embedded actuation for shape control of blades. SMA wires can be implemented inside the blade to pull on the skin for deformation purposes. Efficient solutions for the heating and cooling procedures must be adapted for that.

Considering the different concept of embedded actuators for deformable blades (camber control, flexible flaps, active twist), different sets of requirements are involved. As it has been mentioned in the aerodynamic control concept section, for deformable surface actuation, a torsional weak design should be employed in order to use smart actuators. The current design of wind turbine blades uses the torsion box in order to carry the global loads, and the blade skin carries only the local pressure loads. To apply full blade (chord-wise or span-wise – camber control or active twist) deformations different blade structural properties or load carrying layouts (e.g. ribs) must be considered. Sheets of piezo materials, piezo fiber or SMAs can be used (integrated in the structure, or under the skin) for shape control (e.g. Fig.102). Existing knowledge shows that small deflections can be achieved in that way by using existing smart material properties, but this concept (full blade twist) is not considered feasible for now. Still, large layers of smart materials must be used which add weight and cost to the blade [8]. A feasible concept is the use of integrated or under-the-skin smart actuators to deform small surfaces as trailing edge flaps. Still the flexibility of the skin must be considered.

Research in SMAs

Unique behavior shape memory alloys (SMA) in thermomechanical loads has been studied since early 70's and many successful engineering applications are already in use. SMA elements are able to recover large inelastic strain upon mechanical loading at constant temperature (superelasticity), upon heating (shape memory effect), do reliable mechanical work upon heating (work as thermally driven actuators) due to the intrinsic coupling between the stress and temperature. Figure 91 summarizes basic functional behaviors of SMAs.

However, the SMA responses in thermomechanical loads, even if reversible and reproducible, are nonlinear, hysteretic and path dependent.

$$\varepsilon = f(\sigma, T, \text{history})$$

The same value of macroscopic tensile strain may be realized at a relatively broad range of the applied stress and temperature conditions in a cyclic thermomechanical loads depending on the history (stress-temperature path). This nonlinearity and hysteresis originates from the energy dissipation accompanying thermoelastic martensitic transformation (MT) by which the SMA wire responds to stress and/or temperature variations and causes most of the problems for modeling to be dealt with below.

The general aim of the SMA modeling is to develop constitutive law that would reliably capture any thermomechanical response of SMA element to thermomechanical activation (fig. 95). 3D tensorial SMA models capturing SMA responses under general multiaxial stress conditions are necessary to predict thermomechanical behaviors of more complex SMA elements. On the other hand, 1D uniaxial models are sufficient to deal with the problems accounted while developing linear actuators using SMA wires. Both approaches are followed in the SMA literature for at least 40 years, nevertheless, in

spite of that, no fully accepted and reliable models exist yet. The reason for that is probably the multiplicity of deformation transformation processes derived from martensitic transformation taking place in activated SMA element.

Concerning SMA behavior and modeling approaches, the use of SMA alloys with shape memory and superelastic properties has promoted extensive research on developing constitutive models. A micromechanics model based on the analysis of phase transformation in single crystals of copper based SMA alloys has been presented by Patoor [64] in 1994. Another micromechanical model for SMA alloys capturing different effects of SMA behavior such as superelasticity, shape memory and rubber like effects has been presented by Sun and Hwang [65] in 1995. Phenomenological constitutive models have been presented by Tanaka, Liang and Rogers, Brinson, Boyd and Lagoudas [66-70], among others. The phenomenological model RLOOP developed by Sittner et al [71] is a promising tool for modeling of SMA actuators. A model representative of the rate-dependent models for SMA alloys has been presented by Abeyaratne and Knowles [72-73]. Recently, Fisher [74] has proposed a general framework for SMA constitutive modeling involving evolution of transformation as well as plastic strain.

Most of the mechanical testing on polycrystalline nickel-titanium alloys found in literature has been performed for uniaxial loading. As a result most phenomenological constitutive models are based on uniaxial data. Only a limited amount of experimental data concerning multiaxial loading/unloading of SMA alloys are available e.g. Lagoudas, Shu [75], and Leclercq with Lexcelent, [76].

Concerning the design of SMA based actuators, further functional properties and behavior of SMAs are investigated. NiTi wires commonly exhibit sequential austenite $B2 \leftrightarrow R$ -phase \leftrightarrow martensite $B19'$ transformations, their unique stress-strain-temperature behaviors are readily comprehended and modeled as being solely due to the cubic to monoclinic ($B2 \leftrightarrow B19'$) martensitic transformation (Figure 1). Omitting the R-phase is commonly advocated by the fact that the $B2 \leftrightarrow R$ transformation strains are much smaller. The R-phase transformation strains are indeed small ($<1\%$), since R-phase structure is created by a relatively small rhombohedral distortion [77,78], of the parent cubic austenite lattice preceding the martensitic transformation upon cooling or loading. However, the small strain might be a beneficial feature for e.g. passive structural damping applications [79] aimed at vibrations with small strain amplitudes, smart SMA polymer composites in which the NiTi wire is embedded in hard polymers and can not undergo large strains anyway [80], or for actuator applications requiring very large number of cycles, small actuation temperature range and stable functional properties. However, beyond the small transformation strains, there are additional very interesting features of the R-phase – e.g. the rhombohedral angle varies continuously with the temperature [77,78] or the elastic modulus of NiTi is lowest in R-phase near the R_f temperature and increases upon further loading or cooling in the R-phase state [81].

As described above, the thermomechanical behavior SMA is a rather complex function depending on many parameters which makes the use of such a material in engineering applications more difficult in comparison to more common materials. For facilitating the application of SMA's, there is a necessity of creating a set of parameters describing their thermomechanical properties as completely as possible. Next, sets of parameters for characterizing SMA wires are mentioned based on experimental investigations. Such experiments on SMA's have been done at the Institute of Thermomechanics and Institute of Physics in Prague [63]. Nevertheless, when regarding such results, one could be aware of the fact that the SMA's performance depends also on the geometry (diameter) and the degree of cold work and heat treatment (temperature, time). The experiments done so far were performed on rather thin wires and for estimate the performance of SMA wires used in wind turbines applications, new experimental campaign will have to be conducted on the wires with geometry comparable to that to be applied in real application. Once the real working conditions are known, suggestions concerning heat treatment, alloy composition etc. can be provided, leading to maximizing the performance of SMA wires for a given application.

Basic sets of parameters for characterization of SMA wires, firstly, consist of thermal properties. Such consist of characteristic temperatures of phase transitions and hysteresis. Furthermore, the mechanical characteristics of SMA wires describe their behavior under static and cyclic loading (stress-strain relations). For static conditions, such consist of ultimate tensile strength, yield stress, transformation yield stress of austenite, pseudoelastic stress hysteresis, maximum recoverable transformation strain, strain at failure, Young's modulus of martensite, and Young's modulus of austenite values. For cyclic conditions, such consist of accumulated non-recovered strain for a number of cycles, cyclic accumulated transformation stress change for a number of cycles and cyclic accumulated pseudoelastic hysteresis change for a number of cycles values. Some stress-strain behavior of SMA wires obtained from experiments and the influence of various parameters are shown in figures 96, 97, 98.

An SMA actuator belongs to a specific family of SMA applications demanding a few new characteristics to be added to the previously defined ones in order to assess the suitability of an SMA

wire for actuation purposes. A set of characterizing parameters focusing on the actuator properties has been suggested. Such first experimental works for identifying these parameters have been done at the Institute of Thermomechanics and Institute of Physics in Prague. The actuation characteristics of SMA wires are based on experimental tests under two regimes: at constant stress (recovery strain test) or strain (recovery stress test). These two basic tests provide information about the strain/stress recovery such as achievable values of strain/stress recovery (mechanical parameters), temperature interval (thermal properties) and time (reaction time properties) needed for strain/stress recovery. The crucial thermal parameter for the actuation purposes is the temperature interval required to induce the complete strain or stress recovery. Also, a real SMA actuator is supposed to be heated by electrical current, which allows relatively high frequency actuation. During such a process, the mechanical response is stabilized within several cycles, which is an important parameter indicating the suitability of an SMA wire for actuator applications. Finally, for any actuator working in a feedback control, the response time is a crucial parameter conditioning a good stability of controlled system. Hence, this parameter has to be evaluated also in the case of SMA actuator. We note that the two basic regimes (constant strain/stress) are idealized conditions and the real actuator will work somewhere in between.

It is intended to benefit from the unique shape memory alloys properties by using them as an actuator and/or damping element embedded in composites for the active and/or passive vibration control. In order to apply the SMA wires for these purposes in a correct and most efficient way, it is necessary to understand their dynamical behavior (i.e. the response on an applied dynamic excitation, energy dissipation during vibrations). The unique properties of SMA arise from the first-order martensitic structural transformations taking place during thermomechanical loading and providing a complex dynamical behavior being strongly nonlinear. Due to this, the dynamic response depends on many parameters such as amplitude of vibrations, temperature and prestress. The ongoing experimental observation and identification of the dynamic behavior of SMA wires is crucial point of such projects for two main reasons: First, it will allow to find out the achievable efficiency of their use in vibration control. Second, related to the development of mathematical models of dynamic behavior of SMA wires, the experimental data will provide a necessary confrontation experiment-simulation and possibly calculate internal parameters of such models.

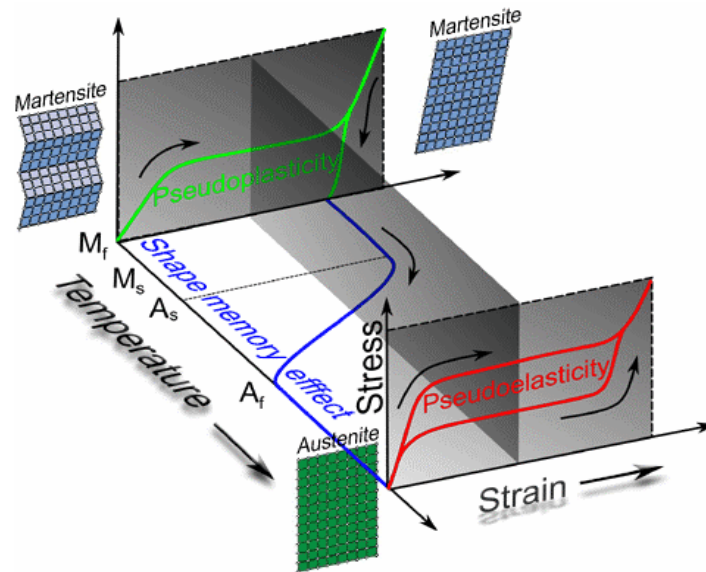


Fig. 95: Basic functional thermomechanical behavior of SMA wire in uniaxial tension

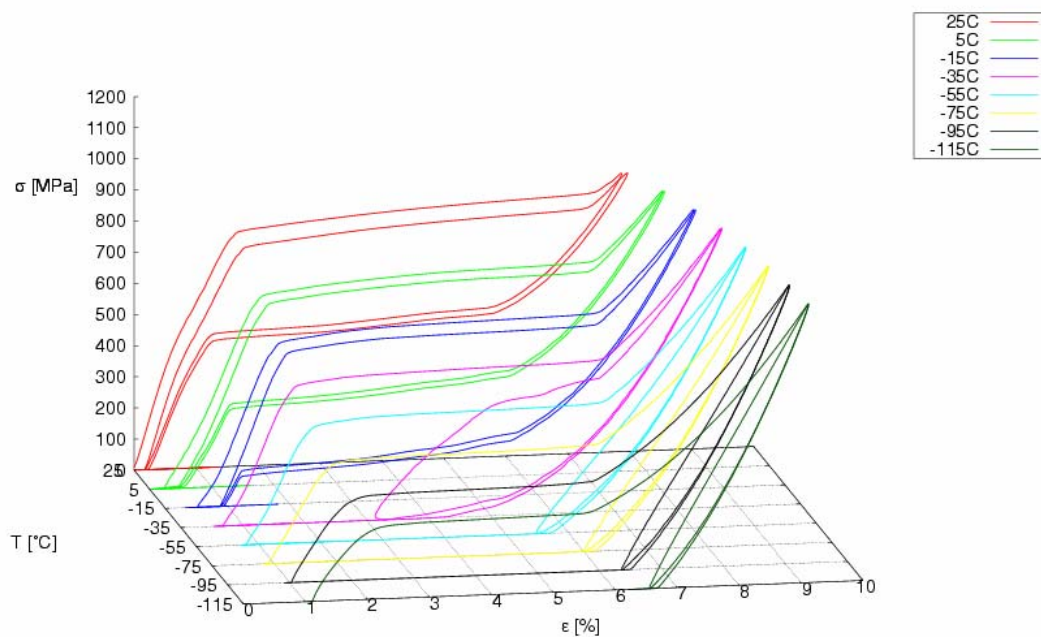


Fig.96: Example of stress-strain curve dependency on temperature. (Memory Metalle superelastic "C" wire, $D=0.050\text{mm}$, annealing conditions $450^\circ\text{C}/30\text{min}$)

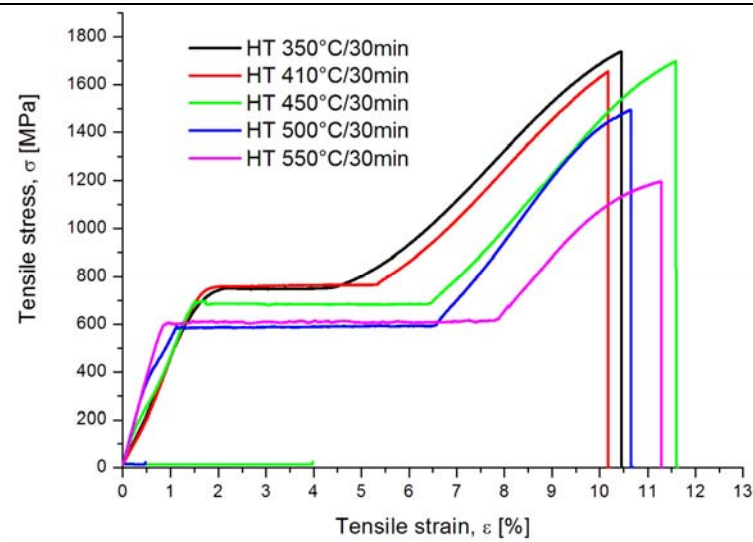


Fig. 97: Influence of heat treatment on the tensile tests until rupture (Memory Metalle superelastic "C" wire, $D=0.050\text{mm}$)

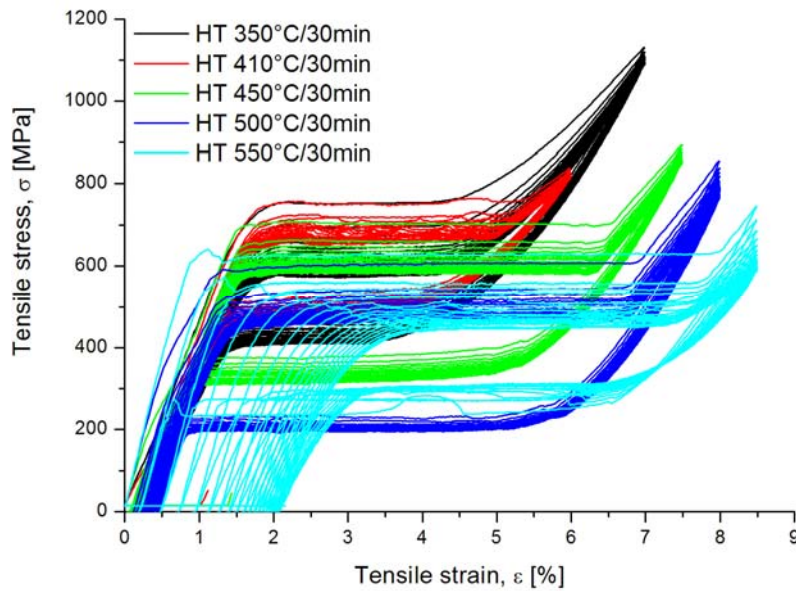


Fig. 98: Influence of heat treatment on cyclic properties (Memory Metalle superelastic "C" wire, $D=0.050\text{mm}$)

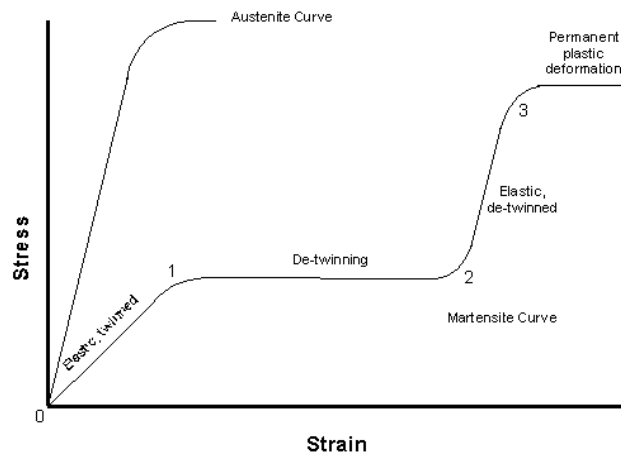


Fig. 99: Stress-strain relation of a SMA [7]

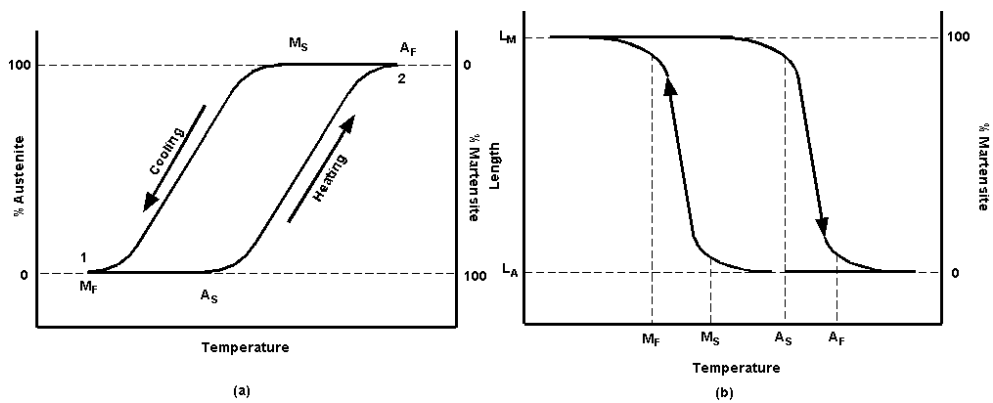


Fig. 100: Hysteresis loops of SMAs [7]

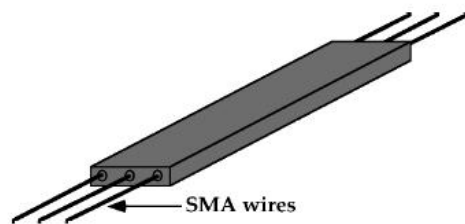


Fig. 101: SMA wires imbedded in structure [3]

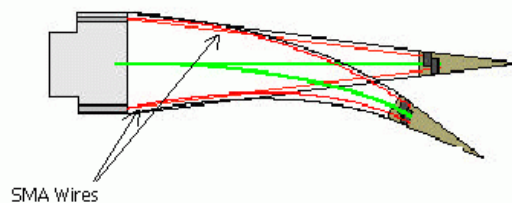


Fig. 102: SMA wires used to pull on the skin of a trailing edge

3.3 Sensors

In this part, available solutions for sensing requirements are analyzed. The function of different options is presented and the implementation for wind turbine active control concepts is discussed.

In the concept of smart blades for rotor control, a point of high importance is the sensing systems. Indeed the aerodynamic loads acting on the blades must be determined and used as inputs in the controller. The goal of the sensing system is to ensure synchronization between the fluctuating loads and deflection of the aerodynamic controls via the controller. But the aerodynamic loads acting on a wind turbine rotor can not be sensed directly. Therefore, the accelerations or structural deformations will have to be sensed.

Sensors for wind turbine blades will require some specific characteristics that are proposed next. Some of them are common to actuators requirements.

- Lightweight: multiplexing capability
- Immunity to electromagnetic waves
- Minimum sensitivity to temperature
- Ease of integration in the structure: manufacturing facilities
- Robustness on a long term
- Minimum calibration requirements
- Precision of measurements. Adequate range and time response.
- Long term stability of measurements
- Reliable operation in harsh environment

3.3.1 Electrical type strain sensors

The different types of electrical-type strain gauges are:

- Resistance strain gauges
- Capacitance strain gauges
- Photoelectric strain gauges
- Semiconductor strain gauges

These types of sensors have been used traditionally to sense blades in order to obtain the strain in different parts of it, especially in the root. With these measurements, aerodynamic loads in the blade can be calculated. Strain gauges are mainly used in laboratory tests or in wind turbine prototypes, but not in serial production [56, 57, 58].

The characteristics of these sensors in measurement range and time response seem to be appropriate to their use in rotor control, even if they only provide one- or two-dimensional strain information. These sensors are sensitive to temperature fluctuations, and a compensating system is consequently required. Generally their main drawback is that their mounting process must be done with high care to assure long life time and high accuracy. Also, these sensors require accurate calibration, and sometimes recalibration during their operating life because of changes in their properties. For instance resistance strain gauges are not suitable for wind turbine applications due to their high calibration requirements and the costly mounting techniques it requires. Comparing to resistance strain gauges, capacitance strain gauges can be more rugged, but their mounting process is still complex. Semiconductor strain gauge shows higher sensitivity, and lower sizes than its counterparts.

None of these types of sensors can assure the number of stress cycles in the lifetime of a wind turbine. They are not robust enough on a long term.

3.3.2 Optical type strain sensors

The strain measurement instruments based on optical methods are:

- Photoelastic strain gauges
- Moire interferometry strain gauges
- Holographic interferometry strain gauges
- Fiber optic strain gauges

The first three kinds of sensors are mainly considered not suitable to be used in a wind turbine rotor, because of their complexity. Only fiber optics strain gauges show good promises and are already used in blade monitoring.

From a sensing point of view, the merits of the optical fiber technology are numerous:

- Very light
- Small in diameter
- Resistant to corrosion and fatigue
- Capable of wide bandwidth operation
- Dielectric in nature
- Immune to electrical interference
- Mechanically flexible, diverse geometry possible
- Do not represent electrical pathways within the host structure
- No protection required against lightning
- Extreme sensitivity
- Do not generate heat or electromagnetic interference
- Low attenuation of signals
- Low maintenance, high reliability
- Possibility for detecting health status of the structure
- High versatility of the measures

Optical fiber sensors permit measurements that are either impractical or uneconomic with conventional measurement technology, such as foil strain gauges. The price of this technology, even if it is still high, begins to decrease thanks to the wide use of fiber optics in telecommunication. Another advantage over conventional technology is the ability to use a single strand of optical fiber to replace hundreds of wires required for measuring a given strain field using foil strain gauges, which entails economy and gain in space. The main drawback of fiber optic sensors is their temperature sensitivity. A single measurement cannot distinguish between the effects of temperature and strain, so the use of a second element is a usual solution. With both measurements, an analysis must compensate for possible temperature fluctuation during strain measurements. Also, these sensors require accurate calibration.

The kind of fiber optic sensor which tends to dominate is the fiber Bragg gratings sensor. Bragg gratings are made by illuminating the core of a suitable optical fiber with a spatially varying pattern of intense UV laser light. This modified fiber serves as a selective mirror: light traveling down the fiber is partially reflected at each of the tiny index variations, but these reflections interfere destructively at most wavelengths and the light continues to propagate down the fiber uninterrupted. However, at one particular narrow range of wavelength, constructive interference occurs and light is returned down the fiber. Maximum reflectivity occurs at the so-called Bragg wavelength (λ_B) given by:

$$\lambda_B = 2n_{\text{eff}} \Lambda$$

Where n_{eff} is the effective refractive index and Λ is FBG period [59].

When the composite changes its strain, n_{eff} and Λ parameters are altered. When there is a variation in the temperature, n_{eff} also changes.

Fiber Bragg Grating technology is already used in blade monitoring. In fact, there are various commercial systems based on these sensors: Smart Fibres, FOS Wind Power, Insensys, LM. These types of sensors exhibit typical precision of ± 1 micro strain with a temperature resolution of 0.1 °C. Another point of importance is that the fiber Bragg gratings sensors can be used to sense different measured quantities as pressure, strain, acceleration for instance. Available sensing systems using fiber Bragg gratings technology

show data acquisition rate from tens of hertz to a few kilohertz which seems to match the rotor control requirements.

Another fiber optic technology has been used in wind turbine blades to detect failures, although it is not as extended as FBG systems. This is the micro bend strain sensor. A LED is used as light source, the light is sent through a set of lenses into the optic fiber. The optic fiber is guided through a fiber-bending device. When the fiber is increasingly bended by the bending device, the transmittance through the fiber is decreased. A laser detection unit measures the light-transmittance through the fiber. The change in transmittances related to the change in displacement between the two halves of the fiber bending device [56].

This sensor is quite cheap with respect to FBG because is based on a multimode optical fiber system. On the other hand the obtained measurements are not as accurate as with FBG system, especially when the number of sensors increases in the same line. Besides that it is very difficult to insert a micro bend transducer into the composite part.

3.3.3 Accelerometers

Accelerometers sense acceleration and 'transform' it into an electric signal thanks to two transducers. The primary transducer sense acceleration and responds to it by a displacement. This displacement is sensed by the secondary transducer which gives an electric signal as response. There are two types of primary transducers which are spring retained seismic mass and double cantilever beam. The secondary transducer can be of different types:

- Piezoelectric
- Potentiometric
- Reluctive
- Servo
- Strain gauge
- Capacitive
- Vibrating element

Firstly, piezoelectric accelerometers are considered not suitable for rotor control because their lower frequency (typically 1Hz) is too high to measure the blade vibrations occurring at frequencies lower than 1Hz. That's why passive accelerometers, which are able to measure accelerations down to zero frequency, have to be chosen. The differences between these types of sensors are their frequency range, their cost, and their frequency response. Costs are not very high. Indeed the widespread use of accelerometers in the automotive industry has pushed their cost down dramatically.

In wind turbine applications, accelerometers are mainly used in maintenance for vibration analysis: bearing, generator and gearbox monitoring, but they are not very extended in blade sensing.

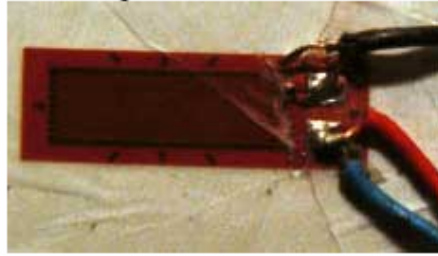
Research has been carried out in Robotiker investigating the use of accelerometers in wind turbine blades. As a result of these researches, a patent (ES 1 075 600) has been obtained.

3.3.4 Acoustic emission monitoring.

The phenomenon of Acoustic Emission occurs due to stress waves generated when a material suffers a small displacement of its surface. It is a non-destructive technique. Transducers are attached to the material in order to detect these waves. AE technology is suitable to be used in blade materials. In load condition, these materials emit a lot of stress waves that can be detected by piezoelectric sensors and they can locate the origin of the waves. This technology is more suitable for small blades. Considering bigger structures, acoustic attenuation could make this technology not so appropriate to get accurate information about loads in the blade. AE monitoring has been used mainly for test and fatigue monitoring and for damage detection more than for loading measurements. Several examples of these functionalities are available [60, 61, 62].

Photograph Soren
Krohn © 1999 DWIA

Measuring Strains



Strain gauges, (i.e. flat electrical resistors which are glued on to the surface of the rotor blades being tested), are used to measure very accurately the bending and stretching of the rotor blades.

Fig. 103: Strains gauges

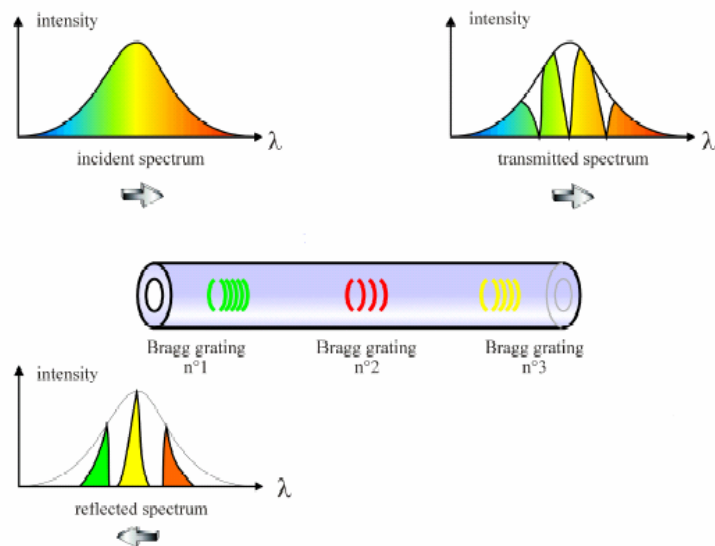


Fig. 104: Optic fiber with 3 FBG

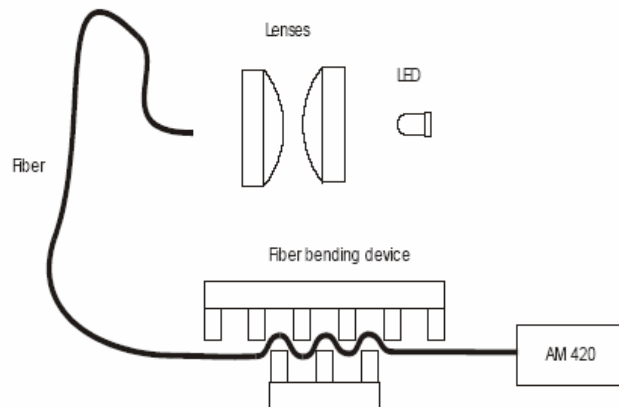


Fig. 105: Sketch of micro bend displacement transducer set up

3.4 Control

In this part, control strategies for active load reduction on wind turbines during operation are presented. Available control techniques and algorithms are summarized. Firstly, different control algorithms which are used or have been developed especially for wind turbine applications. Furthermore, some design developments of smart rotor control are presented. Finally, the use of advanced control techniques, with interesting properties for smart rotor concepts, is explored. Most important references are provided. The report of Wingerden [47] provides detailed list of references.

Also, regarding general theory on flow control, an extensive study of literature on theory, simulation and experiments in active flow control is given in [38]. Overview of possible flow control strategies is given, referenced to relevant literature and categorized by the type of actuation (passive or active) and by means by which the actuation changes in response to flow change (open loop, closed loop, optimal control). Some issues concerning the CFD are also addressed.

3.4.1 Modern control for load reduction

The control algorithm can have a major effect on the loads present in the wind turbine. For example, the pitch controller is used primarily to regulate the generator speed, but changes in pitch angle also have a major effect on the thrust load. This affects the blade out-of-plane bending moments, which drives the foreaft motion of the tower. The foreaft motion affects the relative wind speed seen by the blades. This is fed back to the pitch control via the rotational speed. This strong feedback connection could excite the tower vibration, or even making the pitch control system unstable.

In the literature, information can be found to damp resonant frequencies of certain turbine parts. The first motion is the fore-aft motion of the tower. The first tower fore-aft vibrational mode is very lightly damped, so excitation at this tower resonant frequency needs to be minimal. Because a small amount of excitation is naturally present in the wind, the strength of the response depends on the amount of damping. Bossanyi [48, 50] describes first the use of a notch filter in series with the pitch controller. The notch filter is used to prevent too much pitch action at tower frequency. Thus, the filter needs to be designed such a way that the pitch controller does not reduce the damping at that frequency. The damping which is present is mostly dependent on the aerodynamic damping of the rotor, which can be affected by pitch activity. The second approach described by Bossanyi is better because it increases the aerodynamic damping. The approach uses an extra signal from an accelerometer mounted in the nacelle. This signal is fed back to the pitch controller and this increased pitch activity significantly reduces the tower loads. Research at ECN [53] describe this idea also, and have extended it with a scheduling controller to achieve a constant maximal damping for the whole turbine operating area. In these reports also the drawback of the fore-aft acceleration feedback is mentioned; switching-on the fore-aft acceleration feedback in their simulation package PHATAS-IV, increased the torsional loads of the drive train at tower resonant frequency slightly. Instead of using pitch variations for enabling additional damping for fore-aft tower vibrations, electric torque variations can be used to reduce drive train resonances and sideways tower vibrations. Compared to a fixed-speed turbine, the drive train of a variable-speed turbine operating at constant generator torque can be badly damped, which can therefore lead to very large torque oscillations at the drive train and gearbox. In a fixed speed turbine the induction generator slip acts like a strong damper, and therefore the torsional modes of the drive train are well damped. Also for this problem, Bossanyi [48, 50] and ECN [53] describe a solution, which has been successfully implemented on many turbines. The generator torque can be modified to provide some damping by adding a small ripple to counteract the effect of the resonance. This ripple can be added by using a highpass or bandpass filter on the measured generator speed. Such filters can be placed parallel to damp other resonances, such as in-plane vibrations and sideways tower vibrations. In addition, the ECN [53] have also successfully studied the use of a Kalman filter for reducing vibrations on drive shaft, which cannot be damped by the above described control. Displacements in sideways direction are caused by drive train torque reactions and external forces of waves. Like fore-aft acceleration, sideways acceleration can be fed back to the torque control, see the ECN report [53]. Including this feedback loop and that of the fore-aft tower bending and shaft distortion brings the overall wind turbine control system as illustrated in Fig 106.

Feed forward control of the estimated wind speed can be used to track the optimum tip speed ratio. In order to perform the feed-forwarding of the wind speed, a wind speed observer is developed which estimates the wind speed by using a simple model of the wind turbine. Research of the ECN [53, 54, 55] showed that instead of additional torque action for power optimization that this control can also be used for reducing power variation and fatigue loads. The feed-forward control resist disturbances of the wind speed turbulence and wind gusts by additional pitch control action. The proposed pitch control actions will be an addition to the basic pitch actions for generator speed feedback control. Initially, pitch control was only used at above rated wind speed, but this feed-forward pitch control can be used for the whole operated area with look-up tables. The small additional pitch actions over the whole operated area give a considerable reduction of rotor speed variations and even a small increase of energy yield.

The disadvantage of the previous control method is that the method suggests that the same wind speed turbulence and wind gusts are active on the whole rotor area. As the rotor size increases with respect to the size of the turbulent area, the importance of turbulent wind speed variation across the rotor swept area becomes greater. Since commercial turbines get larger, many of them use individual pitch actuators as independent braking systems instead of needing a high-capacity shaft brake; the idea for individual pitch control is developed. The simplest way to implement is just to add rotational dependent variations to the pitch angle of the individual blades, to reduce the asymmetric loads like wind shear and tower shadow. However, a small phase mismatch due to changes in the tower shadow and wind shear effect will cause higher instead of lower loads. Therefore individual pitch control uses additional sensors to measure the asymmetrical loading in some way. The addition of sensors avoids the danger of mismatch and reduces the stochastic blade loads. The best reduction is achieved by local flow measurements, as described by Larsen [52]. This load-reducing regulation strategy is based on measurement of the inflow parameters angle of attack and relative velocity. The advantage of the individual pitch controller based on local flow properties instead of the measured blade loads is that flow measurements are fast and are not influenced by a time delay between the actual load change and the blade response. The disadvantage is that today's flow measurement devices such as pilot tubes have some robustness issues, thus to unreliable to implement in practice. Most studies of individual pitch control uses strain gauges or accelerometers in each blade tip and lateral and vertical accelerometers in the nacelle to determine out-of-plane loads. Bossanyi [49, 50, 51] and ECN [37] describe the control based on this type of sensors. The main principle of this control is the regulations of the rotor tilt and yaw moments. These non-rotating rotor moments are transformed from the measured blade flapwise and edgewise moments. The coordinate transformations can be expressed for a three bladed turbine as follows:

$$\begin{bmatrix} \theta_{tilt}(t) \\ T_{yaw}(t) \end{bmatrix} = \begin{bmatrix} \cos \varphi_1(t) & \cos \varphi_2(t) & \cos \varphi_3(t) \\ \sin \varphi_1(t) & \sin \varphi_2(t) & \sin \varphi_3(t) \end{bmatrix} \begin{bmatrix} T_1(t) \\ T_2(t) \\ T_3(t) \end{bmatrix}$$

and backwards:

$$\begin{bmatrix} \theta_1(t) \\ \theta_2(t) \\ \theta_3(t) \end{bmatrix} = \begin{bmatrix} \cos \varphi_1(t) & \sin \varphi_1(t) \\ \cos \varphi_2(t) & \sin \varphi_2(t) \\ \cos \varphi_3(t) & \sin \varphi_3(t) \end{bmatrix} \begin{bmatrix} \theta_{tilt}(t) \\ \theta_{yaw}(t) \end{bmatrix}$$

To control the multivariable control problem, a LQG controller has been used successfully to control the two transformed pitch angles. This controller showed excellent performance, but has the disadvantages that the resulting controller is of very high order and it is difficult to guarantee robustness. Most studies decouple the control problem to individual feedback loops, where each loop is controlled using a classic PI-controller, see Fig. 107. Although the performance is less, the classic controller is preferred by the industry, because it is widely applied and straightforward to implement. Eventually, the individual pitch control can also be used to yaw the wind turbine. If a non-zero reference is used for the controller acting on the yawing moment, the pitch action generates a yawing moment to assist (or even replace) the yaw motor in yawing the turbine [51].

3.4.2 Load reduction with smart rotor

Preventing fatigue damage is mostly done in the design phase, but the suppression of vibrations in active operation is becoming more popular, since the wind turbines are becoming larger. Modern control techniques are used and developed to reduce the fatigue in different parts of the turbine. This becomes possible with the use of sensors, like strain gauges and accelerometers. These techniques reduce mostly the fatigue on the drive train, gearbox and tower. The most load-fluctuated parts, the blades, are mostly not included. The main reason is that blade loadings are difficult to control, by the lack of enough control parameters. The only actuator currently used is the pitch, for example in individual pitch control, but this actuator can reduce the low frequent blade vibrations only. The project “smart rotor” introduces the use of aerodynamic control devices like flaps. It is believed that such devices placed on the blades can reduce the vibrations further. Although a parallel study at the Delft University of Technology is researching these new concepts, the literature has some interesting results in this area, as has been discussed earlier. The M.Sc. thesis of Basualdo [17] shows promising results of PID-controlled flaps in simulations with two degrees of freedom (2D). The succeeding M.Sc. thesis of Andersen [19] describes the simulation in 3D and showed also the optimal placement of the flaps on the blade. In the study of Anderson, the blade element momentum method is adapted to the aerodynamics of the flaps. The lift, drag and moment forces of the flaps are added to the blade elements where the flaps are located. This approach is quite different from the one of DUWIND, which includes simple dynamics for the blade deflections, but incorporates a full wind turbine model, including degrees of freedom for the tower and generator and also combining pitch control with smart flap control and testing advanced controllers. Still many factors have to be explored to develop robust tools for realistic enough simulations of smart rotors.

3.4.3 Repetitive learning control

The disturbances acting on an individual wind turbine blade are for a large extend periodic, such as the tower shadow, wind shear and gravity. For relatively slow changing periodic disturbances it is expected that repetitive learning control (RLC) can significantly contribute to the reduction of fatigue of the wind turbine parts. The repetitive control system rejects the unknown periodic disturbances, which cause fluctuations in, for example, the blades. The repetitive controller is a feedback controller (see Fig. 108) compared to an iterative learning controller (ILC), which acts like a feed forward controller. ILC is a closely related and active area of control theory. Other differences include that ILC act on a finite horizon, whereas RLC is continuous, and that the typical assumption of ILC is that each trial starts with that same initial condition, whereas RLC does not start with such assumption.

The basic design for the repetitive controller is illustrated in Fig. 108. The system consists of a plant $P(s)$, compensator $C(s)$ and a memory loop $M(s)$:

$$M(s) = \frac{1}{1 - Q(s)e^{-\tau s}}$$

where $Q(s)$ usually is a low-pass filter, which is needed for both technological and robustness reasons. Nowadays the repetitive control system can also be designed with LMI, and multivariable systems with internal model design and H^∞ design. The drawback of repetitive control is the requirement of the exact knowledge of the period-time (or delay-time τ) of the disturbance signals. Therefore in practical applications with repetitive control, the period-time is required constant. However the disturbances, like tower shadow, wind shear, gravity and even turbulence, depend on the rotational speed of the rotor. Below-rated, the rotational speed, thus also the period-time, is continuously changing. For small changes in period-time, the robustness and performance of the repetitive controller can be increased by placing extra memory loops in series. In the literature several solutions have been proposed for a repetitive control with highly changing period-time. Assuming that the periodicity can be measured accurately, the literature describes two types of methods for solving this problem. First method is to adjust the delay-time τ for the varying period-time. The second method is to adjust the sampling rate (in discrete time). The disadvantage of the first method is that a period mismatch may result in undesirable remaining oscillating errors. As for the second method, the most serious problem is that changing the sampling rate without changing the controller can affect system robustness, and even cause instability. If the angular position of the rotating rotor is available, the sampler could be designed and implemented by using the angular position instead of time, so that the disturbance period is

always exactly one rotation regardless of speed variations. The drawback is that the dynamics are also highly depended on the rotation, so that a controller based on a model could deviate when the rotor speed changes.

3.4.4 Positive position feedback control

Positive position feedback (PPF) is also a control method especially used for vibration suppression. Instead of suppressing periodic disturbances, PPF control is used to reduce vibrations at the resonance frequencies of the controlled flexible structures. The advantages compared to high order controllers designed with LQR and H^∞ is that PPF design is not based on a model, so the controller is not sensitive to model uncertainty or by modeling errors introduced by model reduction. Another advantage is that the resulting controllers of PPF design are of such a low order that they can be easily be implemented in a digital controller. Higher order controllers needs to be reduced, which can lead to lower performance.

Actually there are two methods described in the literature to introduce modal damping; velocity feedback (VF) and positive feedback control (PPF). The PPF controlled system is illustrated in Fig. 109. The PPF controller, denoted by $C(s)$, can be written as a sum of k modal components, each having their own frequency and damping:

$$C(s) = \sum_{n=1}^{n=k} G_n \frac{1}{s^2 + 2\zeta_n \omega_n s + \omega_n^2}$$

The PPF design needs the requirement of the exact knowledge of the natural frequencies. Therefore the varying frequency of the blades, due to centrifugal stiffening, brings the need that the controller can be scheduled. Adaptive methods exist, but scheduling the frequency seems the most attractive method. The varying frequency is closely related to the rotational speed, which is assumed accurately measured. It is expected that this control method can reduce the vibrations on the wind turbine significantly.

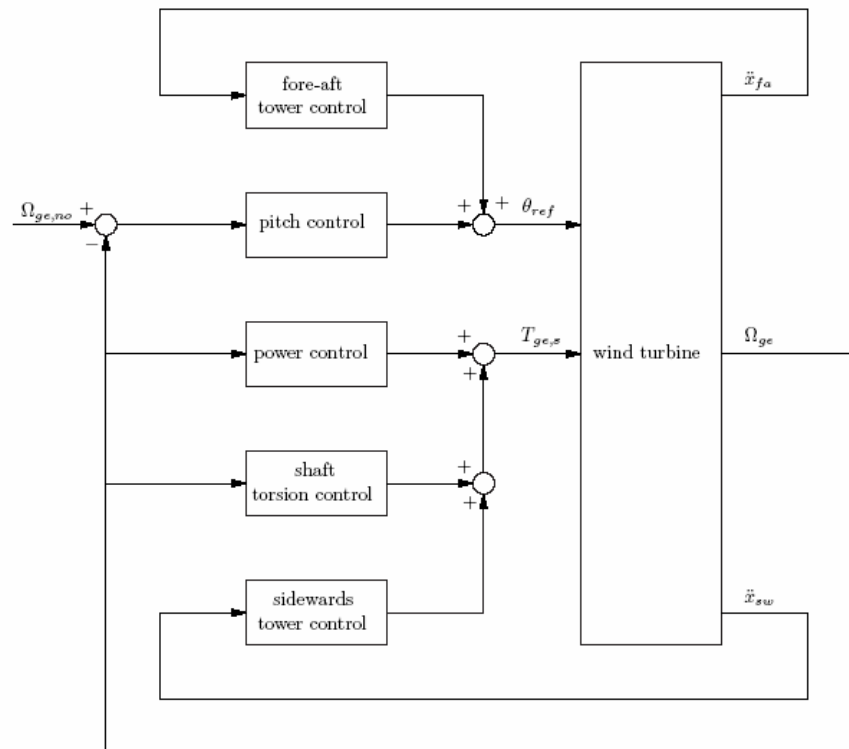


Fig. 106: Block diagram of feedback loops for control

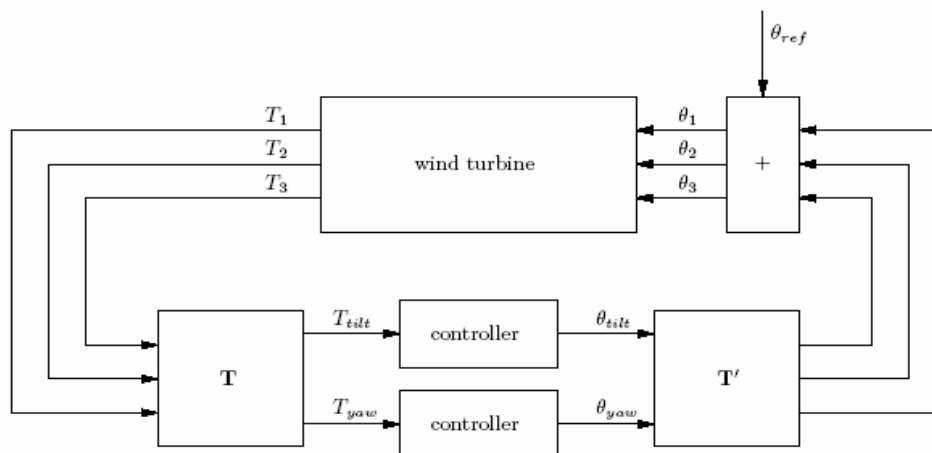


Fig. 107: Block diagram of individual pitch control

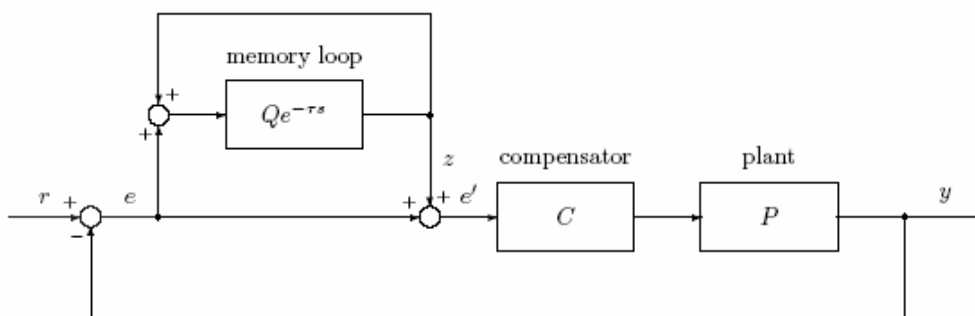
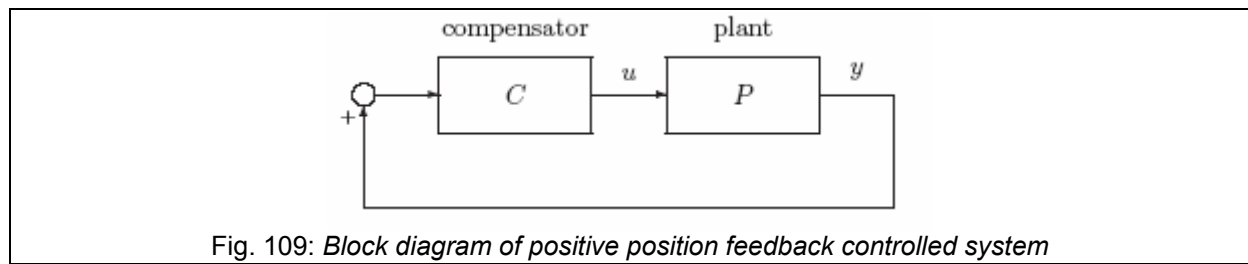


Fig. 108: Block diagram of repetitive learning controlled system



3.5 Modeling-Tools

In this part, an overview of available models and tools needed for the design of smart rotor blades are presented. These models and tools focus on the aero-elastic, structural and control simulations of smart wind turbine rotors. Requirements for such models and available theoretical and software tools are discussed.

3.5.1 Requirements for modelling of smart wind turbine rotors

In order to conduct further research in application of smart rotor control on wind turbine blades, certain requirements for the simulation of concepts must be set. Then, available theoretical and software tools must be suggested and analyzed. The application of smart structures and dynamic control on wind turbine blades includes aspects that are not included in the nowadays standards in wind turbine design. Many differences exist from the ordinary wind turbine design with full-span pitch controlled blades. Summarising the most important issues, we can define such requirements from models and tools:

- **Blade section unsteady aerodynamics:**

In order to model efficiently the use of aerodynamic control devices located on the blades, airfoil unsteady aerodynamic models are required. This comprises the inner problem of describing the aerodynamic environment of a rotor, which is modelling the resulting local unsteady aerodynamic response at each of the blade elements (sections). Quasi-steady aerodynamic models for the airfoil region are considered not realistic for such an application. The fast transient changes in inflow, combined with the fast actuation of the control devices, create a high unsteady aerodynamic environment at the blade element level. The changes in aerodynamic loads from such unsteady phenomena must be calculated accurately, modelling the perturbations to the local angle of attack and velocity field by all elements of aerodynamic forcing and the unsteady response and phase lag connected with them [82]. Also, the unsteady aerodynamic forces under non-attached flow conditions (dynamic stall) should be modelled. The possibility of using aerodynamic control devices for alleviating fast powerful changes in inflow (e.g. gusts) requires that the aerodynamics of that region should be simulated correctly.

- **Unsteady wake modelling:**

Unsteady aerodynamic effects are, in part, a consequence of the time-history of the induced velocity from the vorticity contained in the shed wake, coupled with the induced velocity contributed by the circulation contained in the trailed wake [82]. The outer problem is to model the effects of the induced velocity field produced by the vortical wake trailed from behind each blade. The fast time-varying and spanwise varying load distributions on the blades caused by the aerodynamic control devices, in the case of a smart rotor, will induce a very unsteady and not symmetrical wake environment. The physics of such phenomena must be modelled accurately in order to predict realistic effects on the combination of aerodynamic control devices and rotor aerodynamics.

- **Unsteady wind flow**

The aerodynamic control devices will be used to deal with fast fluctuating loads caused by unsteady wind flow. So, all important periodic and stochastic components of the input wind field should be included. Distortions of the mean wind flow like tower shadow, wind shear and turbulence must be modelled.

- **Actuator dynamics**

It is important to include the dynamics of the control devices located on the blades in the model of the dynamics of the wind turbine rotor. The mass and stiffness distribution together with the inertia forces of the blades will change by including actuation devices on their span.

- **Smart materials**

The use of smart materials on the blades for actuation purposes (camber control, active twist, deformable trailing edge) requires that the structural behaviour of such an approach

should be modelled correctly. Structural models of blade-smart actuator with induced strain actuation are required. The behaviour of surface-mounted or embedded actuators and the interaction with the blade structure should be time-dependent. The modelling of the rotor blades as beams undergoing bending and torsion deformation together with the structural effect of the actuators is essential.

- **Controllers**

The design of the necessary controllers depends on the sensors, actuators and aerodynamic control devices chosen. Appropriate control strategies must be used or developed, which fulfil the specific application on a smart rotor. Traditional controllers on wind turbine design tools do not allow control strategies for embedded and spanwise distributed aerodynamic control. Current methods must be extended and possible solutions for traditional feedback controllers or modern adaptive controllers must be investigated.

3.5.2 Theoretical tools

- **Aerodynamics:**

Available theoretical tools describing the necessary aerodynamics for the application in smart rotor concepts must be analyzed and additional required knowledge must be developed. The most common theoretical tool used for wind turbine analysis and design is Blade Element Theory (BEM), which is based on global momentum balance and assumes stationary or symmetrical inflow conditions and quasi-static 2D flow around airfoil sections. Usually corrections are added to account for 3D effects, dynamic stall and dynamic behaviour of the wake (dynamic inflow). The validity of BEM has been doubted, especially for operation under unsteady inflow conditions as yaw misalignment. Methods based on BEM and the use of corrections require careful handling to come to good results, according to experiences in the certification of Germanischer Lloyd. Dynamic inflow models exist that consider the unsteady aerodynamic lag of the inflow development over the rotor disk usually in response to changes in rotor thrust. Simple mathematical form and numerical efficiency make such models attractive for use as correction in BEM models. Other theoretical tools that describe better the physics of the unsteady wake of a rotor are the vortex wake methods. Such methods represent the circulation and locations of vortical elements on the wake, trailed by the blades. From the geometry and strength of the vortex elements, the induced velocity field can be determined applying the Biot-Savart law. Although such methods have high computational cost, they can give better results and deal efficiently with transient problems, since wake dynamics are described in time-accurate manner without any general assumptions [82]. In such methods, the flowfield around the blades is usually approximated using panel or lifting line methods. At the other hand of the modelling scale are Computational Fluid Dynamics (CFD) methods, that solve numerical the Navier-Stokes fluid equations. The flowfield aerodynamics of a rotor can be realistically simulated this way, although very high computational power is needed and extreme care is needed in the verification of results. The unsteady aerodynamics of blades with active aerodynamic devices can be modelled with CFD, but require extreme computational power and should be carefully treated when dealing with separated flow phenomena. Deformable shape (using moving mesh) or boundary layer manipulation problems (synthetic jets, suction) can be modelled using CFD. At the airfoil section level some theoretical tools exist for modelling the unsteady aerodynamics of airfoils with control devices (deformable shape, trailing edge flaps). A method based on work of Theodorsen, Küssner, Wagner, von Kármán and Sears that treats the unsteady aerodynamic forces on airfoil sections with trailing edge flaps is the one of Leishman [83]. This method provides solution for the unsteady forces on an airfoil section undergoing arbitrary motion (plunge and pitch forcing and trailing edge flap deflection) for potential flow. Also, a method for determining the unsteady aerodynamic forces on a variable geometry airfoil undergoing arbitrary motion was developed by Gaunna [26]. The airfoil is represented by its camberline as in classic thin-airfoil theory, and its deflection is given by prescribed distributed deflection mode shapes. Extension of the method for non-attached flow conditions (stall) is also under development. Methods (usually semi-empirical) for simulating dynamic stall also exist but apply only to plain airfoils, without control devices. Most famous are the Beddoes-Leishman method and the ONERA method. Concerning translational micro tabs (MEM tabs), no analytical unsteady aerodynamics model exists, although there is plenty of data (both steady

and unsteady) from experiments and CFD simulations [27, 28, 29, 30, 31, 32, 33]. Models that describe the boundary layer effects of micro tabs must be developed. Indicial response formulation can be used for an analytical approach. To sum up, some theoretical methods for simulating the unsteady aerodynamics of control devices integrated in wind turbine blades already exist (trailing edge flaps, camber control). Other concepts must be investigated by developing new models and all should be used in integrated aerodynamic tools (e.g. BEM methods, Vortex methods) to investigate their general aerodynamic effect.

- **Dynamics – Structures - Materials:**

Many approaches already exist in modelling of structural dynamics of wind turbine blades. Mainly, the modal analysis approach is used, where blades are modelled as cantilever beams, with airfoils as cross sections and specific degrees of freedom. Other approach is the multi-body modelling, where the structure is modelled using multiple elements (rigid and deformable) and mechanical constraints. Also, finite element methods can be used, which discretize the structure, solving for deformation and stresses. In all of the above models it is possible to implement dynamics concerning control surfaces or structural dynamics of smart materials. In order to do that efficiently, accurate analytical tools should be developed that calculate the achieved deflection/movement of control surfaces depending on the actuation process (discrete trailing edge flaps, micro tabs) or calculate the induced strain actuation of smart materials embedded on the structure (camber control, active twist). Simple constitutive relations of smart material actuators under different loading are required. These dynamic models of distributed actuation processes (with possible spatial variable modal characteristics) on the blades should be integrated into rotor analysis.

- **Control:**

Theoretical tools from classic or modern control theory for active (closed loop) aerodynamic control already exist. Some approaches have been analyzed in section 3.4. In mostly all control strategies, some form of model or surrogate of the system to be controlled is required. It should also be identified through simulations if classic feedback control is adequate for this application, or more advanced (adaptive, self learning) control techniques should be used. Also, control techniques should be adapted specifically to the wind turbine application, load reduction target and specifications of actuators and sensors used.

3.5.3 Software tools

No software tool exists that can simulate a wind turbine rotor with integrated actively controlled aerodynamic devices. In order to evaluate different concepts and perform first-order simulations, various 'academic' tools should be used. Of course, commercial available (e.g. Fluent, Edge) or academic (e.g. EllipSys) CFD packages can be used in order to evaluate the aerodynamic performance of control surfaces. But, unsteady simulations of rotating blades with actively controlled integrated aerodynamic control surfaces will be extremely expensive in computational cost. Analytical models, capturing the most essential physics of the application (unsteady airfoil aerodynamics, unsteady inflow) will have to be used. As already mentioned in section 2.2.3, a 3d aeroelastic model of a rotating blade incorporating adaptive trailing edge flaps has been developed at Risø [19, 22, 23, 24]. Unsteady aerodynamics for a variable camber airfoil [26] and distributed feedback control are included. Results seem promising. Integration of the model into a full wind turbine simulation tool (HAWC2), including pitch control, is in progress. In DUWIND, an aeroelastic software tool for the simulation of a wind turbine, where additional control is provided by means of trailing-edge flaps on the rotor blades, has been developed. The model is based on BEM and includes extensions for dynamic inflow and unsteady airfoil aerodynamics with trailing edge flaps, as described by Leishman [83]. Unsteady wind input is provided, including wind shear, tower shadow and turbulence models. Simple dynamics with degrees of freedom for the blades, tower and transmission are also included. Feedback control for pitch and flaps is modelled. The developers of FlightLab, a helicopter simulation software package widely used, have developed a wind turbine simulation software tool, called Aeolus. Unsteady aerodynamic models are included and additional control structures like servo-flaps will be added. The package is in the final stages of development, before being commercially available. On the other hand, many certified and trusted wind turbine simulation and design software tools exist, commercially available, and widely used by industry. Of course, no active control devices (only pitch control) and unsteady aerodynamic models are included, and the implementation of extra features is not possible. Most famous software packages are: Bladed (Garrahd Hassan), Phatas / Focus (ECN)

and Flex5 (DTU-Vestas-GE). Also, from the National Wind Technology Center (NWTC) of National Renewable Energy Laboratory (NREL) of USA, a series of codes has been developed. Aeroelastic codes include YawDyn, FAST and ADAMS, which use the aerodynamic routines AeroDyn. These software packages are considered more flexible for academic use and extra features can be implemented (especially in ADAMS). ADAMS has already been used for preliminary simulations of smart control devices, as described earlier in section 2.2.1, including extra control, although no unsteady aerodynamic modelling was implemented for the control surfaces (quasi-steady).

For the simulation of the implementation of smart materials into structures, Finite Element Methods can be used. Detailed commercial software packages are widely used (ANSYS, Abacus). In order to do that, structural dynamic characteristics of embedded or surface mounted smart materials should be implemented in such tools. Tools like NREL's PreComp can be used to simulate composite materials in blades, and smart material properties can be added. The great challenge will be the integration of such models into aeroelastic codes, and the active control of their characteristics. Clearly defined relations between controller voltage signal, material strain and achieved aerodynamic shape must be established.

3.6 Design considerations

In this part, issues about the design of smart rotor concepts are presented. Key challenges regarding design requirements, restrictions and limitations are discussed. Since research is not yet at a stage of a clear design, requirements and general considerations are set. Some parameters have already been mentioned in section 3.1.

The realization of a smart wind turbine rotor requires implementation of aerodynamic control surfaces, actuators, sensors and control systems on the blades. Such implementations impose significant changes in the existing design of blades. Although research in smart rotor concepts is still in a preliminary stage, design considerations must be made and restrictions and limitations must be taken into account before proceeding further. Such design requirements may be serious design drivers, sometimes with more significant effect than performance and load reduction results.

Reliability - maintenance

Modern wind turbine blades are considered very reliable, and usually require only limited maintenance at the blade pitch bearing. Conceptual future blades with distributed control devices should be as reliable, without adding maintenance requirements. The reliability of blades with integrated active control devices should be estimated by integrating the reliability of components used in such devices assembly. In the case of smart materials integrated in the blade structure the total structural reliability of the blade should be investigated. Reliability data for specific components (smart materials, sensors, control surfaces) partly exist from manufacturers or from aerospace application investigations, but the total reliability depends on the design of the chosen concept assembly. So, in this stage of research it is not possible to make accurate estimations. This will also affect the maintenance requirements for smart rotor concepts. The requirements will be quite strict, especially focusing on offshore applications, where the accessibility of wind turbines for maintenance is limited. Reliability and maintenance requirements of such concepts will be decisive for future application and should be investigated as soon as first preliminary choice of components has been made.

Size – weight parameters

In all smart rotor concepts, the size of components with regards to available space on the blades should be taken into account. The size of control surfaces is restricted by chord size and spar location, especially near the tip. All new concepts of smart control devices focus on integrated solution without complex mechanical parts, as mentioned in section 3.1. Such solutions can be integrated in blades without sizing problems. The integration of sensors in wind turbine blades has already been investigated in the past for health monitoring purposes [56, 62], and some prototypes already exist (e.g. LM optical fiber blade monitoring system [84]). Embedded solutions of fiber grating optical sensors have been investigated. Weight increase on the blades, due to added control device components, strongly depends on each concept. The use of small discrete control surfaces (trailing edge flaps, microtabs) does not introduce significant weight changes on blades, although the changes in center of gravity with respect to aerodynamic center and elastic center should be investigated for aeroelastic effects. The concepts of using integrated smart materials along the whole span (active twist) will possibly introduce significant weight changes.

Power – cables – electronics

The choice of actuation systems will be decisive for the power requirements. The power needed for actuation will depend on the type, thickness and size of smart materials used in actuators. The requirements in voltage will be in the order of hundreds of Volts. The cable routes and lengths must be investigated in order to find optimal solutions. Control electronics and all other required devices (amplifiers, filters etc) can be placed in the hub, or at the blade root. The size of blades does not place limitations for the cable routes.

Lightning strikes

Statistics show that lightning causes 4 – 8 faults per 100 turbine years in northern Europe and up to 14 faults in southern Germany. 7-10% of lightning events involve wind turbine blades [84]. Even non-conducting blades are often struck by lightning and suffer major damage. It is unknown if distribute smart control systems on the blades, powered with possible high voltage, will attract more lightning strikes. The issues should be investigated. A possible solution is the installation of multiple receptors for lightning protection. Protection systems are available and more advanced systems have been also

investigated with successful results [84]. But, the main blade structure should not be active part of the lightning protection system (as in the case for carbon fiber blades), because of possible damage of sensors, actuators and cables.

Bibliography

- [1] P. S. Veers, Trends in the design, manufacturing and evaluation of wind turbine blades, *Wind Energy*, 3, 245-259, 2003.
- [2] S. Joncas, O. Bergsma, A. Beukers, Power regulation and optimization of offshore wind turbines through trailing edge flap control, *AIAA 0394*, 2005.
- [3] F. K. Straub, A feasibility study of using smart materials for rotor control, *Smart Mater. Struct.* 5, 1-10, 1996.
- [4] F. K. Straub, Smart material-actuated rotor technology – SMART, *Journal of Intelligent Material Systems and Structures* 15, 2004.
- [5] C. Niezrecki, D. Brei, S. Balakrishnan, A. Moskalin, Piezoelectric actuation: state of the art, *The Shock and Vibration Digest*, Vol. 33, No. 4, 2001.
- [6] V. Giurgiutiu, Review of smart-materials actuation solutions for aeroelastic and vibration control, *Journal of Intelligent Material Systems and Structures*, Vol. 11, 2000.
- [7] I. Chopra, Review of state of art of smart structures and integrated systems, *AIAA journal*, 40, 11, 2002.
- [8] L. Krakkers, Ductile piezo-electric actuator materials, Netherlands Institute for Metal Research (internal report), 2006.
- [9] B. Enenkl, V. Kloppe, D. Preibler, Full scale rotor with piezoelectric actuated blade flaps, 28th European Rotorcraft Forum, 2002.
- [10] D. Roth, B. Enenkl, O. Dieterich, Active control by flaps for vibration reduction – Full scale demonstrator and first flight results, 32nd European Rotorcraft Forum, DY04, 2006.
- [11] P. Migliore, G. Quandt, L. Miller, Wind turbine trailing edge aerodynamic brakes, *NREL/TP-441-7805*, 1995.
- [12] L. Miller, Experimental investigation of aerodynamic devices for wind turbine rotational speed control, *NREL/TP-441-6913*, 1995.
- [13] L. Miller, G. Quandt, S. Huang, Atmospheric tests of trailing edge aerodynamic devices, *NREL/SR-500-22350*, 1998.
- [14] B. Marrant, T. van Holten, G. van Kuik, Smart dynamic control of large offshore wind turbines – Inventory of present techniques, Report to NOVEM, 2002.
- [15] B. Marrant, T. van Holten, G. van Kuik, Smart dynamic control of large offshore wind turbines – Inventory of rotor design options, Report to NOVEM, 2002.
- [16] B. Marrant, T. van Holten, G. van Kuik, Smart dynamic control of large offshore wind turbines – Inventory and assessment of available tools, Report to NOVEM, 2002.
- [17] S. Basualdo, Load Alleviation on Wind Turbines using Variable Airfoil Geometry (A Two-Dimensional Analysis), MSc Thesis, DTU, 2004.
- [18] N. Trolborg, Computational Study of the Risø-B1-18 Airfoil Equipped with Actively Controlled Trailing Edge Flaps, MSc Thesis, DTU, 2004.
- [19] P. Andersen, Load alleviation on wind turbine blades using variable airfoil geometry (2D and 3D study), MSc Thesis, DTU, 2005.
- [20] S. Basualdo, Load alleviation on wind turbine blades using variable airfoil geometry, *Wind Engineering*, vol. 29, no. 2, 2005.
- [21] N. Trolborg, Computational study of the Risø-B1-18 airfoil with a hinged flap providing variable trailing edge geometry, *Wind Engineering*, No. 2, 2005.
- [22] T. Buhl, M. Gaunaa, C. Bak, Potential load reduction using airfoils with variable trailing edge geometry, *Journal of Solar Energy Engineering*, (2005) 127, 503-516, 2005.
- [23] T. Buhl, M. Gaunaa, C. Bak, Load reduction potential using airfoils with variable trailing edge geometry, *AIAA-2005-1183*, 2005.
- [24] P. Andersen, M. Gaunaa, C. Bak, T. Buhl, Load alleviation on wind turbine blades using variable airfoil geometry, *Proceedings of the European Wind Energy Conference and Exhibition*, 2006.
- [25] T. Buhl, M. Gaunaa, C. Bak, P. Hansen, K. Clemmensen, Measurements on the Thunder TH-6R actuator, Risø-R-1537(EN) (internal report), 2005.
- [26] M. Gaunaa, Unsteady 2D potential-flow forces on a thin variable geometry airfoil undergoing arbitrary motion, Risø-R-1478(EN) (internal report), 2006.
- [27] D. Yen, C. van Dam, F. Brauchle, R. Smith, S. Collins, Active control and lift enhancement using MEM translational tabs, *AIAA 2000-2242*, 2000.

- [28] D. Yen, C. van Dam, R. Smith, S. Collins, Active Load Control for Wind Turbine Blades using MEM translational Tabs, AIAA 2001-0031, 2001.
- [29] C. van Dam, D. Nakafuji, C. Bauer, D. Chao, K. Standish, Computational design and analysis of a microtab based aerodynamic loads control system for lifting surfaces, UCRL-JC-150324, 2002.
- [30] D. Nakafuji, C. van Dam, J. Michiel, P. Morrison, Load Control for Turbine Blades: A non-traditional Microtab Approach, AIAA 2002-0054, 2002.
- [31] E. Mayda, C. van Dam, D. Nakafuji, Computational Investigation of Finite Width Microtabs for Aerodynamic Load Control, AIAA, 2005.
- [32] J. Baker, K. Standish, C. van Dam, Two-dimensional wind tunnel and computational investigation of a microtab modified S809 airfoil, AIAA 2005-1186, 2005.
- [33] R. Chow, C. van Dam, Unsteady computational investigations of deploying load control microtabs, AIAA 2006-1063, 2006.
- [34] U. Aguirre, Implementation of sensors, actuators and controllers on blades (Experimental work), TUDelft (internal report), 2005.
- [35] A. Glezer, M. Amitay, Synthetic jets, Annu. Rev. Mech, 2002, 34: 503-29, 2002.
- [36] T. Mac Coy, D. Griffin, Active control of rotor aerodynamics and geometry: Status, methods and preliminary results, AIAA 2006-605 (44th ASME), 2006.
- [37] T. van Engelen, E. van der Hooft, Individual pitch control inventory, Tech. rep., Energy research Centre of the Netherlands, 2005.
- [38] S. Collisa, R. D. Joslinb, A. Seifertc, V. Theofilis, Issues in active flow control: theory, control, simulation, and experiment, Progress in Aerospace Sciences 40 (2004) 237–289, 2004.
- [39] E. Stanewsky, Adaptive wing and flow control technology, Progress in Aerospace Sciences 37 (2001) 583–667, 2001.
- [40] E. J. Breitbach, C. Anhalt, H. P. Monner, Overview of Adaptronics in Aeronautical Applications, Air and Space, Europe 3 (2001) pp 148 –151, 2001.
- [41] M. Amitay, A. Glezer, Role of actuation frequency in controlled flow reattachment over a stalled airfoil, AIAA Journal 40, 2, 2002.
- [42] D. Greenblatt, I. Wygnanski, The control of flow separation by periodic excitation, Progress in Aerospace Sciences 36 (2000), pp. 487-545, 2000
- [43] W. Traub, A. Miller, O. Rediniotis, Comparisons of a gurney and jet flap for hingeless control, AIAA Journal of Aircraft 41, 2, 2004.
- [44] L. Vadillo, R. Agarwal, A. Cary, W. Bower, Numerical study of virtual aerodynamic shape modification of an airfoil using a synthetic jet actuator, AIAA paper 2003-4158, 2003.
- [45] H. De Vries, Review of literature concerning flow control and synthetic jets. Intermediate report, Personal communication. University of Twente, 2006
- [46] Inflatable structures in aerospace engineering – An overview, Proceedings of the European Conference on Spacecraft Structures, Materials and Mechanical Testing, 2000.
- [47] J.W. van Wingerden, I. Houtzager, Note: Smart rotor control, TUDelft (internal report), 2007.
- [48] E. Bossanyi, The design of closed loop controllers for wind turbines, Wind Energy 3 (2000), 149–163, 2000.
- [49] E. Bossanyi, Individual blade pitch control for load reduction, Wind Energy 6 (2003), 119–128, 2003.
- [50] E. Bossanyi, Wind turbine control for load reduction, Wind Energy6 (2003), 229–244, 2003.
- [51] E. Bossanyi, Further load reduction with individual pitch control, Wind Energy 8 (2005), 481–485, 2005.
- [52] T. Larsen, H. Madsen, K. Thomsen, Active load reduction using individual pitch, based on local blade flow measurements, Wind Energy 8 (2005), 67–80, 2005.
- [53] E. van der Hooft, P. Schaak, T van Engelen, Wind turbine control algorithms. Tech. rep., Energy research Centre of the Netherlands, 2003.
- [54] E. van der Hooft, T. van Engelen, Feed forward control of estimated wind speed, Tech. rep., Energy research Centre of the Netherlands, 2003.
- [55] E. van der Hooft, T. van Engelen, Estimated wind speed feed forward control for wind turbine operation optimization, Tech. rep., Energy research Centre of the Netherlands, 2004.
- [56] O.J.D. Kristensen, M. McGugan, P. Sendrup, J. Rheinlander, J. Rusborg, A.M. Hansen, C.P. Debel, B.F. Sorensen, Fundamentals for Remote Structural Health Monitoring of Wind Turbine Blades Annex E – Full-Scale Test of Wind Turbine Blade, Using Sensors NDT, RISO-R-1333(EN), May 2002.
- [57] Project: Dynamics of medium and large W.E.C.S formulation of a method for measuring loads on HAWT blades, 1st FWP. ENNONUC 3C, April 1992.
- [58] C. Anderson (NREL), Test and demonstration of a new technology 50Kw wind turbine blade on a high-wind site, URN 03/975, 2003.
- [59] C. Doyle (Smart Fibres). Fibre Bragg Grating Sensors, An introduction to Bragg gratings and interrogation techniques, 2003.

- [60] A.G. Dutton (ERU), M.J. Blanch (ERU), P. Vionis (CRES), D. Lekou (CRES), D.R.V. van Delft (Delft University), P.A. Joosse (Delft University), Anastassopoulos (Envirocoustics Abee), T. Kossivas (Geobiologiki S.A.), T.P. Philippidis (University of Patras), Y.G. Kolaxis (University of Patras), G. Fernando (Cranfield University), A. Proust (Euro Physical Acoustics, S.A.), Acoustic Emission Monitoring during Certification Testing of Wind Turbine Blades. (AEGIS Project), February 2003.
- [61] M.J. Sundaresan (NREL), M. J. Shulz (NREL), A. Ghoshal (NREL), Structural Health Monitoring Static Test of a Wind Turbine Blade, August 1999.
- [62] L. Lading, M. McGugan, P. Sendrup, J. Rheinlander, J. Rusborg, Fundamentals for Remote Structural Health Monitoring of Wind Turbine Blades Annex B – Sensors and Non-Destructive Testing Methods for Damage Detection in Wind Turbine Blades, RISO-R-1341(EN), May 2002.
- [63] M. Landa, SMA Actuators (internal report), 2007
- [64] Patoor, E., Eberhardt, A., Berveiller, M., In: Brinson, L.C., Moran, B. (Eds.), Proceedings of ASMEWAM'94: Mechanics of Phase Transformation and Shape Memory Alloys, vol. AMD189/PVD292. ASME, pp.23–37, 1994.
- [65] Sun, Q.P., Hwang, K.C., J. Mech. Phys. Solids 41 (1), 1–33, 1993.
- [66] Tanaka, K., Nishimura, F., Hayashi, T., Tobushi, H., Lexcelent, C., Mech. Mater. 19, 281–292, 1995.
- [67] Liang, C., Rogers, C.A., J. Intell. Mater. Syst. Struct. 1, 207–234, 1990.
- [68] Brinson, L.C., J. Intell. Mater. Syst. Struct. 4, 229–242, 1993.
- [69] Boyd, J.G., Lagoudas, D.C., 1996a. Int. J. Plasticity 12(6), 805–842, 1996.
- [70] Boyd, J.G., Lagoudas, D.C., 1996b. Int. J. Plasticity 12(7), 843–873, 1996.
- [71] P. Šittner, R. Stalmans and M. Tokuda Smart Materials and Structures, Vol. 9, pp. 452, 2000.
- [72] Abeyaratne, R., Knowles, J.K., 1994a. Physica D 79, 269–288, 1994.
- [73] Abeyaratne, R., Knowles, J.K., 1994b. Arch. Ration. Mech. Anal. 126(3), 203–230, 1994.
- [74] Fischer, F.D., Oberaigner, E.R., Tanaka, K., Nishimura, F., Int. J. Solids Struct. 35 (18), 2209–2227, 1998.
- [75] Lagoudas, D.C., Shu, S., J. Mech. Sci. 41, 595–619, 1999.
- [76] Leclercq, S., Lexcelent, C., J. Mech. Phys. Solids 44 (6), 953–980, 1996.
- [77] Miyazaki S., Wayman C.M., Acta Metallurgica, 36, pp.181–192, 1988.
- [78] Šittner P., Lugovyy D., Neov D., Landa M., Lukáš P., Novák V., J. de Physique IV France, 115, pp. 269–278, 2004.
- [79] Williams K. A., Chiu G. T. and Bernhard R. J., J. Sound and Vibration, 280/1–2, pp.211–234, 2005.
- [80] Bidaux J.E., Manson A., GOTTHARDT R., *Proc. of the 2nd International Conference on Shape Memory and Superelastic Technologies SMST1997*, A. R. Pelton et al eds., SMST, Santa Clara, USA, pp.287–294, 1997.
- [81] P. Šittner, V. Novák, P. Lukáš, M. Landa, Journal of Mechanical Engineering and Technology ASME, 128, 2006, 268–278, 2006.
- [82] J. G. Leishman, Challenges in modeling the unsteady aerodynamics of wind turbines, AIAA 2002-0037, 2002.
- [83] J. Gordon Leishman, Unsteady lift of a flapped airfoil by indicial concepts, Journal of Aircraft, Vol. 31, No. 2, 1994.
- [84] T. Thomsen (LM), Reliability of large rotor blades, AusWIND, 2004
- [86] J.W. Waanders, Piezoelectric Ceramics-Properties and Applications, N.V. Philips Gloeilampenfabrieken, Philips Co., Eindhoven, The Netherlands, 1991
- [87] J. Sihora, I. Chopra, Fundamental Behavior of Piezoceramic Sheet Actuators, Journal of Intelligent Material Systems and Structures, Vol.11, p.47–61, 2000.
- [88] H. Strehlow, H. Rapp, Smart Materials for Helicopter Active Control, In AGARD, Smart Structures for Aircraft and Spacecraft 16, 1993.
- [89] H.Y. Zhang, Y.P. Shen, Three-dimensional analysis for rectangular 1–3 piezoelectric fiber-reinforced composite laminates with the interdigitated electrodes under electromechanical loadings, Composites: Part B 37, 603–611, 2006.
- [90] H.A. Sodano, G. Park, D.J. Inman, An investigation into the performance of macro-fiber composites for sensing and structural vibration applications, Mechanical Systems and Signal Processing 18 (2004) 683–697, 2004.
- [91] R. Barret, Active plate and wing research using EDAP elements, Smart Materials and Structures. Vol.1, p.214–226, 2002.
- [92] R. Barret, Post-buckled precompressed piezoelectric flight control actuator design, development and demonstration. Vol.15, p.1323–1331, 2006.
- [93] S. Aimmanee, M.W. Hyer, Deformation and Blocking Force Characteristics of Rectangular THUNDER-type Actuators, King Mongkut's University of Technology Thonburi, <http://www.kmutt.ac.th/cocare/conference/>.

- [94] S. Aimmanee, M.W. Hyer, Analysis of the manufactured shape of rectangular THUNDER-type actuators, *Smart Materials and Structures*, Vol.13, p.1389–1406, 2004.
- [95] K.J. Yoon, et al., Design and Manufacture of a Lightweight Piezo-composite curved actuator, Technical Note, *Smart Materials and Structures*, Vol.11 p.163–168, 2002.
- [96] K.J. Yoon, et al., Analytical Design Model for a Piezo-composite Unimorph Actuator and its Verification using Lightweight Piezo-composite Curved Actuators, *Smart Materials and Structures*, Vol.13, p.459–467, 2004.
- [97] K.Y. Kim, et al., Performance evaluation of lightweight piezo-composite actuators, *Sensors and Actuators A* 120, p.123–129, 2005.
- [98] M. Bothwell, Ramesh Chandra, I. Chopra, Torsion Actuation with Extension-Torsion Composite Coupling and a Megnetostrictive Actuator, *AIAA Journal*, Vol.33, No.4, p.723-729 1995.
- [99] T. Malysh and J. Erhart, Electric Field Applicability Limits for PZT Ceramics, *Ferroelectrics*, 319:45–56, 2005.
- [100] Bohm, et al., Czochralski growth and characterization of piezoelectric single crystals with langasite structure: $\text{La}_3\text{Ga}_5\text{SiO}_{14}$ (LGS), $\text{La}_3\text{Ga}_{5.5}\text{Nb}_{0.5}\text{O}_{14}$ (LGN) and $\text{La}_3\text{Ga}_{5.5}\text{Ta}_{0.5}\text{O}_{14}$ (LGT). Part II, Piezoelectric and elastic properties, *Journal of Crystal Growth*, Volume 216, p.293-298, 2000.
- [101] www.piezo.com
- [102] www.smart-material.com
- [103] www.faceinternational.com
- [104] www.actiflow.com
- [105] www.morganelectroceramics.com/access-pzbook.html
- [106] www.airmar.com/